Ivana Magario

Enzyme reaction engineering for the conversion of emulsified di-rhamnolipid by free and immobilized Naringinase

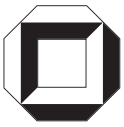

universitätsverlag karlsruhe

Ivana Magario

Enzyme reaction engineering for the conversion of emulsified di-rhamnolipid by free and immobilized Naringinase

Enzyme reaction engineering for the conversion of emulsified di-rhamnolipid by free and immobilized Naringinase

by
Ivana Magario

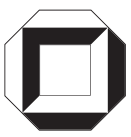

universitätsverlag karlsruhe

Dissertation, Universität Karlsruhe (TH)
Fakultät für Chemieingenieurwesen und Verfahrenstechnik
Tag der mündlichen Prüfung: 04.07.2008

Impressum

Universitätsverlag Karlsruhe
c/o Universitätsbibliothek
Straße am Forum 2
D-76131 Karlsruhe
www.uvka.de

Universitätsverlag Karlsruhe 2009
Print on Demand

ISBN: 978-3-86644-329-7

ENZYME REACTION ENGINEERING FOR THE CONVERSION OF EMULSIFIED DI-RHAMNOLIPID BY FREE AND IMMOBILIZED NARINGINASE

zur Erlangung des akademischen Grades eines
DOKTORS DER INGENIEURWISSENSCHAFTEN (Dr.-Ing.)

der Fakultät für Chemieingenieurwesen und Verfahrenstechnik der
Universität Fridericiana Karlsruhe (TH)

genehmigte
DISSERTATION

von
Dipl.-Ing. Ivana Magario
aus Córdoba / Argentinien

Referent: Prof. Dr. Christoph Syldatk
Korreferent: Prof. Dr. Matthias Franzreb
Tag der mündlichen Prüfung: 04.07.2008

Acknowledgements

I would like to thank the following persons for their support during my Ph.D. thesis:

Prof. Dr. Syldatk for his guidance and support as well as for giving me the possibility to carry out the Ph.D. project in his department and so offering me a great opportunity of learning.

Dr. Anke Neumann for her constant guidance, patience, her helpful pieces of advice at academic and human level and especially for her kind friendship making me feel as if I were her younger sister!

Dr.-Ing. Rudolf Hausmann, from whom I have learnt so much! For his enormous help especially at the end of the thesis, his positive energy, constant motivation and engagement and his contagious passion for research!

Dr. Oliver Vielhauer for his support, guidance, his helpful pieces of advice at the right moment, and for showing me how interesting chemistry can be.

Prof. Dr. Oliveros for the interesting discussions, her pieces of advice and for teaching me with high motivation.

PD. Dr. Matthias Franzreb from the Institute of Technical Chemistry, Water Technology and Geotechnology Division, *Forschungszemtrum Karlsruhe*, who accepted to report on my thesis as well as to Dr. Sonja Berensmeier from the same institution for her kind collaboration with enzyme technology issues.

All co-workers of the Institute of Biochemical Engineering under the direction of Prof. Dr.-Ing. h.c. Matthias Reuss for accompanying me during the first year of my thesis at the University of Stuttgart. I would like to thank specially Dr. Pedro Brandão for his support and friendship and also for introducing me in the interesting world of biocatalysis. I express my gratitude to Dr. Luciano Aguilera for his helpful pieces of advice, friendship, his support and nice company at the very beginning of my residence in Germany.

Rebecca Lorenz, Xiaotian Ma and Thomas Bosch for their experimental input throughout the project, for the shared hours in the lab and for giving me the opportunity to teach.

For the financial support of this work I would like to thank the European Union and the University of Karlsruhe.

All colleagues of the Chair of Technical Biology; Vanessa, Birgit, Sandra, Ana, Ulrike, Ralph, Frank, Matthias, Sebastian, Berna, Jens for their friendship, nice company, the countless German lessons and for the friendly atmosphere in our nice office room!

My parents, Luis and María, my sister Gisela and my brother Francisco for their unconditional and lovely support making the long physical distance seem shorter!

My friends, Felipe, Simona, Jessica, Marta, Matteo, Ricardo and especially to Carolina for being always there and sharing so many nice moments!

Special thanks to my Hernán for his love, friendship, patience, unconditional support, and his motivating trust in me, especially in the hard times of this work.

Abstract

Process optimization based on reaction engineering methods was conducted for the enzymatic conversion of di-rhamnolipid. An L-rhamnose molecule from a di-rhamnolipid is cleaved by α-L-rhamnosidase contained in Naringinase from *Penicillium decumbens* leading to the high tensoactive mono-rhamnolipid.

For selection of reaction conditions, the biocatalyst stability was first studied in dependence of the process conditions temperature, pH and enzyme concentration. Enzyme deactivation kinetics by a series mechanism with formation of an intermediate state was proposed for fitting deactivation data. Based on multivariate statistical methods (response surface methodology), empirical models were constructed for prediction of half-life values under different process conditions. Following observations were gained: 1) Naringinase is most stable in the pH range of 4.5 - 5.0, being quite sensitive to lower pHs (< 3.5); 2) Naringinase preserves its activity for long times (>100 h) when incubated at temperatures below 65°C and; 3) the intermediate state may correspond to unfolding and self-digestion of its carbohydrate portion, being both processes controlled by the pH and temperature of incubation. (**section 4.1**)

Highest initial reaction rates at pH 4.0 – 5.0 and 70°C were found for di-rhamnolipid conversion. Thus, at these conditions di- and mono-rhamnolipid are co-emulsified as large aggregates building a macro-emulsion (*i.e.* turbid emulsion). In order to increase reaction rates by increasing substrate solubility, water miscible organic solvents were added to di-rhamnolipid emulsions. However, little or none-effect on reaction rates was observed, although most emulsions turned clear after solvent addition. Considering these observations together with Naringinase stability data, pH 4.5 with no co-solvent addition, and 60°C were selected as process conditions for further studies. Initial reaction rates were equal to 4.5 ± 0.3 U per mg Naringinase preparation or 58 ± 7 U per mg protein. (**section 4.2**)

The following task was the set-up of a kinetic model for describing reaction-time courses. Since reaction rates were dependent on the aqueous but not on the total di-rhamnolipid concentration and due to the biphasic nature of the system, diffusive transport of the involved species was postulated for modeling: A diffusive transport of di-rhamnolipid molecules from the aggregates to the aqueous phase has to occur due to the decomposition of this species by the enzyme. Equally, a diffusive mass transport of the emerging reaction product mono-rhamnolipid occurs in the opposite direction whereas the product L-rhamnose accumulates in the aqueous phase. Michaelis-Menten kinetics with competitive L-rhamnose inhibition was assessed for the enzymatic reaction. Since a linear relation between reaction rate and enzyme concentration was observed, di-

rhamnolipid diffusion from the aggregates to the aqueous phase was considered to be not rate-limiting. Experimental determination of the model parameters A_s/K_M (rate constant), $cmc_{di\text{-}RL}$ (di-rhamnolipid critical micelle concentration) and K_I (L-rhamnose inhibition constant) enabled the kinetic model to be compared with experimental data. Excellent agreement of experimental and expected values was obtained for conversion of 1 - 10 mM di-rhamnolipid emulsions. However, enzyme deactivation as well as micelle-phase volume should be taken into account when conversions of high rhamnolipid concentrated emulsions are assayed during a larger reaction time. Furthermore, mono-rhamnolipid consumption due to its consecutive enzymatic conversion into 3-(3-hydroxydecanoyloxy)decanoic acid and L-rhamnose was considered in the model equations. Good agreement between experimental and expected values was achieved. (**section 4.2**)

The second part of this work was focused on the selection of a suitable carrier for Naringinase immobilization. Non-porous micro-magnetic beads in comparison to conventional porous carriers like Eupergit and Sepharose were tested. These carrier materials were evaluated with respect to activity yield, activity loading and operational stability. Unspecific immobilization of foreign proteins present in the Naringinase preparation was investigated. Thus, immobilization of an enriched preparation was tested as well as Naringinase specific adsorption to a pre-coupled protein (Concanavalin-A) that binds specifically to sugar moieties of its carbohydrate portion. A two-fold increase in activity yield was in accordance with the increase of specific activity achieved upon enzyme enrichment. Furthermore, the effect of protein and activating-reagent concentration on immobilized enzyme activities on micro non-porous carriers was investigated by response surface methodology. Highest activity loading of 97 U per g carrier and activity yields of 69 % were obtained with micro non-porous carriers at a protein loading of 2.5 mg per g carrier. (**section 4.3**)

The kinetic analysis of initial reaction rates with the immobilized enzyme was of special interest. Thus, the influence of diffusion limitation within porous and on non-porous carriers was investigated. The variation of the reaction effectiveness factor with increasing enzyme loading was compared with experimental efficiencies utilizing immobilized preparations with different protein loadings. Efficiencies were also determined with the high-soluble substrate p-nitro-phenyl-rhamnoside. Excellent agreement between theoretical and experimental tendencies was observed for porous carriers and intrinsic enzyme activities were thereby estimated for this support-type. Intrinsic activity of Naringinase coupled on Eupergit 250L was 7-fold higher than free-enzyme activity upon di-rhamnolipid conversion. This may correspond to a lumped value due to adsorption or partition of rhamnolipid molecules on the hydrophobic matrix of Eupergit 250L. Experimental efficiencies on non-porous micro-beads were much lower than theoretical values. On the other hand, a simple multi-layer immobilization model a-

llowed experimental tendencies to be interpreted. In conclusion, non-porous microbeads demonstrated to be the most suitable carrier for conversion of a low-soluble substrate like rhamnolipids, where mass diffusional resistances in the three-phase reaction system are completely overcome. However, the smaller particle surface available limited the specific activity obtained at high protein loadings. (**section 4.4**)

Zusammenfassung

In dieser Arbeit wurde eine Prozessoptimierung basierend auf reaktionstechnischen Methoden für die enzymatische Umsetzung von di-Rhamnolipid durchgeführt. Die Abspaltung eines L-Rhamnose Moleküls von einem di-Rhamnolipid wurde somit zur Gewinnung des reinen mono-Rhamnolipids und der wertvollen L-Rhamnose mittels enzymatischer Hydrolyse untersucht. Eingesetzt wurde hierfür das Enzym Rhamnosidase des kommerziellen Präparates „Naringinase“ aus *Penicillium decumbens*.

Zur Ermittlung geeigneter Reaktionsbedingungen wurde zuerst die Biokatalysatorstabilität in Abhängigkeit von den Prozessparametern Temperatur, pH-Wert und Enzymkonzentration untersucht. Dabei wurde ein Serien-Mechanismusmodel mit Bildung eines Enzymzwischenzustandes zur Anpassung an das experimentell ermittelte Deaktivierungsprofil vorgeschlagen. Weiterhin wurde eine Reihe von Stabilitätsversuchen, deren Bedingungen mit Hilfe von multivariater statistischer Versuchsplanung (response surface methodology) sorgfältig ausgewählt worden sind, durchgeführt. Diese Versuche dienten dazu, empirische Modelle zu bilden um die Enzymhalbwertzeit unter verschiedene Prozessbedingungen vorhersagen zu können. Folgende Ergebnisse wurden dabei gewonnen: 1) In dem pH-Bereich von 4,5 – 5,0 ist Naringinase am stabilsten und bei niedrigeren pH-Werten (< 3,5) sehr empfindlich; 2) Naringinase ist bei Inkubationstemperaturen niedriger als 65°C über lange Zeiträume aktiv (>100 h); 3) Die postulierte Bildung von einem Zwischenzustand könnte auf eine Entfaltung und Selbstverdauung seiner Zuckerreste zurückgeführt werden, wobei diese Prozesse von dem Inkubations-pH-Wert aber auch von der Inkubationstemperatur abhängen. (**siehe Kapitel 4.1**)

Die höchste Anfangsreaktionsrate für die Umsetzung von di-Rhamnolipid wurde bei pH 4,0 – 5,0 gefunden. Bei diesen Bedingungen sind mono- und di-Rhamnolipide co-emulgiert und liegen als große Aggregate in einer trüben Emulsion vor. Um die Reaktionsrate durch eine gesteigerte Substratlöslichkeit zu erhöhen wurden wasserlösliche organische Lösungsmittel zu der di-Rhamnolipid Emulsion gegeben. Obwohl dies in den meisten Fällen zu einer klaren Lösung geführt hat, konnte wenig bis kein Effekt auf die Reaktionsrate beobachtet werden. Aufgrund dieser Ergebnisse und der Stabilitätsdaten der Naringinase wurden pH 4,5; 60°C und keine Solventzugabe als Prozessbedingungen für weitere Studien gewählt. Die Anfangsreaktionsraten betrugen 4,5 ± 0,3 U pro mg Naringinase Pulver oder 58 ± 7 U pro mg Protein. (**siehe Kapitel 4.2**)

Anschließend wurde ein kinetisches Model entwickelt um den Reaktionsverlauf zu beschreiben. Da die Reaktionsrate von der wässrigen, aber nicht von der Gesamtrhamnolipidkonzentration abhängt und wegen des zweiphasigen Charakters des System wurde folgendes postuliert: Um den Abbau der di-Rhamnolipid Moleküle durch das

Enzym zu ermöglichen, muß ein diffusiver Transport der di-Rhamnolipid Moleküle von den Aggregaten zur wässrige Phase erfolgen. Ebenso erfolgt ein diffusiver Stofftransport des gebildeten Produktes mono-Rhamnolipid in die entgegengesetzte Richtung. Das zweite Produkt, L-Rhamnose, akkumuliert in der wässrigen Phase. Die enzymatische Umsetzung wurde als Michaelis-Menten Kinetik mit kompetitiver L-Rhamnose-Inhibierung beschrieben. Da eine lineare Korrelation von der Enzymkonzentration und der Reaktionsrate gefunden wurde, konnte die Diffusion des di-Rhamnolipid von den Aggregaten in die wässrige Phase als nicht geschwindigkeitsbestimmend angesehen werden. Durch die experimentelle Bestimmung der Reaktionsparameter As/KM (Geschwindigkeitskonstante), cmcdi-RL (kritische Mizellkonzentration von di-Rhamnolipid), und KI (L-Rhamnose-Inhibierungskonstante) konnte das kinetische Model mit Versuchsdaten verglichen werden. Für die Umsetzung von di-Rhamnolipid-Emulsionen bei 1 – 10 mM Substratskonzentration wurde eine sehr gute Übereinstimmung von gemessenen und erwarteten Werten gefunden. Bei der Betrachtung der Umsetzung bei höher konzentrierten Emulsionen über eine längere Reaktionszeit sollten jedoch die Enzyminaktivierung und das Volumen der Aggregate mitberücksichtigt werden. Des Weiteren wurde die konsekutive Umsetzung des Produktes mono-Rhamnolipid in ß-Hydroxydecanoyl-ß-hydroxydecansäure und L-Rhamnose in die Modelgleichungen miteinbezogen. Gute Übereinstimmung zwischen experimentellen und erwarteten Werten wurde beobachtet. (**siehe Kapitel 4.2**)

Der zweite Teil dieser Arbeit befasst sich mit der Auswahl eines geeigneten Trägers für die Immobilisierung der Naringinase. Unporöse magnetische Mikropartikel wurden mit konventionellen porösen Eupergit- und Sepharose-Träger verglichen. Dabei wurden Aktivitätsausbeute, Aktivitätsbeladung und operationelle Stabilität betrachtet. Die unspezifische Bindung von Fremdproteinen des Naringinase-Pulvers an die Träger wurde auf zwei Weisen untersucht. Erstens wurde die Immobilisierung von einem angereicherten Enzympräparat betrachtet. Zweitens wurde die spezifische Adsorption der Naringinase an mit Concanavalin-A vorgekoppeltes Träger untersucht. Concanavalin-A bindet spezifisch die Zuckerreste der glycosilierten Naringinase. Der zweifache Anstieg der Aktivitätsausbeute korreliert mit dem Anstieg der spezifischen Aktivität, der durch die Enzymanreichung erzielt wurde. Mit Hilfe von Response Surface Methodology wurde der Effekt von der Protein- und Aktivierungsreagenz- Menge auf die Enzymaktivität der immobilisierten Naringinase auf magnetischen Mikropartikeln untersucht. Dabei wurde die höchste Aktivitätsbeladung von 97 U per g Träger mit einer Aktivitätsausbeute von 69 % mit den magnetischen Mikropartikeln bei einer Proteinbeladung von 2,5 mg g^{-1} erreicht. (**siehe Kapitel 4.3**)

Von besonderer Bedeutung war die kinetische Analyse der Anfangsreaktionsraten mit dem immobilisierten Enzym. Daher wurde der Einfluss von internem bzw. externem Stofftransport bei porösen und nicht-porösen Trägern untersucht. Die theoretische Ab-

hängigkeit des Wirkungsgrades von der Enzymbeladung wurde mit experimentell ermittelten spezifischen Trägeraktivitäten von Immobilisaten verschiedener Enzymbeladung verglichen. Dabei wurden Enzymaktivitäten mit di-Rhamnolipid als Substrat sowie mit dem löslichen Substrat p-Nitrophenyl-Rhamnosid betrachtet. Bei den porösen Trägern wurde gute Übereinstimmung zwischen dem theoretischen und experimentellen Aktivitätsverlauf gefunden. Dadurch konnten die intrinsischen Enzymaktivitäten für die porösen Träger abgeschätzt werden. Die intrinsische Aktivität von an Eupergit 250L gekoppelter Naringinase war für die di-Rhamnolipid Umsetzung siebenfach höher als die von freier Naringinase. Dieser unerwartet hohe Wert könnte auf Adsorption oder Partition von Rhamnolipid-Molekülen an dem hydrophoben Eupergit-Trägermaterial zurückgeführt werden. Anderseits waren experimentell bestimmte Aktitvitätsbeladungen bei den nicht-porösen Mikropartikeln viel niedriger als die theoretischen und ließen sich anhand von einem einfachen Mehrschicht-Immobilisierungsmodel gut interpretieren. Schließlich zeigten sich nicht-poröse Mikropartikel als der geeignete Trägertyp für die Umsetzung von schwer-löslichen Substraten wie Rhamnolipiden. Somit werden Stofftransportwiderstände bei dem dreiphasigen Reaktionsystem überwunden. Jedoch limitierte die geringere verfügbare Partikeloberfläche die spezifische Trägeraktivität bei hohen Proteinbeladungen. (**siehe Kapitel 4.4**)

Contents

1 Introduction

1.1 Microbial Biosurfactants and Rhamnolipids

Surfactants are surface-active agents, which will adsorb at an air-water or oil-water interface and at the surface of solids (Attwood and Florence 1983). Chemically, they are amphipathic compounds containing both hydrophobic and hydrophilic moieties. A biosurfactant is a biologically produced surfactant. Of special interest are microbial biosurfactants, which are produced by bacteria, fungi, or yeast as extracellular compounds or bound to its cell membrane. Different molecule structures showing surface active properties were found to be secreted by microorganisms. The hydrophilic portion of biosurfactants often contains a mono-, oligo- or polysaccharide, an amino acid or peptide, a carboxylate or phosphate group whereas the hydrophobic portion is composed of saturated or unsaturated fatty acids, hydroxyl fatty acids or fatty alcohols (Lang 2002). According to Rosenberg and Ron (1999) and Lang and Trowitzsch-Kienast (2002), biosurfactants are chemically classified as:

- Low-molecular-mass biosurfactants: glycolipids, lipopeptides, fatty acids and phospholipids
- High-molecular-mass biosurfactants: lipoproteins, polysaccharides-proteins, lipopolysaccharides, etc.

This wide variety of compounds supposes that different groups of biosurfactants have different physiological roles in the growth of the producing microorganisms. Indeed, biosurfactants are suggested to increase the surface area of hydrophobic water-insoluble substrates, increase the bio-availability of hydrophobic water-insoluble substrates and to regulate the attachment-detachment of microorganisms to and from surfaces (Rosenberg and Ron 1999).

Biosurfactants are becoming important biotechnology products due to their specific modes of action, relative ease of preparation and widespread applicability (Singh et al. 2007). Advantages over chemical surfactants are their bio-degradability, production from renewable materials and its lower toxicity. However, due to its relative high production costs (US$ 20-5/kg for 20-100 m^3 fermentation process) compared to chemical surfactants (US$ 1-3/kg) (Lang and Wullbrandt 1999) biosurfactants can not compete with the well-established petroleum-based surfactants (Lang 2002). At the present the majority of surface-active agents are from chemical origin; however, increasing environmental concern has led to the consideration of biological surfactants as alternatives to the chemically synthesized compounds (Nitschke et al. 2005). By the year 2010,

biosurfactants could capture 10 % of the surfactant market, reaching US$ 200 million in sales (Nitschke et al. 2005). The reduction of its production costs requires enhancement of biosynthesis efficiency, application of non-pathogen microorganisms, selection of inexpensive medium components by *e.g.* use of agro-industrial by-products and industrial wastes.

The major interest of biosurfactants is found in applications, where bio-compatibility and low toxicity are specially required properties (Lang and Trowitzsch-Kienast 2002). For evaluating its potential uses, research has been conducted in the following areas:

- Environmental applications: Hydrophobic pollutants in soils and water as *e.g.* polycyclic aromatics, and poly-chlorinated biphenyls, can be eliminated by bioremediation facilitated by the addition of biosurfactants. As they increase the oil/water surface area, they accelerate degradation of oils by bacteria improving its uptake from soils and water. Biosurfactants can also complex heavy metals as Pb^{+2}, Zn^{+2}, Cd^{+2} and uranium ions (UO_2^{+2}) thus promoting its elimination from contaminated areas. Examples of environmental applications are reviewed by Banat et al. (2000); Kosaric (2001); Lang and Trowitzsch-Kienast (2002) and Mulligan (2005).

- Cleaning industry: Biosurfactants also show advantages over chemical surfactants for detergents formulations since they are much less harmful to the environment and they are compatible with enzymes often found in detergent formulation (Rosenberg and Ron 1999).

- Petroleum industry: Biosurfactants has been also used in studies on enhanced oil recovery and also for cleaning-up of storage tanks and pipes. Examples are reviewed by Lang and Trowitzsch-Kienast (2002).

- Food industry: Emulsion forming, stabilization and anti-adhesive activities are some properties of biosurfactants that could be explored for food processing and formulation (Nitschke and Costa 2007). High-molecular-mass biosurfactants coats oil-droplets forming very stable oil in water emulsions (e.g. salad dressing). They also improve texture and creaminess of soft chesses and ice creams and this property is especially important for low-fat products (Rosenberg and Ron 1999).

- Biomedical applications: Several biosurfactants have strong antibacterial, antifungal and antiviral activity. Other medical relevant uses include their role as anti-adhesive agents to pathogens, making them useful for treating many diseases and as therapeutic and probiotic agents (Singh and Cameotra 2004). Studies of biosurfactants as adjutants for vaccines as well as on anti-tumor tests are reviewed by Lang and Trowitzsch-Kienast (2002). Medicine applications are reviewed by Cameotra and Makkar (2004); Singh and Cameotra (2004) and Rodrigues et al. (2006).

Biosurfactants are also potentially useful in agriculture (formulation of herbicides and pesticides), in the textile and paper industry and in cosmetic applications due to anti-irritating effects and skin-compatibility (Rosenberg and Ron 1999; Maier and Soberon-Chavez 2000).

Glycolipids are the most-intensive investigated classes of biosurfactants. The carbohydrate moiety is bound to the lipid group via a glycosidic linkage (*e.g.* rhamnolipids and sophorolipids) or via an ester linkage (*e.g.* trehalose glycolipid). They are produced by different microorganisms from hydrophobic as well as from hydrophilic carbon sources. Enzymatic glycolipid production processes are also widely described. Thus, lipase-, protease- and glycosidase-assisted catalytic syntheses from sugar moieties and fatty acids or fatty alcohols were successfully applied (Lang and Trowitzsch-Kienast 2002).

Rhamnolipids (RL) are glycolipids produced *e.g.* by *Pseudomonas* sp. having L-rhamnose moieties (Rha) attached by a glycosidic linkage to the lipid tail, a ß-hydroxy-fatty acid (C_n). RL are produced as an extracellular mixture of different species. Figure 1 shows the structures of the main components rhamnolipid 3 (R3) and rhamnolipid 1 (R1) commonly produced and also of derived structures from those.

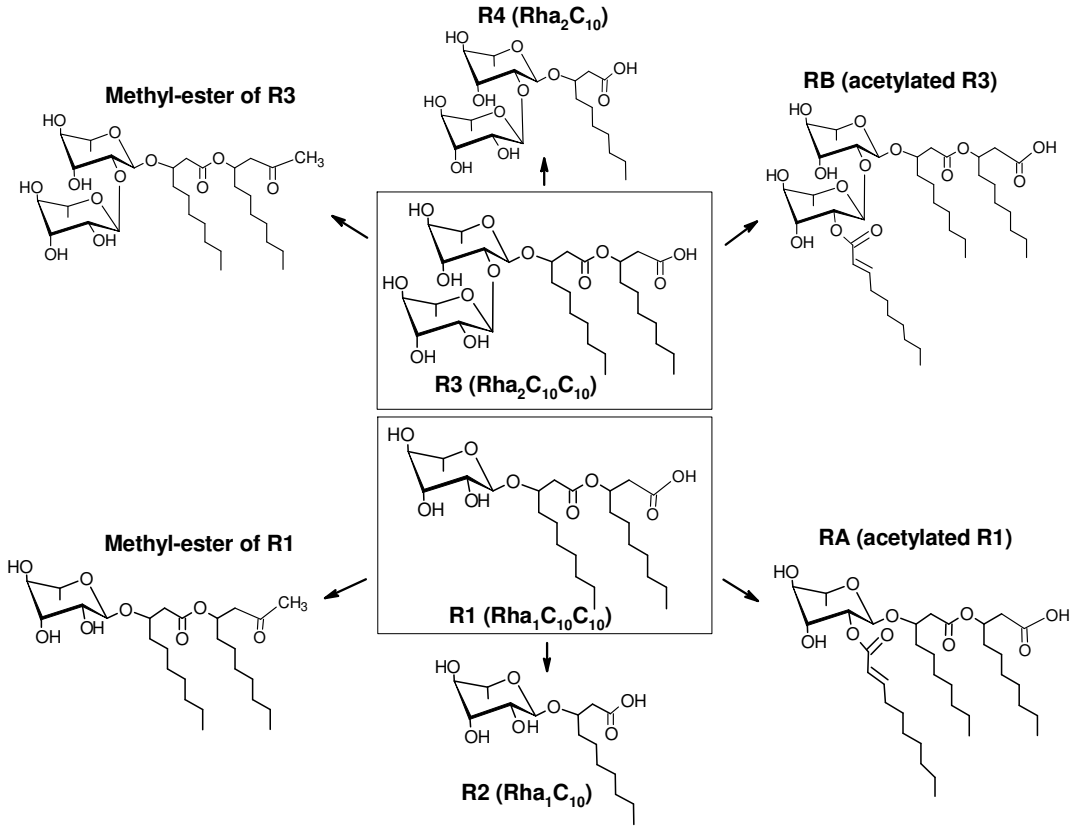

Figure 1: Rhamnolipid structures produced by different *Pseudomonas* species

RL with acetylated L-rhamnose units (RA and RB) were described and also structures with methyl esters of the fatty acids moieties were encountered as main products by

cultivation and *P. aeruginosa* 158 (Lang and Wullbrandt 1999). The species R2 and R4 where also found by resting cells of *Pseudomonas* sp. DSM 2874 (Syldatk et al. 1985). Numerous minor species have also been detected by high performance liquid chromatography mass spectrometry (HPLC-MS) and up to 28 different RL have been identified. These species vary according to the number of L-rhamnose units (Rha_1 and Rha_2), fatty acids chain lengths (C_8, C_{10}, C_{12}) and presence of unsaturated fatty acid chains (Nitschke et al. 2005).

Following aspects of rhamnolipids will be shortly overviewed:

1.1.1 Microbial production of rhamnolipids

Overproduction of RL is achieved by growth-limitation conditions. Restrained conditions of nitrogen and multivalent ions are necessary. Carbon sources as glycerol, glucose, n-alkanes and triglycerides contained in *e.g.* vegetable oils are suitable for production. One of the main problems of cultivation is the extreme high foam formation during production. Following biotechnological methods has been described: batch or fed-batch cultivation under growth limiting conditions, batch cultivation with resting free cells, semi-continuous production with immobilized cells (in fluidized bed reactor followed by RL isolation on Amberlite XAD-2 columns) and continuous cultivation in a chemostat (Lang and Wullbrandt 1999). The nature of the carbon source, concentration of nitrogen and multivalent ions, cultures conditions such pH and temperature, aeration rate, fermentation strategy, and bacterial strain are production parameters affecting the efficiency of the process and/or the composition of the RL mixture (Nitschke et al. 2005).

1.1.2 Biosynthetic pathway and genetics of rhamnolipids

RL production by *Pseudomonas* is dependent on central metabolic pathways, such as fatty acid synthesis and dTDP-activated sugars as well as on enzymes participating in the production of alginate (Maier and Soberon-Chavez 2000). Thus, the sugar and lipid moiety of RL are formed by *de novo* synthesis and are independent of the substrate used (Lang and Wullbrandt 1999; Nitschke and Costa 2007). Genetic regulation of RL biosynthesis is controlled by the quorum sensing system (production of diffusible autoinducers at high cell density activating specific transcriptional regulators) (Maier and Soberon-Chavez 2000). Investigation at genetic level has being carried out for the construction of enhanced strains for overproduction of RL (Frank Rosenau, *Forschungszentrum Jülich,* personal communication) and for RL production in recombinant *Escherichia coli* (Ochsner et al. 1995).

1.1.3 Surface activity of (bio)surfactants and rhamnolipids

An amphiphilic molecule will tend to accumulate at the air/water or oil/water surface in order to place the hydrophobic tails in the gaseous or oil phase. Since the forces of intermolecular attraction between water molecules and non-polar groups are less than those existing between two water molecules, the contracting power of the surface is reduced and so, the surface tension (Attwood and Florence 1983). This is the reason why surfactants are capable to produce stabile emulsions of two immiscible liquids. The surface tension of a surfactant solution decreases with the surfactant concentration up to a point in which no further decrease is observed. The surface is saturated with surfactant molecules and they start to build aggregates in the bulk solution called micelles: the hydrophobic tails are placed in the core surrounded by the hydrophilic moieties in contact with water. The concentration at which micelles start to form is called the critical micelle concentration (*cmc*) and is an important parameter for evaluating the surface activity of surfactants.

In the past 20 years many authors reported *cmc* and surface tension values obtained by RL produced by different strains. Table 1 summarized *cmc*, surface and interfacial tension values of different kinds of RL. For comparison, *cmc* values of other biosurfactants are also shown. The absence of one of the fatty acid chain causes a deeply decrease of the surface activity (R2 and R4) whereas other variations in structures does not influence the surface activity to a great extend.

Table 1: *cmc*, surface (σ) and interfacial (γ) tension data of RL and of various biosurfactants

Surfactant	*cmc* (mg l^{-1})	σ_{cmc} * (mN m^{-1})	γ ** (mN m^{-1})	Reference
R1 ($Rha_1C_{10}C_{10}$)	20	31	8	Syldatk et al. (1985)
R2 (Rha_1C_{10})	200***	25	<1	Syldatk et al. (1985)
R3 ($Rha_2C_{10}C_{10}$)	20	31	3	Syldatk et al. (1985)
R4 (Rha_2C_{10})	200***	30	<1	Syldatk et al. (1985)
RA ($C_{10}ORha_1C_{10}C_{10}$)	40	-	-	Ishigami et al. (1987)
RB ($C_{10}ORha_2C_{10}C_{10}$)	120	-	-	Ishigami et al. (1987)
$Rha_2C_{10}C_{12/12:1}$	37	36	-	Mata-Sandoval et al. (1999)
Sophoroselipid	82	37	1-2	Cooper and Paddock (1984)
Surfactain	25	27	<1	Cooper et al. (1981)
Trehalose-monocorynomycolate	4	32	14	Kim et al. (1990)

* Surface tension of water 72 mN m^{-1}

** γ of the system water/surfactant/n-hexadecane. γ of water/n-hexadecane, 43 mN m^{-1}

*** Determined in deposit water

1.1.4 Tested applications and current uses of rhamnolipids

RL were principally tested in soil bioremediation studies. They have been shown to enhance the biodegradation of different hydrocarbons in pure cultures but also in soil sys-

tems however they also inhibited biodegradation in some cases. RL also enhanced biodegradation in system co-contaminated with organics and toxic metals. They also showed high flushing properties removing organics compounds from contaminated solids by either mobilization of the non-aqueous liquid phase or by solubilisation of these hydrophobic pollutants. The solubilisation capacity of RL for many organics was much higher than the for chemical surfactants SDS, Tween 80 and alkyl benzyl sulfonate. RL also have high affinity to metal ions as cadmium, copper, lanthanum, lead and zinc and their use in removing such metals from contaminated areas has also been demonstrated (Maier and Soberon-Chavez 2000).

R1 and R3 showed antimicrobial activity restricting the growth of *Basillus subtilis* and antiphitoviral effects against tobacco mosaic virus and potato X virus were also observed. They also showed zoosporicidal activity on different genera of zoosporic phytophatogens (Lang and Wullbrandt 1999; Maier and Soberon-Chavez 2000). Piljac and Piljac (1993) patented a pharmaceutical preparation based on RL for treatment of dermatological diseases, viral infections and for cosmetic purposes.

RL were also tested in food industry to *e.g.* preserve freshness of fruits, emulsify flavor oils, as flavors' precursors and for crystallization of sugar. Van Haesendonck and Vanzeveren (2006) patented the use of RL for improvement of dough stability, volume and shape, for microbial conservation of bakery products and also for properties improvements of butter creams.

Jeneil Biosurfactants Corporation is producing RL at large scale offering products with different grade of purity. Furthermore, RL are being used as cosmetic additives in Japan (Maier and Soberon-Chavez 2000) whereas the Belgian company Ecover applied RL for formulation of household glass-cleaning agents (Dirk Develter, personal communication).

1.2 Enzymatic Modification of Rhamnolipids

Biosurfactants obtained after microbial production often comprises a mixture of different species. However, for industrial applications pure species are generally more desirable than mixtures. Moreover, single species are more feasible for serving as starting material for organic synthesis as well as for testing new properties (*e.g.* in medical or pharmaceutical uses). The advantages and potential applications of biosurfactants can be spread by modifications and even improvements of their properties may be achieved through production of new species. Finally, biosurfactant modification can also be targeted to the obtainment of its valuable hydrolysis products, mono- or oligosaccharides as well as the fatty acid or hydroxyl fatty acids.

Modifications of the original structure of biosurfactants after microbial production can be achieved by enzymatically or chemically catalysed reactions (Lang and Trowitzsch-

Kienast 2002). Interesting examples of such modifications were widely applied in case of sophorolipids (Bisht et al. 1999; Bisht et al. 2000; Lang and Trowitzsch-Kienast 2002; Hut and Ju 2003; Singh et al. 2003; Zhang et al. 2004).

In this context, a promising modification schema for RL can be as followed:

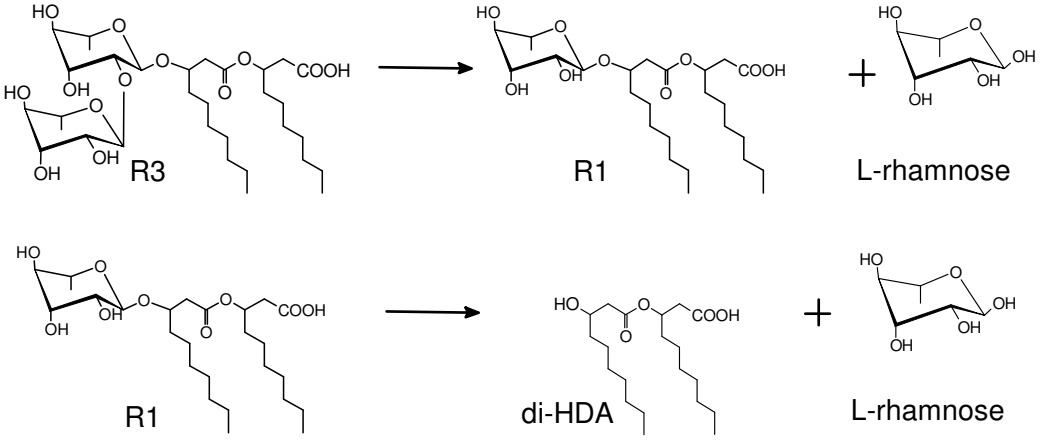

Figure 2: Hydrolysis of rhamnolipid 3 and rhamnolipid 1

In Figure 2 one L-rhamnose molecule is first cleaved from R3 leading to the formation of R1. This cleavage can be enzymatically catalysed by an L-rhamnosidase activity. A second L-rhamnose molecule can be also cleaved from R1 for a final production of 3-(3-hydroxydecanoyloxy)decanoic acid (di-HDA) and two L-rhamnose molecules. Motivations and advantages of such modification are:

- Production of the single species R1 from the fermentation mixture often composed of the two main products R3 and R1. This mono-rhamnolipid showed higher surface and interfacial activity than R3 at concentrations below the *cmc* and this behavior was attributed to the more favorable hydrophilic/hydrophobic balance of R1 molecules (Ozdemir et al. 2004). Pure R1 may be also achieved by physical means, *e.g.* by adsorption chromatography of the RL mixture on silica gel. However, through this method big amounts of organic solvents would be needed for RL elution from the adsorbent. The enzymatic modification would be a more environmental-friendly process.

- The side-product L-rhamnose is therewith also obtained. This desoxy-sugar is used as starting material for chemical syntheses as *e.g.* formation of the high-valuable flavor agents Furaneol®, as inducer of recombinant protein expression in *E. coli* and is also of interest for pharmaceutical purposes (Lang and Trowitzsch-Kienast 2002; Trummler et al. 2003). Its current difficult and expensive production process lies in the fact that L-rhamnose is obtained from plant raw materials (Rutin, Hesparadin, Naringin) or from microbial polysaccharides difficult to handle and containing other sugar monomers which are hard to separate (Lang and

Trowitzsch-Kienast 2002). Production of L-rhamnose from RL may solve the problem of foreign sugar monomers in the downstream processing and therefore be a promising alternative for its production.

- For *Pseudomonas aeruginosa* 7108 it was shown that the ratio R3 to R1 increased with production time from 1:2 to 4:1 and this observation was independent of the carbon source (vegetable oils) used (Leitermann et. al. unpublished). Thus, this ratio seems to be a characteristic of the strain used and may hardly be changed upon process conditions. Therefore, for those strains the proposed modification would be an interesting solution for obtaining high RL yields and simultaneously high R1 amounts.
- The second modification step leads to the production of one extra L-rhamnose molecule from R3 and also to di-HDA. This hydroxy-fatty acid is also an interesting chiral precursor for chemical synthesis.

In the past the interest of RL was often targeted to the production of L-rhamnose and therefore in these studies RL were hydrolyzed by acidic catalysis after biotechnological production for obtaining this desoxy sugar (Linhardt et al. 1989; Giani et al. 1993; Mixich et al. 1996). Moreover, enzymatic hydrolysis of RL were also reported by Meiwes et al. (1997) and by Trummler et al. (2003). Trummler et al. (2003) achieved hydrolysis of RL and therewith production of pure R1 by directly adding the enzyme Naringinase during *Pseudomonas sp.* resting cells fermentation. Unfortunately, this integrated microbial/enzymatic process was not industrially feasible due to the chemical decomposition of L-rhamnose in the bioreactor.

The advantages of an enzymatic hydrolysis of RL over the chemical hydrolysis are besides the milder pH and temperature and lower salts content in the reaction system, that the grade of RL hydrolysis can be controlled. Thus, due to the higher enzyme selectivity, the reaction can be directed for R1 and L-rhamnose production or let to go further to the final formation of L-rhamnose and di-HDA. Moreover, production of R1 and/or of di-HDA by acid hydrolysis is not possible since every glycosidic and ester bond is indistinctly cleaved leading to L-rhamnose and 3-hydroxy decanoic acid (HDA) as final products. On the other hand, an enzymatic hydrolysis may be more expensive than the chemical hydrolysis. Fortunately, L-rhamnosidases are found in commercial technical preparations like Naringinase. These preparations are relative inexpensive and should not increase the production cost mainly if enzyme re-use by immobilization is considered.

2 Research Proposal

Rhamnolipids are well-studied microbial glycolipids with well-tested potential applications. Most rhamnolipid producing bacteria lead to a mixture of different species, which differ in their tensoactive properties. The composition of this mixture is, however, difficult to be affected by *e.g.* varying process conditions. On the other hand, an increasing need for pure species with higher tensoactive properties as *e.g.* mono-rhamnolipid is arising in view of their specific applications as *e.g.* in the biomedical field. Enzymatic modification of the rhamnolipid mixture can therefore be attempted to produce one single species with simultaneous gaining of valuable hydrolysis products. On previous investigations it was demonstrated that an inexpensive L-rhamnosidase-containing-enzyme-preparation was capable of cleaving the di-rhamnolipid structure to produce mono-rhamnolipid and L-rhamnose. Based on this work, a two-step production process was proposed: microbial production of rhamnolipids followed by enzymatic modification with L-rhamnosidase.

The aim of this work was to build the background for the development of a biotechnological process for the production of mono-rhamnolipid by enzymatic modification of di-rhamnolipid resulting from the production with *Pseudomonas* sp. The gained knowledge about the description of the enzymatic reaction of an aggregates-building substrate should serve as basis for understanding similar reacting system involving biosurfactants other than rhamnolipids.

Once substrate, products as well as biocatalysts are selected a process optimization scheme should be conducted for a rational selection of operating conditions (Biselli et al. 2002). The present reaction is a simple one-substrate reaction where reversible reaction can be neglected since it was found to go forward till 100 % conversion. The enzyme selectivity is here not an issue since the present reaction does not imply formation of enantiomeric isomers. However, a consecutive enzymatic reaction with R1 consumption takes also place and should be also investigated. The complicity of the system lies rather in the nature of their reactants and products, namely in their surface activity and their tendency to build aggregates. Following questions arise:

- How do these aggregates affect the substrate availability for the enzyme? Can the substrate availability and thus reaction rates be enhanced by the use of co-solvents?
- Can the aggregates be treated as second phase for describing enzyme kinetics? Is the substrate diffusion a relevant issue?
- How does this surface active substrate interact with immobilized enzyme? Is the substrate diffusion a relevant issue?

To elucidate these questions and perform a process optimization of industrial interest, this work was focused on following aspects:

- Study of the effect of reaction conditions on the biocatalyst stability
- Study of the effect of reaction conditions on the biocatalyst activity as well as on the physical properties of the reaction system. Evaluation of the use of organic solvents for increasing reaction rates
- Kinetic analysis and mathematical modeling of the main and also of the consecutive enzymatic reaction for description of reaction-time courses
- Enzyme immobilization for its re-use: evaluation of porous and non-porous carriers and optimization of immobilization parameters
- Kinetic analysis of the immobilized-enzyme-catalyzed reaction

The outline of this work can be further clarified with the squeamish representation of Figure 3.

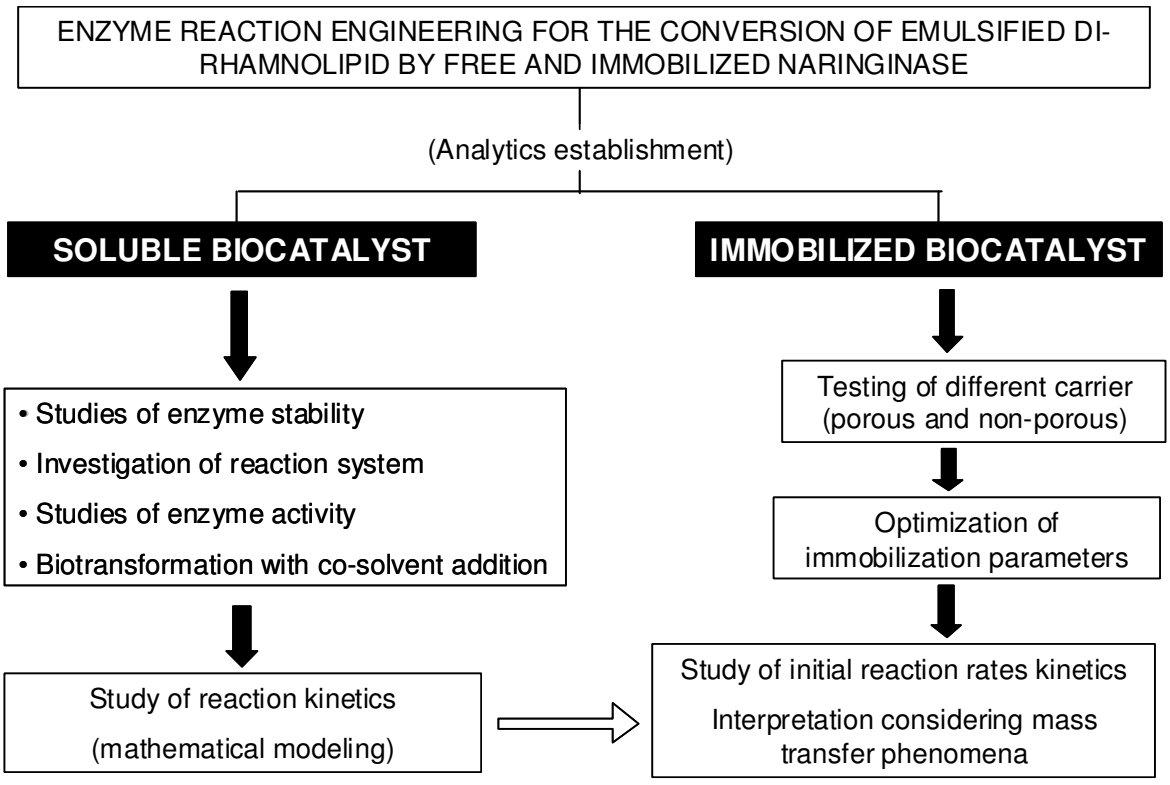

Figure 3: Outline of this work

3 Particularities of Reaction System and Biocatalyst

3.1 Reaction System

Characteristics of the reaction system have to be considered for process optimization. Physicochemical properties such as substrate and products solubility or occurrence of parallel non-enzymatic reaction as well as variation of these properties with reaction conditions have to be taken into account for finding the optimal operating conditions (Biselli et al. 2002). Moreover, such data are crucial for interpretation of kinetic data. Finally, physicochemical properties of the reaction system are also important for process design, reactor type selection and downstream processing.

The present reaction system contains a surface-active substrate (R3) and a surface-active product (R1). Both molecules tend to adsorb to surfaces (air/liquid, oil/liquid and solid/liquid) and to build aggregates by interacting on each other. That makes the availability for enzyme-substrate-complex building and destruction more difficult and less predictable. Thus, it would be not surprising that the simple Michaelis-Menten kinetic model for soluble "non-surface active" substrates would here not apply. For example, under conditions of "virtual" substrate solubility, the actual aqueous substrate concentration (monomers) may be much lower than the nominal value due to the formation of micelles. There are some works reporting about kinetic analysis and modeling of enzymatic conversion of surface-active substrates. The enzymes present in such conversions were commonly lipases and phospholipases showing interfacial activation at substrate concentration above the *cmc* (Panaiotov et al. 1997). However, less information is known about kinetic analysis and modeling with hydrophilic enzymes as L-rhamnosidases (Chopineau et al. 1998). An overview of this reaction models are described under the discussion section of section 4.2.

Following RL properties are considered to be relevant for process design and optimization and are therefore listed below together with available data from the literature.

3.1.1 Solubility and its pH dependency

The aqueous solubility of RL is pH-dependent increasing with pH as can be observed from the picture in Figure 4. This behavior is caused by the acid-base equilibrium of its carboxylate group. At low pH values RL molecules are fully protonated and uncharged and its solubility is lower than its *cmc* value and thus solid hydrated surfactant are in equilibrium with monomers and no micelles are present (Attwood and Florence 1983). At higher pH, RL molecules become de-protonated and charged increasing its solubility

beyond its *cmc* value and, so, monomers at a concentration equals to the *cmc* are in equilibrium with micelles, building an isotropic microemulsion system.

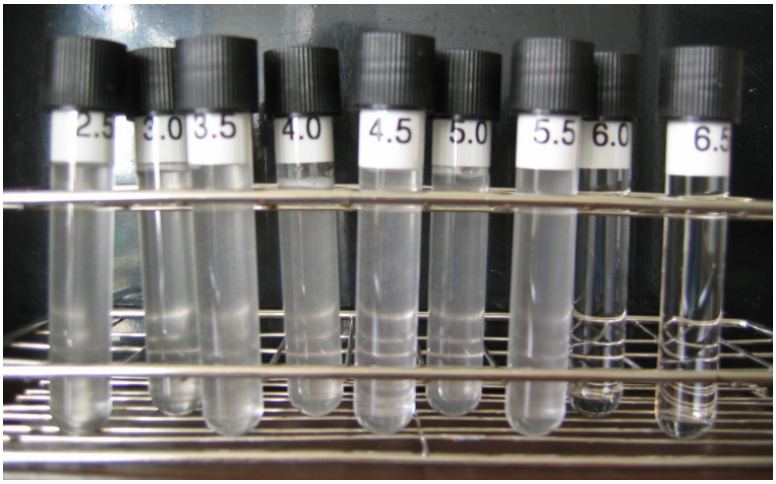

Figure 4: Array of R3 solutions at different pH values. Conditions: 0.65 g l^{-1} R3 concentration and room temperature

Ishigami et al. (1987) determined a pK_a-value of 5.6 for RA and RB (see Figure 1) by potentiometric titration. Furthermore, Lebron-Paler et al. (2006) found pK_a-values of 4.3 – 5.5 for a mixture of mono-rhamnolipids (mainly R1) by potentiometric and spectrochemical titrations. On the other hand, at the present no data concerning the pK_a-value of R3 were reported.

3.1.2 Critical micelle concentration (*cmc*)

At concentrations beyond the *cmc*, dissolved surfactant monomers are in equilibrium with micelles and the monomer concentration remains constant and equal to the *cmc* (Attwood and Florence 1983). The *cmc* value of a surfactant is often affected by the pH of the solution, ionic strength, temperature, presence of additives, etc. Under the assumption that an enzyme attack is only possible for monomers, the *cmc* value and its variation with process conditions should be taken into account for kinetic analysis. Table 2 summarized available data of *cmc* of purified RL under different conditions of pH and in the presence of the reaction products R1 and L-rhamnose at room temperature. A clearly decrease of *cmc* with pH is recognized for both R1 and R3. Moreover, at higher ionic strength a decrease of *cmc* is likewise observed whereas this effect was no longer observed under acidic conditions (Sanchez et al. 2007). The presence of L-rhamnose also tends to decrease the *cmc* of both RL and from mixture of R1 and R3. The monomer concentration of a surfactant is also affected by the presence of a second surfactant and under this situation the monomer concentration is no longer equals to its *cmc*. This situation applies during production of R1 from R3. This topic is treated in the "reaction kinetic modeling" section in chapter 4.2.

Table 2: *cmc* values of R3 and R1 at different conditions of pH, ionic strength and in the presence of L-rhamnose (Rha)

Surfactant	pH	C_{NaCl}* (M)	*cmc* (mM)	Reference
R3 ($Rha_2C_{10}C_{10}$)	acid	-	0.04-0.07	Parra et al. (1989), Ozdemir et al. (2004)
	neutral	-	0.15-0.3	Parra et al. (1989); Ozdemir et al. (2004)
	basic	-	0.3	Parra et al. (1989)
	neutral	0.5	0.08	Helvaci et al. (2004)
	neutral	1	0.04	Helvaci et al. (2004)
R1($Rha_1C_{10}C_{10}$)	acid	-	0.04-0.06	Parra et al. (1989); Ozdemir et al. (2004)
	neutral	-	0.08-0.1	Parra et al. (1989); Ozdemir et al. (2004)
	basic	-	0.08	Parra et al. (1989)
	neutral	0.5	0.05	Helvaci et al. (2004)
	neutral	1	0.04	Helvaci et al. (2004)
R3:R1= 1:1	neutral	-	0.15	Peker et al. (2003)
R3:Rha= 1:1	neutral	-	0.5	Peker et al. (2003)
R1:Rha= 1:1	neutral	-	0.7	Peker et al. (2003)
R3:R1:Rha=1:1:1	neutral	-	0.10	Peker et al. (2003)

* Concentration of sodium chloride in the system

3.1.3 Aggregate formation

At concentrations above the *cmc*, a surfactant undergoes aggregate formation. The size and type of these aggregates varies with concentration and temperature leading to the formation of liquid crystalline phases due to interaction of aggregates at high concentrations (see Figure 5).

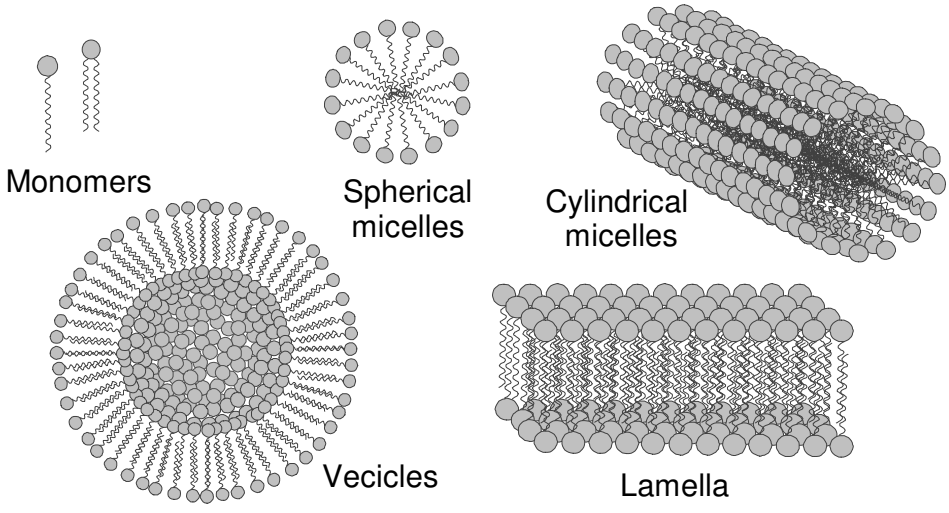

Figure 5: Aggregate formation of surfactant molecules in aqueous solution (Attwood and Florence 1983; Champion et al. 1995)

Many authors observed aggregate formation of RL (Ishigami et al. 1987; Champion et al. 1995; Peker et al. 2003; Helvaci et al. 2004; Ozdemir et al. 2004; Lebron-Paler et al.

2006; Sanchez et al. 2007). Variation of RL aggregates with pH was detected by Ishigami et al. (1987); Champion et al. (1995) and Lebron-Paler et al. (2006). Figure 6 shows effect of pH and of RL concentration on the morphology and size of RL aggregates detected by different authors. Ishigami et al. (1987) postulated a pH-sensitive conversion of molecular aggregates of RA and RB. RL aggregates become greater with decreasing pH and with increasing concentration. Variations in morphology with ionic strength and under the presence of L-rhamnose were also observed by Peker et al. (2003) and Helvaci et al. (2004).

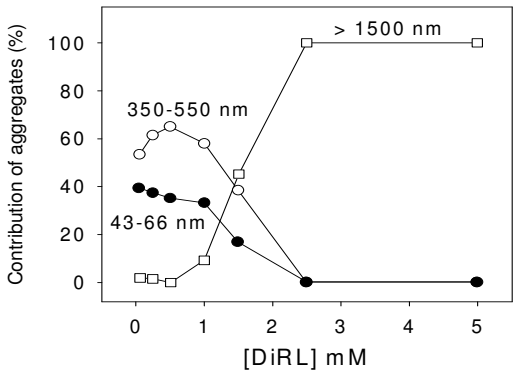

Contribution of aggregates of different sizes as function of di-rhamnolipid concentration. Conditions: pH 7.4 in 5 mM Hepes, 150 mM NaCl– 25°C (Sanchez et al. 2007)

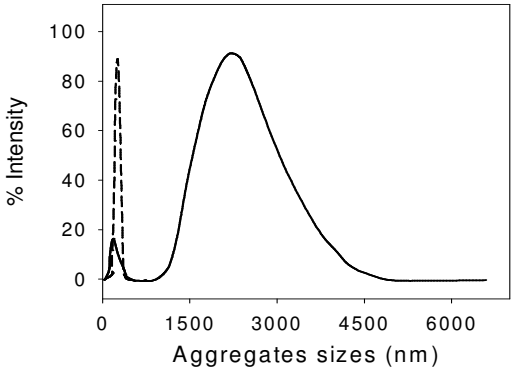

Mono-rhamnolipid aggregates sizes at pH 3.2 (full line) and pH 7.17 (dotted line). Conditions: 1 mM in deionised water at room temperature (Lebron-Paler et al. 2006)

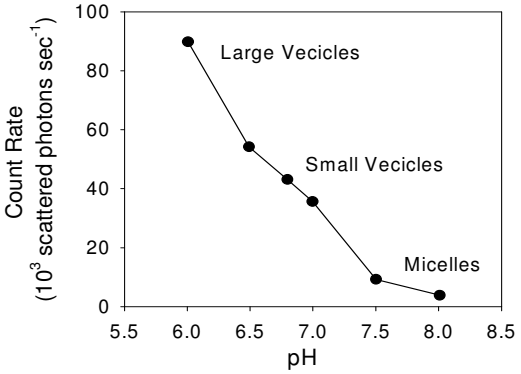

Effect of pH on rhamnolipid photon scattering intensity. Conditions: 1.5 µM monorhamnolipid in 0.01 mM Pipes buffer (Champion et al. 1995)

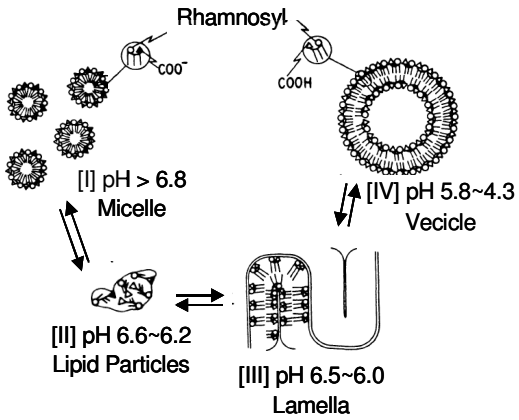

pH sensitive conversion of molecular aggregates of RA and RB (Ishigami et al. 1987)

Figure 6: Light scattering measurements of size and type of RL aggregates at different pH and RL concentration observed by different authors

3.1.4 Chemical stability

RL are very stabile molecules. The glycosidic bonds between L-rhamnose molecules and with the fatty acid portion can be cleaved by acidic hydrolysis at pH 0 – 3 and tem-

peratures of 120 – 150 °C (Syldatk 1984; Linhardt et al. 1989; Giani et al. 1993; Mixich et al. 1996). However, at these conditions the ester bond between both hydroxy-fatty acid chains is also cleaved. A basic hydrolysis of this last bond can be achieved in 0.5 M sodium hydroxide and 60°C (Syldatk 1984).

3.1.5 Sorption to solid surfaces

Surfactants also tend to adsorb to solid surfaces as *e.g.* on the walls of a container or on particulate matter present in the solution. This adsorption process involves a chemical interaction between adsorbent and solid matter such as ionic interaction, hydrogen bond formation or hydrophobic interactions through van der Wall's forces (Attwood and Florence 1983). Such a sorption process should be taken into account when the reaction is to be performed by enzyme immobilized to a solid carrier. Thus, these matrices may act also as adsorbents, where RL may adsorb on, mainly on hydrophobic polymers due to interactions with its fatty acid tails. Therefore, the kinetic of the reaction by immobilized enzyme may be affected by RL sorption.

In view of a promising downstream processing after microbial production, studies of RL sorption on polystyrene resins (XAD-2) showed that 50 - 60 mg RL per g of resin could be adsorbed and that this capacity is not affected by the pH of the system (Reiling et al. 1986; Matulovic 1987). Li et al. (2006) could absorb 15 mg RL per g of a sucrose/silica adsorbent. Since RL can be used as washing agent for enhanced removal of metal and organic contaminants from soils, there are studies on RL sorption on soil matrices of different compositions (Noordman et al. 2000; Ochoa-Loza et al. 2007). Noordman et al. (2000) observed that the more hydrophobic RL components were preferentially adsorbed and also suggested that adsorption of RL to soil is not a partitioning process but mainly an interfacial adsorption process.

3.1.6 Foaming properties

Foam formation in liquid systems makes difficult its handling. Foam formation is caused due to the elasticity of the foam film, which is inversely proportional to the compressibility of the film monolayer: the more elastic the film, the easier the foam formation. The foam properties of RL were investigated by Peker et al. (2003) and Ozdemir et al. (2004). They found that 1) The rate of foam formation increases with RL concentration; 2) Foam volume decreases with pH of the bulk solution; 3) Foam stability was greater at lower pH-values and; 4) The presence of L-rhamnose decreases foam rate formation.

3.2 The Biocatalyst: α-L-Rhamnosidase

α-L-rhamnosidases (EC. 3.2.1.40) catalyze the hydrolysis of terminal non-reducing α-L-rhamnose residues from polysaccharides and glycosides. α-L-rhamnose is widely distributed in plants and bacteria as a component of the polysaccharides of cell walls and of various bioactive products as aroma and flavors compounds *e.g.* terpenol glycosides of wine and flavonoid glycosides in citrus (Monti et al. 2004). Therefore, α-L-rhamnosidases are produced by a number of mammalian tissues, plants, bacteria and fungi. Bacterial α-L-rhamnosidases were purified and characterized from *Bacillus* sp. (Hashimoto et al. 1999), *Clostridium stercorarium* (Zverlov et al. 2000), *Pseudomonas paucimobilis* (Miake et al. 2000) and *Sphingomonas* sp. (Hashimoto and Murata 1998). Moreover, α-L-rhamnosidase was also purified from the cell extract of the yeast *Pichia angusta* (Yanai and Sato 2000). As demonstrated in screening works reported by Monti et al. (2004) and by Scaroni et al. (2002) several fungi are capable of producing α-L-rhamnosidase under the addition of proper inducers as α-L-rhamnose, Naringin, Hesperidin or Rutin. However, purification and characterization of this enzyme were mainly carried out from cultures of *Aspergillus* sp. (Mutter et al. 1994; Manzanares et al. 1997; Manzanares et al. 2000; Gallego et al. 2001; Manzanares et al. 2001) and *Penicillium* sp. (Meiwess et al. 1994; Norouzian et al. 1999; Mamma et al. 2004). Meiwess et al. (1994) patented the production and purification of α-L-rhamnosidase from *Penicillium* sp. DSM 6825 and DSM 6826 with ester derivates of rhamnolipid 2 as inducers. Seven different α-L-rhamnosidases have been cloned and expressed: two from *Aspergillus aculeatus* (Manzanares et al. 2003), two from *Bacillus* sp. GL1 (Hashimoto et al. 2003), one from *Clostridium stercorarium* (Zverlov et al. 2000) and one from a thermophilic bacterium PRI-1686 (Birgisson et al. 2004). Moreover, the last two recombinant α-L-rhamnosidases are thermostable.

The fungal α-L-rhamnosidase is an extracellular enzyme often expressed together with β-glucosidase activity (EC 3.2.1.21) forming the enzyme complex called Naringinase (Dunlap et al. 1962; Young et al. 1989; Puri and Banerjee 2000). Puri and Banerjee (2000) reviewed the main properties of this enzyme complex. Historically, its production and major application was targeted for the debittering of citrus juices. Indeed, α-L-rhamnosidase converts the bitter glycoside Naringin to the less bitter Prunin by cleavage of an alpha-(1->2) bond between L-rhamnose and glucose. Subsequent hydrolysis of glucose from Prunin by the β-glucosidase portion yields finally the aglycone Naringenin. The α-L-rhamnosidase activity of Naringinase finds further applications in the production of the antiviral active Prunin, for aroma enhancement of wine, in steroid transformation, in the structural study of bacterial polysaccharides and also in the production of L-rhamnose from glycosides (Cheetham and Quail 1991; Puri and Banerjee 2000).

Despite of its industrial interest, the commercial availability of the α-L-rhamnosidase is limited. Technical crude lyophilized preparations are obtained from Sigma Aldrich under the trade name Naringinase and Hesperidinase from *Penicillium decumbens* and *Aspergillus niger*, respectively. A much more purified enzyme preparation from *Penicillium sp.* is also available. α-L-rhamnosidase as a side activity is also found in plant-structural-material-degrading enzyme preparations (Cheetham and Quail 1991).

Trummler et al. (2003) found that the crude Naringinase from Sigma Aldrich could hydrolyze R3 quantitatively; however, the recombinant thermostable α-L-rhamnosidase from *Clostridium stercorarium* did not. Moreover, bacterial α-L-rhamnosidases are often intracellular enzymes which are more difficult to recover and much less stable than the extracellular fungal enzymes. Taken into account these observations the present optimization study was restricted to the use of commercially available fungal α-L-rhamnosidases. Since rhamnolipid activity was detected only with *Penicillium* α-L-rhamnosidases (see Appendix 7.1), most of the work was carried out with the α-L-rhamnosidase from *Penicillium decumbens*. Therefore, relevant biochemical properties of this specific α-L-rhamnosidase will be briefly described here.

3.2.1 Biochemical characterization

Penicillium decumbens α-L-rhamnosidase is a glycoprotein with 50 % glycosidation grade and a molecular weight of 90 kDa. It shows optimal activity at pH 3.5 - 4.5 and 57 °C and its activity is dependent of the ionic strength of the solution (Romero et al. 1985; Young et al. 1989). Gabor and Pittner (1984) reported that this enzyme tend to oligomerization and also to self-digestion with loss of 160-170 mol glucose per mol of enzyme. In this state, the enzyme losses 25 % of its initial activity and is less stable than the original state. It also showed a not-clear isoelectric point at a pH value of about 5.0. By exclusion chromatography Schalkhammer and Pittner (1986) observed a dependency of molecular weight with pH of the buffer. Chemical modification of the active site region supported the idea that tyrosine is essential for activity (Schalkhammer and Pittner 1986). The amino acid composition of the peptides was analyzed (Young et al. 1989) however its primary structure is not known. Young et al. (1989) purified a commercial enzyme preparation by application in a Mono Q column. They observed activity elution in two peaks being the second peak the major and coming together with the ß-glucosidase portion. Gunata et al. (1988) separated both activities by chromatofocusing. They also observed isoenzymes of rhamnosidases eluting at pH 6.2 and 5.7.

3.2.2 Substrate specificity

Michon et al. (1989) demonstrated that Naringinase is an exoglyconase specific to α-L-rhamnopyranosyl linkages from glycosides independently of the point of attachment of

their interglycosidic linkages. It rapidly hydrolyses glycosidic linkages between two sugar moieties whereas it also cleaves this bond between L-rhamnose and an aglycone moiety. Thus, Naringinase proves to be active against Naringin, p-nitrophenyl-α-L-rhamnoside (pnpR), and a number of naturally occurring glycosides (Romero et al. 1985; Turecek and Pittner 1986). Rhamnosidases of *Penicllium* sp. DSM 6825 and DSM 6826 showed inverse substrate specificity compared with the *Penicillium decumbens* rhamnosidase since it was more active against the cleavage of L-rhamnose from R1 than from R3 (Meiwes et al. 1997).

3.2.3 Stability

Naringinase is a rather stable enzyme showing less than 25 % decrease in activity at 60°C after 15 minutes incubation at acidic pH (Tsen et al. 1989). In contrast to the other fungal α-L-rhamnosidases, less information is published about its pH stability profiles and deactivation kinetics of the free form. Most studies deal with stabilities in immobilized state (Manjon et al. 1985; Tsen et al. 1989; Ellenrieder and Daz 1996). Ellenrieder and Daz (1996) observed increasing stability at higher Naringinase concentrations. They also achieved thermo-stabilization by cross-linking modification with glutaraldehyde and by addition of bovine serum albumin.

3.2.4 Inhibitors

L-Rhamnose and glucose are competitive inhibitors of the rhamnosidase activity of Naringinase (Romero et al. 1985). Metal ions as Ca^{+2}, Zn^{+2}, and Mg^{+2} inhibited activity whereas Mn^{+2} causes a 30 % increase in activity of a partial purified enzyme of *Penicillium decumbens* PTCC 5248 (Norouzian et al. 1999). On the other hand, Naringinase proved to be active in the presence of organic solvents as chloroform, cyclohexane, and ethyl acetate as well as with several alcohols as methanol, ethanol and propanol (Turecek and Pittner 1986; Martearena et al. 2003). Ionic surfactants are known to denature enzymes by disturbing the forces that maintain the delicate protein structure. Naringinase demonstrated to be active against the biosurfactants R3 and R1 (Trummler et al. 2003), however damaging effects with time were not investigated.

3.3 Biocatalyst Immobilization

Immobilized enzymes are enzymes with artificially restricted mobility by fixation to or within a solid material (Chaplin and Bucke 1990; Tischer 1995). Enzyme immobilization is often applied to improve the space-time-yield of an enzymatic process. Immobilized-enzyme catalyzed reaction applied to the modification of RL may be advantageous in the following aspects:

- Enzyme re-use: This is often essential for the economics of the process. When the enzyme is fixed to a solid carrier, it becomes insoluble and therewith easier to separate from solution allowing its re-use and preventing it from contaminating the product (Chaplin and Bucke 1990). On the other hand, an alternative efficient approach for enzyme re-use with soluble enzymes is the use of membrane reactors. By passing the reaction medium through nanopores-membranes soluble enzymes are retained inside the reactor due to its greater sizes compared to the reaction products. However, for modification of RL this approach would be not practicable since the large RL aggregates (40 – 4500 nm) are greater than the enzyme molecules (~ 17 nm).
- Facilitating downstream processing: The reaction product L-rhamnose can in this way easier be recovered from the aqueous phase without contaminating soluble enzyme.
- Possibility of continuous mode operation: by *e.*g. use of a reactor column with immobilized enzyme (plug-flow-reactor, PFR) or use of a continuous stirred-tank reactor (CSTR).

Enzyme stability may be highly enhanced by immobilization and often is the main reason of applying this approach in an enzymatic process (Chaplin and Bucke 1990; Tischer 1995). However, Naringinase is an already rather stable enzyme and therefore this property is not pursuit as being a crucial advantage.

3.3.1 Methods of enzyme immobilization

There are many well-tested methods of immobilizing enzymes. In Figure 7 these methods are schematically presented and classified by the type of interaction between enzyme and carrier. Covalent binding means that enzymes can be covalently ***attached*** to a solid carrier, be chemically ***incorporated*** to a polymeric network or simply ***cross-linked*** each other or with foreign proteins forming insoluble aggregates. Adsorptive binding means a non-covalent attachment of the enzyme to a solid carrier by electrostatic ***ionic adsorption***, hydrophobic or polar induced ***adsorption*** or being chelated through ***metal binding***. Finally, enzymes can be immobilized by physical methods, and so they can be ***entrapped*** into a ***gel matrix***, ***microcapsules*** or pre-formed devices such as ***membranes*** (Tischer 1995). There are also combined methods in which *e.g.* enzyme adsorption to a matrix followed by enzyme cross-linking or enzyme entrapment to a gel matrix combined with covalent attachment to it (Tischer 1995). Table 3 listed some advantages and disadvantages of these methods. The matrix should be grafted with specific functional groups for obtaining the desirable enzyme attachment. Thus, matrices with *e.g.* anionic (CM-, carboxymethyl) or cationic (DEAE-, diethylaminoethyl) groups are applied for ionic enzyme adsorption whereas matrices with *e.g.* amino, carboxyl, aldehyde, or e-

poxy groups are used for covalent enzyme binding. Indeed, functional groups of the protein as amino, carboxyl, hydroxyl, or sulphidryl groups form a bond with the functional group of the matrix. Common amino-acid residues relevant for immobilization are lysine, arginine, histidine, aspartate, glutamate, tyrosine, serine and threonine and cysteine. They have to be exposed at the protein surface for reaction. Some functional groups need to be further activated for enabling reaction as *e.g.* amino groups with glutaraldehyde or carboxy groups with carbodiimide. An enormous number of matrices and coupling reactions and activation methods are described in the literature (Tischer 1995; Buchholz and Kasche 1997).

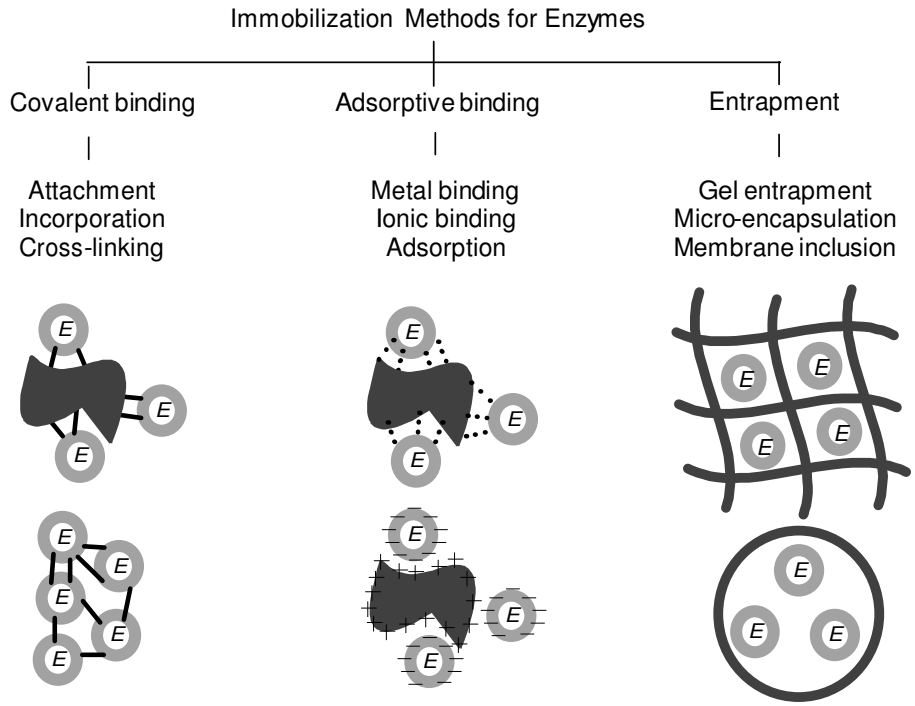

Figure 7: Different enzyme immobilization methods (Chaplin and Bucke 1990; Tischer 1995)

Table 3: Generalized comparison of different enzyme immobilization techniques (Chaplin and Bucke 1990)

Characteristic	Adsorption	Covalent binding	Entrapment	Membrane confinement
Preparation	Simple	Difficult	Difficult	Simple
Cost	Low	High	Moderate	High
Binding force	Variable	Strong	Weak	Strong
Enzyme leakage	Yes	No	Yes	No
Applicability	Wide	Selective	Wide	Very wide
Running Problems	High	Low	High	High
Matrix effects	Yes	Yes	Yes	No
Large diffusional barriers	No	No	Yes	Yes
Microbial protection	No	No	Yes	Yes

Table 4: Properties of matrices relevant for enzyme immobilization (Buchholz et al. 2005)

Properties	***Desired***
Chemical	
• Hydrophilicity/ Hydrophobicity	
• Swelling properties	Low
• Chemical stability	High
• Microbial stability	Good
Morphological	
• Particle diameter, particle distribution	0.2 - 1 mm / narrow distribution
• Pore size	30 – 60 nm
• Surface for adsorption/compressibility	Large
Mechanical	
• Resistance to pressure/compressibility	Good/low
• Elasticity	Sufficient (no abrasion by stirrer)
General	Food grade (application in food manufacture) Low cost

Table 4 summarized the main properties of matrices to be considered for enzyme immobilization. An optimal carrier material should offer a high surface area for immobilization, have a high density of functional groups, be not damaging for the enzyme upon adsorption and/or covalent binding, and be mechanical and chemical stable under process conditions. Morphologically, enzyme carriers are often spherical particles of porous or non-porous matrices. Porous matrices offers higher surfaces areas for immobilization but substrate diffusion inside the pores may limit the efficiency of an enzymatic reaction whereas non-porous particles are commonly free of substrate diffusion limitations, however having less surface area available for immobilization. The nature of the carrier materials can be classified as (Buchholz et al. 2005):

- Inorganic materials such as silica, alumina, zeolites and porous glass. They are characterized by high pressure stability.
- Organic natural materials such as agarose, cellulose, chitin, and dextrans. They are characterized by favorable compatibility with proteins but less chemical stability.
- Organic synthetic materials: polymers and derivates of acrylamide, methycrylate, polystyrene and polyvinylalcohols. They are characterized by high chemical stability but they may be damaging upon enzyme adsorption due to high hydrophobicity of the matrix.

Special classes of synthetic materials are magnetic materials in which the magnetic properties of the carrier facilitate their handling for separation from the reaction medium. The magnetic material (*e.g.* Fe_3O_4) is combined with a non-magnetic material in the following arrangements: 1) A magnetic core coated with a natural or synthetic

polymer or an inorganic material; 2) Encapsulation of magnetic solids within natural gels or synthetic polymers; and 3) Infiltration of porous matrices with fine magnetic sub-micron particles or aqueous mixtures ions capable of forming magnetic ferrites (Bozhinova 2004).

3.3.2 Naringinase immobilization

Table 5 lists reported immobilization methods successfully applied to the Naringinase preparation of *Penicillium decumbens*. About 9 covalent binding methods, 2 entrapment methods and 1 adsorption method were tested on different carrier types and morphologies. The results are difficult to compare since immobilized activities were assayed at different conditions with different substrates like p-nitrophenyl-rhamnoside (pnpR), Naringin or Rutin. None immobilized preparation was tested with rhamnolipids as substrate. The interest of immobilized Naringinase was rather targeted to its use in columns for juice debittering (Manjon et al. 1985; Tsen et al. 1989; Puri et al. 1996; Soares and Hotchkiss 1998; Puri et al. 2001; Sekeroglu et al. 2006), to increase heat stability (Ellenrieder and Daz 1996) or for its use in the preparation of Rutin and aglycones from naturally occurring glycosides (Roitner et al. 1984; Turecek and Pittner 1986).

In most cases high protein and activity yields were obtained and improved heat stability was also detected. Manjon et al. (1985) characterized the hydrolysis kinetics of the model substrate pnpR with glycophase-controlled pore glass derivates and detected internal diffutional limitations. Moreover, they performed plug-flow reactor modeling for simulation of substrate conversion with residence time and validated the model with experimental data (Manjon et al. 1987). However, this method is rather laborious and expensive. On the contrary, inexpensive and simple methods resulted also in high activity yields like covalent attachment to hen-egg-white beads or the entrapment into alginate beads (Puri et al. 1996; Puri et al. 2001).

3.3.3 Carrier and coupling methods

In order to select the optimal immobilized biocatalyst for a specific application comparative studies with the same enzyme immobilized on different supports can provide important information on the properties of the supports that are important to improve the process (Buchholz et al. 2005). Therefore, within the scope of this work different carrier materials and coupling methods were applied. A brief overview of every tested support-type will be described in the next sub-sections.

Table 5: Reported immobilization of Naringinase from *Penicillium decumbens*

Carrier type	Carrier morphology	Method	Binding properties	Substrate	Stability	Reference
Amine functionalized silane-coated CPG **	100-200 mesh particles 253 Å mean pore diameter	covalent binding by activation with glutaraldehyde	3.4 mg/g_{wet} *** 2.8 U/g_{wet}	Naringin	-	(Roitner et al. 1984)
		covalent binding by pyridine-aldehyde and CNBr-activation	7.0 mg/g_{wet} *** 12.5 nkat/$mg_{protein}$	pnpR *	stable for months	(Turecek and Pittner 1986)
Glyco-phase CPG **	200-400 mesh particles 40, 100, 200, and 460 Å mean pore diameter	covalent binding by diazo coupling to arylamine derivate beads	14.3 mg/g_{dry} *** 127.7 U/g_{dry} (data with 460 Å pore diameter)	pnpR *	> 192 hs operation in column reactor	(Manjon et al. 1985)
Cellulose triacetate and cellulose acetate	fibers films (juice packaging films)	entrapment	40 % activity yield 60-90 % protein yield	pnpR * Naringin	improved stability	(Tsen et al. 1989; Soares and Hotchkiss 1998)
Silane coated magnetic beads	15 – 36 µm particles 100 Å mean pore diameter	covalent binding by activation with epoxy, aldehyde and carboxyl groups	~ 20 mg/g *** best, aldehyde method	Rutin Naringin	60 % activity after 320 h	(Dreker 1998)
-	-	cross-linking with glutaraldehyde	70 % activity of the native enzyme	pnpR *	improved stability	(Ellenrieder and Daz 1996)
Protein rich support	keratine, collagen and fibroin fibers pre-treated with papain	covalent binding by activation with glutaraldehyde	Best activity yield: keratine support Best protein yield collagen	pnpR *	improved stability	(Ellenrieder and Daz 1996)
Seeds of *Ocimum-basilicum*	-	Covalent binding through ethyl-enediamine arms	92 % protein yield 57 % activity yield	Naringin	50 % activity after 7 days	(Norouzian et al. 1999)
Hen-egg white beads	cross-linked with glutaral-dehyde	covalent binding by activation with glutaraldehyde	70 % protein yield 140 % activity yield	Naringin	-	(Norouzian et al. 1999; Puri et al. 2001)
Calcium alginate beads	2% alginate (gave highest activity)	entrapment	80 % protein yield 72 % activity yield No enzyme leaching	Naringin	half-life upon 12 use-cycles	(Puri et al. 1996; Norouzian et al. 1999)
Celite beads	~ 10 µm mean particle diameter	adsorption	83% activity yield	Naringin	68 % activity in 2nd cycle	(Sekeroglu et al. 2006)

* pnpR: p-nitro-phenyl-rhamnoside
** CPG: controlled pore glass
*** mg/g: protein to carrier mass ratio

3.3.3.1 Micro-non-porous magnetic beads (M-PVA)

For a non-porous material, the particles need to be rather small for offering a great specific surface area available for immobilization. However, difficulties to remove small particles from the reaction solution and to run a continuous process occur (Bozhinova 2004). For enhancing the handling, small non-porous particles with magnetic properties

may be a good choice. Magnetic carrier technology offers a novel and convenient way to selectively separate the magnetic matrix with immobilized enzyme from the reaction system (Bozhinova 2004). The carrier-supplier Chemagen AG offers magnetic beads of 1 - 3 µm consisting of a matrix of polyvinyl alcohol, which is subsequently aminated using an eight-atom spacer (supplier information). Moreover, due to its superparamagnetic nature the typical aggregation tendency of magnetic materials due to remanent magnetism is completely avoided (Bozhinova 2004).

The main applications of M-PVA are laboratory scale separations of diverse biological materials such as DNA, RNA, proteins, and cells. Despite the common use of magnetic adsorbent particles in laboratory bioseparation the technique is not available for larger scales by now. Franzreb et al. (2006) have summarized the current state of development of magnetic adsorbent particles for protein separation. Polymer coated micro-non-porous and porous magnetic beads have been studied as carrier materials for enzyme immobilization (Pieters and Bardeletti 1992; Bahar and Celebi 1999; Shimomura et al. 1999; Guo and Sun 2004; Liu et al. 2005; Qiu et al. 2005; Wang et al. 2007). However, in few cases performance comparisons of magnetic micro-beads with non-magnetic carrier are reported (Bilkova et al. 2002; Bozhinova et al. 2004).

In this work non-porous magnetic beads (M-PVA) were applied for Naringinase immobilization through two different coupling mechanisms, the glutaraldehyde method and the carbodiimide method. Figure 8 describes the coupling reactions.

3.3.3.2 Methacrylate beads

Methacrylate beads are widely applied enzyme supports known under the trade name Eupergit®. This is a copolymer of methacrylamide, N,N'-methylene-bis-(methacrylamide), and two monomers containing oxirane groups (Degussa Röhm Pharma polymers, basic information). They possess a sophisticated porous structure consisting of relatively large cavities and channels constructed from a network of small micro-beads (Bozhinova 2004). Two different types were tested, Eupergit C and Eupergit 250 L differing on its porous sizes and having similar bead sizes around 190 – 170 µm. Figure 9 shows an electro scanning micrograph of the structure of Eupergit 250 L. The coupling reaction for enzyme binding is shown in Figure 8.

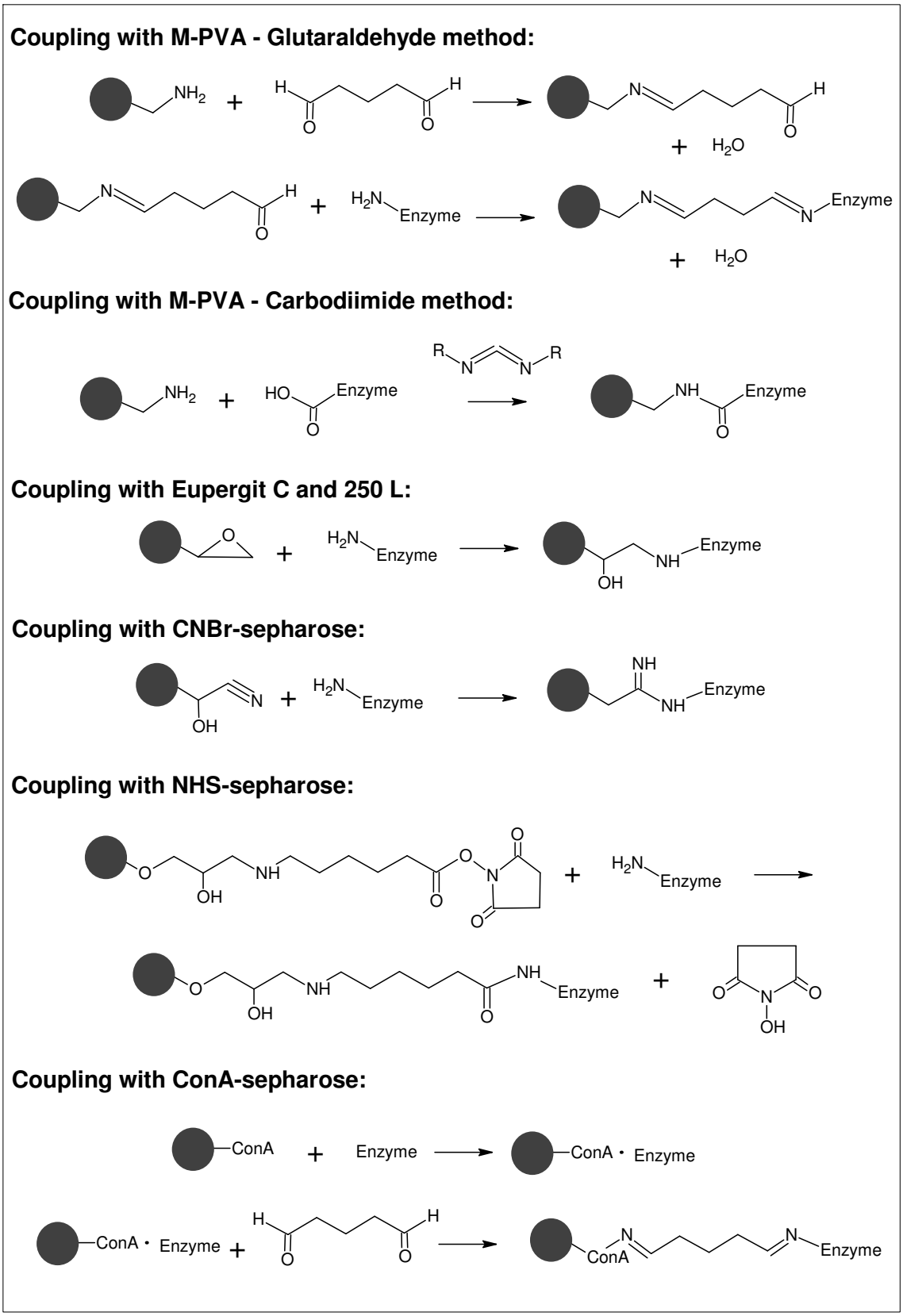

Figure 8: Coupling reactions with the different tested carrier materials

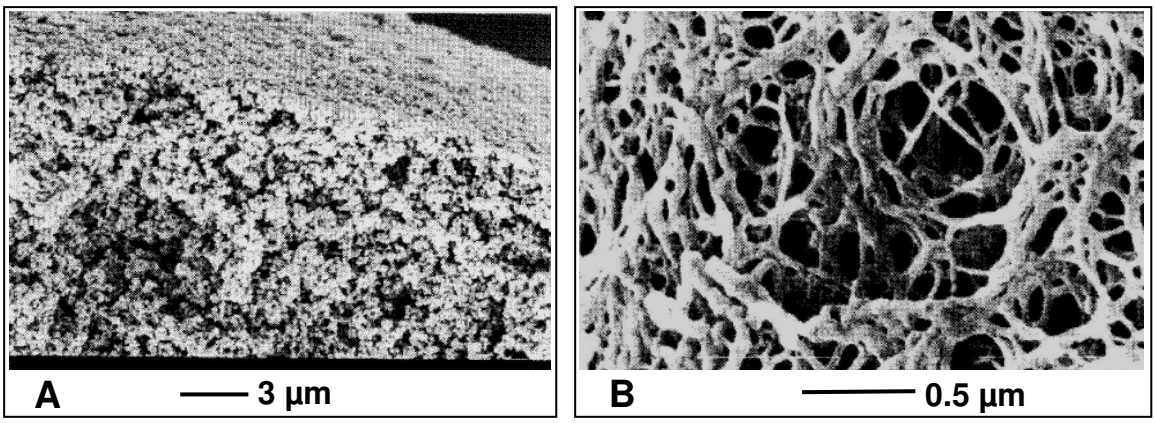

Figure 9: Scanning electron microscopy pictures of Eupergit 250L (A) and of the porous network of a 2 % agarose gel (B) (Buchholz et al. 2005).

3.3.3.3 Sepharose beads

They are enzyme-purification-chromatographic material widely applied also as immobilization supports and known under the trade name Sepharore. They are composed of agarose, a linear polysaccharide consisting of alternating residues of ß-D-galactose and 3,6-anhydro-alpha-L-galactose. The polysaccharides are organized as single fibers spun into a yarn of fibers, forming a remarkable network of pentagonal pores (Bozhinova 2004). Figure 9 shows the structure of a 2 % agarose gel. Sepharose beads are available in a number of different functionalities from protein ionic binding, non-specific covalent binding to affinity techniques for special target proteins. Following coupling methods were tested for Naringinase immobilization:

- Anionic binding with diethylaminoethyl functionalized Sepharose beads (***DEAE-Sepharose***). They consist of 4 % agarose beads of 90 µm diameter. This is a mild and simple method for achieving immobilization enabling bead regeneration after enzyme deactivation whereas it is not specific and enzyme leaching may occur. This method was successfully applied for Naringinase from *Aspergillus niger* on DEAE-sephadex A-25 (Ono et al. 1977).

- Covalent binding with cyanogen bromide activated Sepharose beads (***CNBr-Sepharose***). They consist of 4 % agarose beads of 90 µm diameter. Cyanogen reacts with hydroxyl groups on Sepahrose to form reactive cyanate ester groups. It is a simple and rapid method for covalent immobilization whereas non-specific (Amersham-Biosciences 2002). Figure 8 shows the coupling reaction.

- Covalent binding with N-hydroxysuccinimide activated Sepharose beads (***NHS-Sepharose***). They consist of 6 % high cross linked agarose beads of 34 µm diameter. In comparison with CNBr-Sepharose this bead type may reduce possible negative matrix effect with the enzyme since they possesses a 10-atom spacer groups

between enzyme and support. Figure 8 shows the structure of the spacer arm and the coupling reaction.

- Specific adsorption and cross-linking on Concanavalin-A (ConA) coupled to Sepharose by the cyanogen bromide method (***ConA-Sepharose***). They consist of 4 % agarose beads of 90 µm diameter with precoupled Concanavalin-A in a density of 10 – 16 mg ConA per ml drained medium. Con A is a tetrameric metalloprotein isolated from jack beans (*Canavalia ensiformis*) that binds molecules containing α-D-mannopyranosyl, α-D-glucopyranosyl and sterically related residues. ***ConA-Sepharose*** is used for purification of glycoproteins, polysaccharides and glycolipids (Amersham Biosciences, product information). Saleemuddin and Husain (1991) reviewed glycoprotein immobilization reported on ConA coupled matrices. Since the commercial enzyme preparation is rather impure, foreign proteins may also be immobilized thus affecting the specific activity of the biocatalysts. Thus, high specific immobilization of the glycoprotein Naringinase may be achieved by this method. Figure 8 shows the coupling reaction.

3.3.3.4 Calcium alginate entrapment

This simple and inexpensive calcium alginate entrapment method was also tested since literature data reported that Naringinase entrapped in alginate beads was stable without showing enzyme leaching (Puri et al. 1996).

3.3.4 Carrier selection and characterization

The characterization of immobilized biocatalysts should involve (Buchholz et al. 2005):

- Physical and chemical characterization: particle shape and radius, pores sizes, surface area, swelling, compressibility in columns or abrasion in stirred vessels.
- Immobilization protocol: method and detailed reaction conditions, immobilization yield, enzyme leakage
- Kinetic characterization: initial rate activity measurements, determination of intrinsic properties of the immobilized enzyme, description of substrate diffusional effects, substrate partition effects, space-time-yield at process conditions
- Stability determinations: operational and storage stability and productivity (space-time-yield integrated over the time the biocatalyst is used)

In this work the selection of a suitable enzyme carrier for the conversion of RL was mainly based on the kinetic characterization of every carrier. High coupled activities and at the same time high activity yields were always aimed. On a first stage, initial rate activities against rhamnolipid conversion and also against the model substrate p-nitro-

phenyl-rhamnoside were measured for all carriers. After selecting the most-promising carrier materials (see section 4.3) the immobilization protocol for each method was optimized by varying the mass ratio protein to carrier (see sections 4.3 and 4.4). Special care was focused on the description of substrate diffusional effects for the interpretation of immobilized activity data (see section 4.4). An estimation of the intrinsic activity of the immobilized enzyme on the different supports was also possible.

Following aspects were studied:

3.3.4.1 Mass transfer phenomena

When substrate diffusion is much lower than the enzymatic reaction, diffusion becomes a rate-limiting process in an immobilized biocatalyst catalyzed process. Substrate molecules must diffuse through the surrounding layer of the particle (external transport) in order to reach the catalytic surface and be converted to product. In order for the entire enzyme amount to be utilized, substrate must also diffuse within the pores in the surface of the immobilized enzyme particle (internal transport). Figure 10 show the substrate and products profiles that may occur under diffusion limitations (Chaplin and Bucke 1990).

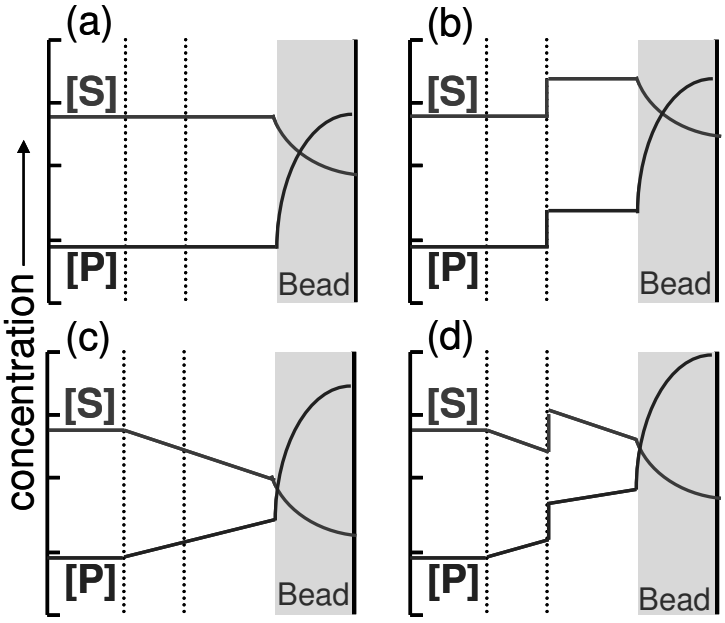

Figure 10: Schematic diagram showing the concentration gradients of substrate [S] and product [P]. (a) concentration gradient due to reaction and internal diffusion; (b) as (a) but with additional concentration gradients due to partitioning effects; (c) as (a) but with an additional concentration gradients due to external diffusion; (d) concentration gradients due to the combined effects of partition and diffusion (modified from Chaplin and Bucke 1990)

The extension of internal diffusion limitation increases with particle radius, high intrinsic enzyme activity, and high protein loading whereas decreases with pores diameters

and low reaction temperatures. The extension of diffusion limitation can be estimated by the effectiveness factor, which is a ratio between the actual reaction rate and the reaction rate without diffusion effects. Mass transfer limitations may be even more pronounced when the substrate concentration in the bulk solution is low due to a low concentration gradient as driving force for diffusion. This situation may apply in case of the aggregates-building RL, where monomers at a concentration as low as its *cmc* value (0.04 – 0.15 mM) remain in solution. Therefore, for overcoming diffusion limitation, the use of non-porous particles or porous particles with big pores (> 100 nm) may be advantageous.

3.3.4.2 Matrix and coupling effects

The interaction of the matrix may alter the protein structure irreversible leading to activity lost. Enzyme bound in a non-productive mode due to the inaccessibility of the active site and distortion of the active site producing an inactive immobilized enzyme may also occur (Chaplin and Bucke 1990). The coupling method may also involve amino acid rests of the active site, thus making them inaccessible for enzyme attack. For interpretation of observed immobilized activities also the nature of the substrate is important. Surface active molecules like RL will adsorb on the matrix and/or partition into the microenvironment of the enzyme. Partition causes changes in the local concentration of the molecules which, in turn, affects the apparent kinetic constants of the enzyme (Chaplin and Bucke 1990). Different matrix materials (*e.g.* hydrophobic like Eupergit and hydrophilic like Sepharose) and also different coupling methods may distantly affect intrinsic activities and may help to find the optimal biocatalyst.

4 Publications and Manuscripts

This PhD. thesis is based on the following publications and manuscripts, which are specified in detail in the following sections (4.1 – 4.4):

1. Running Title: Stability of α-L-rhamnosidase from *Penicillium decumbens*

Magario, I.; Neumann, A.; Oliveros, E.; Syldatk, C. Deactivation kinetics and response surface analysis of the stability of α-L-rhamnosidase from *Penicillium decumbens*

(In press, to appear in: *Applied Biochemistry and Biotechnology*, DOI: 10.1007/s12010-008-8204-5)

This article describes: 1) stability data on the α-L-rhamnosidase from *Penicillium decumbens* and its variation with pH, temperature and enzyme concentration; 2) The description of experimental residual activities by a series-type deactivation mechanism; and 3) A set-up of a response surface model for prediction of stability values required for the selection of reaction conditions for di-rhamnolipid conversion into mono-rhamnolipid.

2. Running Title: Kinetic analysis of a di-rhamnolipid bioconversion

Magario, I.; Vielhauer, O.; Neumann, A.; Hausmann, R.; Syldatk, C. (2009) Kinetic analysis and modeling of a liquid-liquid conversion of di-rhamnolipids by Naringinase from *Penicillium decumbens*. *Biotechnology and Bioengineering*, 102 (1): 9-19. DOI: 10.1002/bit.22057

This manuscript specifies a mathematic description of the kinetics of di- and mono-rhamnolipid conversion by free α-L-rhamnosidase from *Penicillium decumbens*. The effect of pH, temperature and co-solvent addition on di-rhamnolipid conversion rates is also described. For the kinetic analysis, substrate transfer from the micelle to the aqueous phase for its subsequent decomposition by the enzyme was postulated.

3. Running Title: Enzyme carrier evaluation for conversion of di-rhamnolipid

Magario, I.; Neumann, A.; Syldatk, C.; Vielhauer, O.; Hausmann, R. Evaluation of enzyme carriers as biocatalysts for the conversion of emulsified di-rhamnolipid

(Submitted)

This manuscript presents results regarding: 1) Activity coupling, activity yield and stability of α-L-rhamnosidase immobilization on porous and non-porous supports through different coupling reactions; and 2) Optimization of coupling conditions on a non-porous type support by response surface methodology.

4. Running Title: Non-porous micro-carriers for a diffusion rate-controlled enzymatic conversion

Magario I.; Ma X.; Neumann A.; Syldatk C.; Hausmann R. (2008) Non-porous magnetic micro particles: Comparison to porous enzyme carriers for a diffusion rate-controlled enzymatic conversion. *Journal of Biotechnology* 134: 72-78. DOI:10.1016/j.jbiotec.2007.12.001

This article describes the kinetic analysis of initial reaction rates of the conversion of di-rhamnolipid into mono-rhamnolipid by immobilized α-L-rhamnosidase on porous and non-porous supports. This analysis is based on the estimation of the effectiveness factor of the immobilized enzyme at different protein loaded preparations considering substrate transfer and enzymatic reaction.

4.1 Stability of α-L-Rhamnosidase from *Penicillium decumbens*

DEACTIVATION KINETICS AND RESPONSE SURFACE ANALYSIS OF THE STABILITY OF ALPHA-L-RHAMNOSIDASE FROM *PENICILLIUM DECUMBENS*

In press, to appear in:

Applied Biochemistry and Biotechnology

DOI: 10.1007/s12010-008-8204-5

I. Magario *, A. Neumann, E. Oliveros [a],C. Syldatk

Institute of Engineering in Life Sciences, Chair of Technical Biology, University of Karlsruhe (TH), Germany

[a] Lehrstuhl für Umweltmesstechnik, Engler-Bunte-Institut, Universität Karlsruhe.

Current address: Laboratoire des IMRCP, UMR CNRS 5623, Université Paul Sabatier

* Corresponding author: I. Magario
Tel: +49-721-608-6736/8428
Fax: +49-721-608-4881
E-mail: Ivana.Magario@tebi.uni-karlsruhe.de

Key words: Naringinase; Doehlert array; response surface methodology; series-type deactivation kinetics; α-rhamnosidase, enzyme stability

Abstract

The stability of the mixed enzyme preparation Naringinase from *Penicillium decumbens* was studied in dependence of the temperature, the pH value and the enzyme concentration by means of response surface methodology. Deactivation kinetics by formation of an intermediate state was proposed for fitting deactivation data. Empirical models could then be constructed for prediction of deactivation rate constants, specific activity of intermediate state and half-life values under different incubation conditions. From this study it can be concluded that, 1) Naringinase is most stable in the pH range of 4.5 - 5.0, being quite sensitive to lower pHs (< 3.5); 2) the glyco-enzyme is a rather thermo-stable enzyme preserving its initial activity for long times when incubated at its optimal pH up to temperatures of 65°C. Enriched α-L-rhamnosidase after column treatment and ultrafiltration presented similar deactivation kinetics pattern and half-life values as the unpurified enzyme. Thus, any influence of low molecular weight substances on its deactivation is most probably negligible. The intermediate state of the enzyme may correspond to unfolding and self-digestion of its carbohydrate portion, lowering its activity relative to the initial state. The digestion- and unfolding-grade of this intermediate state may also be controlled by the pH and temperature of incubation.

Introduction

Naringinase is an enzyme complex consisting of α-L-rhamnosidase (EC 3.2.1.40) and β-glucosidase (EC 3.2.1.21) [1-5]. Historically, its production and major application was targeted for the debittering of citrus juices. Indeed, α-L-rhamnosidase converts the bitter glycoside naringin to the less bitter prunin by cleavage of an α-(1→2) bond between L-rhamnose and glucose. Subsequent hydrolysis of glucose from prunin by the β-glucosidase portion yields finally the aglycone naringenin. The α-L-rhamnosidase activity of Naringinase finds further applications in the production of prunin, for aroma enhancement of wine, in steroid transformation, in the structural study of bacterial polysaccharide and in the production of L-rhamnose from glycosides [2, 6-9]. Furthermore, *Penicillium*-α-L-rhamnosidases are known to be capable of hydrolysing L-rhamnose from rhamnolipids [10, 11]. Meiwess et al. [11] reported that a commercial *Penicillium*-Naringinase was able to cleave quantitatively the glycosidic bond between the two L-rhamnose units of dirhamnolipids. The subsequent bond cleavage between L-rhamnose and the (R,R)-3-(3-hydroxydecanoyloxy)decanoic acid portion of the resulted mono-rhamnolipid was also achieved, however at rather low rates.

α-L-rhamnosidases are mainly produced by the fungal species *Aspergillus* and *Penicillium* [1, 2, 6-8, 10, 12-16] whereas bacterial and plant sources are also reported. α-L-Rhamnosidase from *Penicillium decumbens* is an extracellular glycoprotein (50% glycosidation grade) of 90 kDa showing optimal activity at pH 3.5 - 4.5 and 57 °C [3, 17]. In contrast to the other fungal α-L-rhamnosidases, less information is published about its stability profiles of the free form and most studies deal with stabilities in immobilised state [18-21].

For optimization of enzymatic processes not only high activities but also high stabilities of the catalyst are desirable [22]. It is well known that temperature is the most important variable affecting enzyme deactivation by weakening non-covalent interactions that stabilize the protein structure, leading to unfolding and subsequent changes that reduce the catalytic activity [23]. Variation in the pH-value can also irreversibly change this delicate structure by alteration of the charge of the amino acid responsible for maintenance of the secondary and tertiary structure [24]. Extreme pH-values lead similarly to chemical modification fully inactivating the enzyme. Enzyme concentration is also known to affect inactivation by modifying aggregation and subunit dissociation grade [23]. There are many examples of enhanced stabilities at high enzyme concentrations [5, 25].

The objective of this study was to quantify the effect of temperature, pH and enzyme concentration on *Penicillium*-α-L-rhamnosidase stability for a rational selection of process conditions in view of its promising application for enzymatic modification of

rhamnolipids. For that, optimal experimental design techniques were applied for collecting stabilization data in a minimum set of optimal-located experimental points for building of a response surface model. The efficiency of the technique for enzyme stability studies was demonstrated.

Materials and Methods

Naringinase from *Penicillium decumbens* was purchased from Sigma Aldrich (Steinheim, Germany) (Lot 110K16471, 511 U g^{-1} Naringinase or α-L-rhamnosidase activity, and 55 U g^{-1} ß-glucosidase activity). The model substrate p-nitrophenyl-α-L-rhamnoside (pnpR) used for activity assays was obtained from Extrasynthese (Genay, France). All other chemicals were of analytical grade.

Enzyme stability assay

Different enzyme solutions were incubated in plastic cups at controlled temperature under 1400 rpm agitation in a thermoblock unit. At different times, aliquots were withdrawn and the enzyme activity was immediately measured. For determination of initial enzyme activity a first sampling at room temperature before incubation was carried out. Incubation buffers (0.1 M) were as follows: sodium formate for pH 2.50 - 3.38; sodium acetate for pH 4.25 - 5.13, and sodium phosphate for pH 6.00. Naringinase stability tests at low concentration were carried out at pH 5.5 and 40 – 60 °C and a Naringinase concentration of 0.01 g l^{-1}. For avoiding protein adsorption on the vessel walls, plastic cups were pre-treated by incubation of a BSA or Naringinase solution into them. Incubation was conducted at 1 g l^{-1} powder concentration in sodium acetate buffer pH 5.5, 60°C and 1400 rpm for 1 h.

Enzyme enrichment

Enrichment of α-L-rhamnosidase from the commercial powder was carried out with an ÄKTAexplorer equipment coupled to a control system (UNICORN) (Amersham Biosciences, Uppsala, Sweden)). For selection of running buffer pH, small scale assay were carried out on a 1 ml-Hitrap-Q-FF column (Amersham Biosciences, Uppsala, Sweden) with different equilibration buffers: 50 mM Tris-HCl for pH 7.5 and 7.0 and 50 mM potassium phosphate for pH 6.5. Larger protein amounts (5 g Naringinase powder equivalent to 0.4 g protein) were applied on a 20 ml Hiload Q-sepharose HP (Amersham Biosciences, Uppsala, Sweden) column and eluted in 50 mM potassium phosphate buffer pH 6.5 at 4 ml min^{-1} after 12 column-volume (CV) equilibration time with a 40 CV linear gradient from 0 to 0.5 M potassium chloride. Fractions containing α-L-rhamnosidase were pooled, desalted and concentrated in a stirred ultrafiltration cell

(Amicon Inc., Beverly, USA) with a 30 kDa exclusion size membrane (Millipore, Bedford, USA).

Enzyme activity assay

50 µl of an enzyme solution were added to 950 µl of a 4 or 8 mM pnpR solution (in sodium acetate buffer pH 5.5) in a plastic cuvette at 60 °C. The final protein concentration in the cuvette was 0.6 - 2 mg l^{-1} for Naringinase solutions, 2 mg l^{-1} for enriched enzyme solutions and 0.45 – 36 mg l^{-1} for pooled fraction after column treatment. The increase of p-nitrophenolate (pnp) concentration was followed by monitoring the absorption at 400 nm (Molar absorption coefficient for pnp: 1.17 l $mmol^{-1}$ cm^{-1} at pH 5.5 and 60 °C) during 5 minutes reaction time in a photometer provided with a heated cell changer (Amersham Biosciences, Uppsala, Sweden) and coupled to the software Swift II reaction kinetics (Biochrom Ltd., Cambridge, UK). One unit was defined as the protein amount that converts 1 µmol pnp from pnpR in 1 minute at 60 °C and pH 5.5. Activity assays for stability tests were performed by double determinations with 8 mM pnpR solution in 0.5 M sodium acetate buffer whereas simple determinations at 4 mM pnpR solution in 0.1 M sodium acetate buffer were carried out for activity assays of pooled fractions after enrichment.

Protein determination

The protein concentration of collected fractions from α-L-rhamnosidase enrichments were determined by the Bradford method [26] (Bio-rad laboratories, Munich, Germany) using bovine serum albumin (BSA) as standard.

Response surface methodology

The *experimental design methodology* [27-30] was used for studying the stability of Naringinase. This methodology is based on multivariate methods where the levels (settings or values) of the *independent variables* (*e.g.* processing conditions, X_i) are simultaneously modified from one experiment to another. These methods find their major application when the effect of one variable is affected by the setting of another one. Such "interaction effects" between variables are difficult to detect by a traditional experimental setup where one variable is changed at a time. The experimental design methodology makes use of statistical tools for selecting a minimum *set of experiments* adequately distributed in the experimental region (*experimental matrix*). These experiments are chosen so that the coefficients of the mathematical model (usually a polynomial equation) representing the variations of the *experimental response of interest* (dependent variable $Y = f(X_i)$) may be evaluated with the best possible precision. The least-square estimates of the coefficients of the model (b_j) are calculated from the values of

the response *y* for each experiment in the chosen experimental matrix. The resulting model allows the drawing of contour plots (lines or curves of constant response value) and of three-dimensional representations of the responses (Response Surface Methodology) [29, 31-33]. Once tested, the model may be used to predict the value of the response(s) under any conditions within the experimental region.

Model selection

Due to the complexity of the events involved in protein inactivation, the dependency of the variables on the responses were not expected to be linear, the experimental responses were therefore fitted to an empirical quadratic polynomial model of the form:

$$Y = b_0 + \sum b_i \cdot X_i + \sum b_{ii} \cdot X_i^2 + \sum \sum b_{ij} \cdot X_i \cdot X_j \qquad (1)$$

In equation 1, b_0 is the average of all experimental responses, b_i the main effect coefficient of the variable X_i, b_{ii} the second order effect coefficient of the variable X_i and b_{ij} the interaction effect coefficient between variables X_i and X_j $(i \neq j)$.

Experimental design

Among all possible experimental designs associated to a quadratic model [27-30], a Doehlert array was selected for two reasons: besides providing a uniform array of optimally selected experiments within the experimental region, it allows a stepwise approach, investigating in a first step the influence of two variables and extending then the treatment to more variables [31-34]. In a first step, a Doehlert matrix for 2 variables was used for investigating the temperature and pH effects. This matrix contains 7 uniformly distributed experiments (Table 1, experiments 1-7) that may be represented in normalized variables (X_i) by the apexes and the centre of a hexagon. In a second step, a third variable (enzyme concentration) was introduced by adding 6 experiments (Table 1, experiments 8 to 13), resulting in a matrix containing 13 experiments that may be represented by the apexes and centre of a cube octahedron [33].

Determination of the experimental region

Considering the application of the Naringinase for biotransformation of rhamnolipids, the range of each variable was determined according to possible process conditions. The temperature range was selected from 50 °C to 80 °C, the pH-value was set between 2.5 and 6.0 and the Naringinase concentration between 0.1 g l^{-1} and 1 g l^{-1}. Because different variables have different units and ranges of variation, the value of the variables are coded or normalized as: $X_i = (U_i - U_0)/\Delta U$, where X_i is the normalized variable (range from –1 to +1), U_i the value of the effective variable, U_0 the value at the center of the

variable range, and ΔU_i the step (= ($U_{i,max}$ - $U_{i,min}$)/2). Table 1 lists the series of experiments in normalized and effective variables.

Table 1: Doehlert array of experiments for 3 variables. Set of variable-levels: temperature at 7 levels, pH-value at 5 levels, and Naringinase concentration at 3 levels

	pH-Value		Temperature		Enzyme powder concentr.	
Exp. N°	Coded	Effective (-)	Coded	Effective (°C)	Coded	Effective (g/L)
Experimental matrix for temperature and pH						
1	+1.0000	6.00	0	65	0	0.525
2	-1.0000	2.50	0	65	0	0.525
3	+0.5000	5.13	+0.8660	78	0	0.525
4	+0.5000	5.13	-0.8660	52	0	0.525
5	-0.5000	3.38	-0.8660	52	0	0.525
6	-0.5000	3.38	+0.8660	78	0	0.525
7	0	4.25	0	65	0	0.525
Extended matrix for coupling of enzyme concentration						
8	+0.5000	5.13	+0.2887	69	+0.8165	0.913
9	-0.5000	3.38	-0.2887	61	-0.8165	0.137
10	+0.5000	5.13	-0.2887	61	-0.8165	0.137
11	0	4.25	+0.5774	74	-0.8165	0.137
12	-0.5000	3.38	+0.2887	69	+0.8165	0.913
13	0	4.25	-0.5774	56	+0.8165	0.913
Repetitions at the centre of the experimental region						
14 to 18	0	4.25	0	65	0	0.525
Control experiments						
A	0.1400	4.50	-0.3300	60	0	0.525
B	0.5000	5.13	0	65	0	0.525

The reproducibility of the experimental responses was determined by 5 repetitions of the experiment at the center of the experimental region (all variables at normalized value 0). The fitting of the stability curves to the proposed deactivation model and also of initial pnpR activities to the Michaelis-Menten equation was made by the least-square regression method using the Levenberg-Marquardt algorithm (Sigma plot 9.01, Systat software, Inc., San Jose, USA). The calculation of the enzyme half-life values from the activities-time expression was carried out with the program Mathcad 13 (Mathsoft® Needham, USA). For building the experimental matrices, calculating the coefficients of the model (equation 1), evaluating the significance of regression and performing the validity tests, the NEMROD program was used [34].

Results

Kinetics of α-L-rhamnosidase at assay conditions

For establishing the activity assay, the kinetic parameters of the conversion of pnpR by α-L-rhamnosidase were determined at 60 °C and pH 5.5 in 0.1 M sodium acetate by measurement of the initial reaction rate at different initial pnpR concentrations. After fitting the data to the Michaelis-Menten equation, the maximal specific activity and the

Michaelis-Menten constant (K_M) were evaluated to be 13.3 ± 0.4 U mg^{-1} (relative to powder amount) and 6.1 ± 0.3 mM, respectively. Product effects like backward reactions and inhibition phenomena were not considered since initial reaction rates were taken for the calculation. The K_M value thus obtained was higher than the one reported by Romero et al. [3] at pH 3.5 (1.52 mM) and therefore a higher initial pnpR concentration was used for greater accuracy in the activity assays.

Stability at low protein concentration

First stability assays were performed at low enzyme powder concentration (0.01 g l^{-1}) resembling the conditions of rhamnolipid activity assays. In the temperature range from 40 to 60 °C the activity rapidly decreased within the first 30 min incubation time but afterwards remained constant at about 45% of the initial value for 5 hours (data not shown). Incubation without agitation caused a similar behaviour but the remaining activity after 30 min was higher (80 % of the initial value). Ellenrieder and Daz [5] found thermo-stabilization of Naringinase by the presence of BSA. Therefore, 1 g l^{-1} BSA was added to the incubation buffer and the rapid activity decrease within the first 30 min was no longer observed. The activity remained constant and equal to the initial value until 5 h. Moreover, this decay was gradually reduced with higher enzyme concentrations, completely disappearing at 0.1 g l^{-1} Naringinase powder concentration and indicating subunit dissociation. However, when handling with very dilute enzyme solutions a significant percentage of protein can be adsorbed on the walls of the incubation vessel accounting for the former observations [35]. In order to detect this, stability assays at a concentration of 0.01 g l^{-1} Naringinase were performed in pre-treated vessels with BSA or Naringinase absorbed on their surfaces [36]. The apparent deactivation at the beginning was hereby no longer observed. The lower limit of the variable enzyme concentration was therefore set up to 0.1 g l^{-1} for the response surface study in order to avoid adsorption of a high percentage of protein on the vessel-walls.

Proposed deactivation model

Figure 1 shows the decreasing activity as a function of time at different conditions of temperature and pH-values. In a half-logarithmic diagram a non-linear behaviour between time and residual activity is observed for all cases. The decay of the first part of the curve is more pronounced than the second part. Actually, for all experiments carried out for the response surface analysis, it was not possible to fit acceptably the experimental data to the common single-exponential decay. However, for all conditions an adequate fitting to a two-exponential equation of the form [25],

$$a = C_1 \cdot e^{-q_1 t} + (1 - C_1) \cdot e^{-q_2 t} \tag{2}$$

could be achieved. In equation 2, a is the normalized residual activity related to the initial value and C_1, q_1 and q_2 are the equation parameters, which can be evaluated by the fitting.

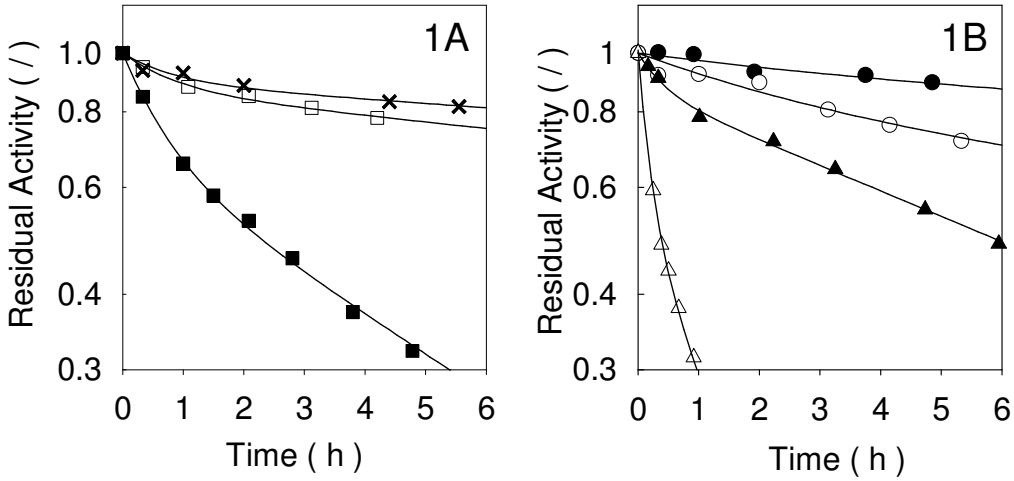

Figure 1: Stability of Naringinase at different conditions. Figure 1A: Effect of pH-value on enzyme stability at 65°C: pH 4.25 (x); pH 6.00 (□); pH 2.50 (■). Figure 1B: Effect of temperature on enzyme stability at pH 3.38; 52°C (●); 61°C (○); 69°C (▲); 78°C (Δ)

This multiple-exponential behavior in the stability curve is always observed when more than one independent, potentially active form of the enzyme is involved on the deactivation kinetics [25]. As with single-exponential decay, a certain number of possible deactivation mechanisms could be applied to explain the double-exponential behavior. However, the value of the physical parameters of the mechanism can only be determined from deactivation data when the number of equation parameters equals the number of the physical ones. Otherwise, the parameters are evaluated as "lumped" or as apparent rate constants of a more complicated mechanism [25]. Therefore, double-exponential deactivation behaviour is often explained by the most simple series type mechanism: the initial enzyme form *(E)* first deactivates to a still active intermediate state *(E_1)*, which slower deactivates to the final fully inactivated state *(E_d)*:

$$E \xrightarrow{k_1} E_1 \xrightarrow{\beta_1 \; k_2} E_d \qquad \text{(A)}$$

In scheme A, β_1 is the specific activity of the intermediate state E_1 related to the initial state *(E)* and k_1 and k_2 are the respective rate constants of the first and second deactivation reactions. Assuming that these steps are irreversible, the second rate constant k_2 is equal to the parameter q_2 from equation 2. Further assuming that no parallel reactions from E to E_d take place and that only the form E is present at the initial state, the activity-time expression corresponding to the former deactivation scheme is [25]:

$$a = \left(1 + \frac{\beta_1 \cdot k_1}{k_2 - k_1}\right) e^{-k_1 t} - \frac{\beta_1 \cdot k_1}{k_2 - k_1} e^{-k_2 t} \quad (3)$$

Comparing equations 2 and 3, the value of the physical parameters β_1, k_1 and k_2 can be then evaluated from the equation parameters C_1, q_1 and q_2. The physical parameters were then taken as responses for the experiments (Doehlert matrix). Moreover, when a equals 0.5 a half-life value ($t_{1/2}$) can be calculated from equation 2 and can be taken as a further response as well.

Response surface analysis

The experimental responses β_1, k_1, k_2 and $t_{1/2}$ of every stability assay under defined incubation conditions according to the corresponding Doehlert array (Table 1) are summarized in Table 2. In all cases the rate constant k_1 was higher than the second rate constant k_2 which agrees with the proposed deactivation model. However, as can be seen from the repeated experiments at the centre, the standard deviation (s) of the response k_1 was rather high compared with the s of the other responses. Probably, more experimental points at the very beginning of the stability assays could have been required for measuring this rapid deactivation decay with acceptable accuracy. Therefore, this response was not taken into account for the analysis. Taking the first experiments 1 to 7 and the centre repetitions 14 to 18 and by multiple regressions analysis of the responses k_2 ($\log k_2$) and β_1, polynomial models were obtained at constant Naringinase concentration (0.525 g l^{-1}). The coefficients of the models are given in equations 4 and 5, respectively. In these equations, X_1 and X_2 represent the normalized variables for pH and temperature, respectively.

$$\log(k_2) = -1.85_{(\pm 0.03)} - 0.47_{(\pm 0.04)} X_1 - 1.11_{(\pm 0.04)} X_2 + 0.67_{(\pm 0.05)} X_1^2 + 0.42_{(\pm 0.05)} X_2^2 + 0.23_{(\pm 0.08)} X_1 X_2 \quad (4)$$

$$\beta_1 = 0.85_{(\pm 0.02)} + 0.12_{(\pm 0.03)} X_1 - 0.18_{(\pm 0.03)} X_2 - 0.08_{(\pm 0.04)} X_1^2 - 0.14_{(\pm 0.04)} X_2^2 + 0.12_{(\pm 0.06)} X_1 X_2 \quad (5)$$

The standard deviations of the responses are 0.07 and 0.05 for $\log k_2$ and β_1, respectively. The multiple regression coefficients R^2 are equal to 0.995 (R^2 adjusted of 0.991) for $\log k_2$ and 0.932 (R^2 adjusted of 0.873) for β_1. The results of F-tests have shown that the polynomial regressions are statistically significant at a confidence level higher than 95% (F = 241.8 for $\log(k_2)$ response and F = 16.1 for β_1 response) ($F_{5\%}(5;6) = 4.39$), indeed the chosen variables affect significantly the experimental responses (Table 2). The good agreements between experimental and calculated values (Table 2) confirm the validity of the polynomial models obtained (equations 4 and 5). The experimental responses of the control assays, shown also in Table 2, are in agreement with the calculated values from the model equations within experimental error.

Table 2: Responses of the experimental matrix assays

Exp.-Nr.	k_1 x 10^2 (h^{-1})	k_2 x 10^2 (h^{-1})		$ß_1$ (/)		$t_{1/2}$ (h)	
	Exp*	Exp*	Calc**	Exp*	Calc**	Exp*	Calc**
1	127	2.5	2.2	0.86	0.89	23	26
2	205	17.4	19.2	0.68	0.65	2.3	2.0
3	482	25.7	28.4	0.71	0.68	1.6	1.4
4	93.6	0.2	0.2	0.92	0.89	309	268
5	20.8	1.1	1.0	0.85	0.88	52	61
6	408	58.9	53.3	0.44	0.47	0.40	0.46
8	78.2	2.9	3.2 (2.9)	0.75	0.77 (0.84)	16	15 (18)
9	31.5	3.0	2.6 (2.0)	0.73	0.71 (0.83)	16	18 (27)
10	116	0.7	0.8 (0.6)	0.86	0.91 (0.91)	78	84 (105)
11	170	8.9	9.5 (8.5)	0.76	0.72 (0.70)	5.3	4.5 (4.7)
12	13.1	9.5	9.1 (7.5)	0.83	0.78 (0.69)	5.8	5.3 (5.3)
13	254	0.5	0.5 (0.5)	0.92	0.96 (0.91)	120	141 (138)
Control experiments							
A	52.0	0.3	0.6	0.86	0.91	165	103
B	118	1.5	1.2	0.88	0.89	38	48
Repetitions at the centre of the experimental region							
7	118	1.6		0.88		36	
14	290	1.7		0.92		36	
15	309	1.3		0.82		38	
16	442	1.3		0.81		37	
17	530	1.3		0.82		39	
18	70.0	1.3		0.86		44	
average	293	1.4		0.85		38	
s***	178	0.2		0.04		3	

* Experimental responses

** Response calculated by the corresponding prediction model: equations 4; 5 and 6 for experiments 1 - 6 and equations 7 and 8 for experiments 8 - 13. In parenthesis, the calculated values from pH-temperature prediction model (equations 4; 5 and 6)

*** Standard deviation of the experimental response

From a practical point of view it could be interesting also to predict the value of the half-life of the enzyme under given process conditions. Taking the logarithm value of $t_{1/2}$ an empirical quadratic model for this response could be calculated as shown in equation 6:

$$\log(t_{1/2}) = 1.58_{(\pm 0.01)} + 0.56_{(\pm 0.02)} X_1 - 1.27_{(\pm 0.02)} X_2 - 0.72_{(\pm 0.03)} X_1^2 - 0.53_{(\pm 0.03)} X_2^2 - 0.10_{(\pm 0.04)} X_1 X_2 \qquad (6)$$

Figure 2 shows the three-dimensional representation and the contour plots of the prediction models for $log(k_2)$, $ß_1$ and $t_{1/2}$. In order to display the direct value of half-life, equation 6 was plotted in Figure 2 after solving it for $t_{1/2}$. The prediction model for $\log(k_2)$ shows that k_2 decreases with decreasing temperature, indicating as expected, an increasing stability at lower temperatures. The k_2 value also depends on the pH and this behaviour varies with the temperature reflecting the contribution of the interaction coefficient in equation 4. The model parameter $ß_1$ ranged from 0.25 to 0.90 suggesting that the intermediate state E_1 is less active than the initial state for all conditions. Hereby the higher the incubation temperature, the lower the activity of the intermediate state and

this dependency is also influenced by the incubation pH. Variations of the β_1 value with pH were already observed with glucose phosphate isomerase [25].

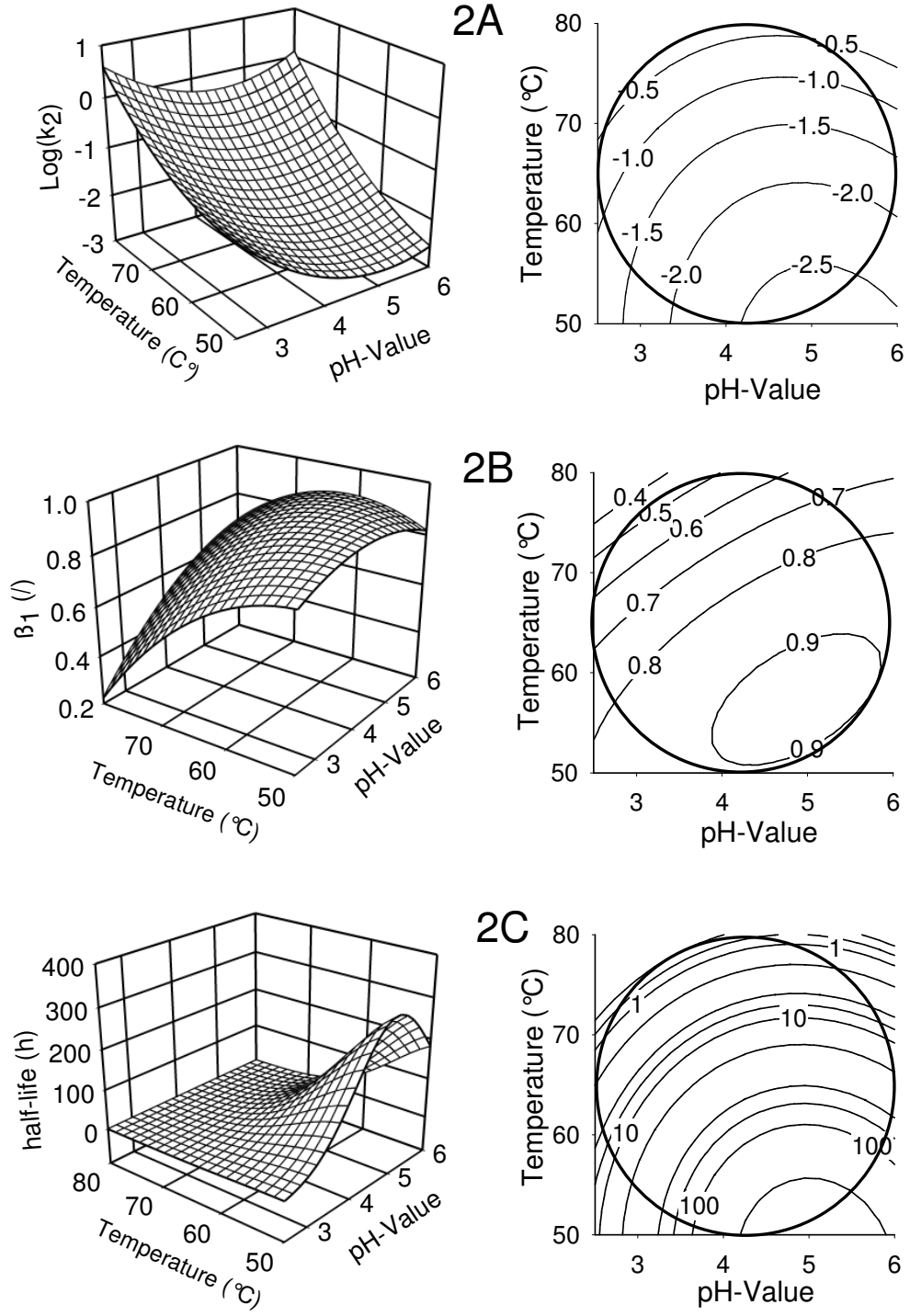

Figure 2: Three dimensional representation of the response surfaces for log(k_2), (2A); ß$_1$ (2B); and half-life, (2C). The corresponding contour plots are plotted on the right of each response surface (the circle denotes the experimental region)

For extending the analysis to the third variable, Naringinase concentration, experiments 8 - 13 (Table 1) were carried out and then the coefficients of the corresponding models

for 3 variables (experiments 1 - 17) were calculated by multiple regression analysis and are given in equation 7 and 8. In these equations, X_1 and X_2 and X_3 represent the normalized variables for pH, temperature and Naringinase concentration, respectively.

$$\log(k_2) = -1.85_{(\pm 0.03)} - 0.49_{(\pm 0.03)} X_1 + 1.09_{(\pm 0.03)} X_2 - 0.03_{(\pm 0.03)} X_3 + 0.67_{(\pm 0.06)} X_1^2 + 0.42_{(\pm 0.06)} X_2^2 + 0.11_{(\pm 0.05)} X_3^2 + 0.23_{(\pm 0.08)} X_1 X_2 - 0.03_{(\pm 0.09)} X_1 X_3 + 0.07_{(\pm 0.09)} X_2 X_3 \quad (7)$$

$$\beta_1 = 0.85_{(\pm 0.02)} + 0.09_{(\pm 0.03)} X_1 - 0.16_{(\pm 0.03)} X_2 + 0.03_{(\pm 0.03)} X_3 - 0.08_{(\pm 0.05)} X_1^2 - 0.14_{(\pm 0.05)} X_2^2 - 0.01_{(\pm 0.04)} X_3^2 + 0.12_{(\pm 0.07)} X_1 X_2 - 0.17_{(\pm 0.07)} X_1 X_3 - 0.09_{(\pm 0.07)} X_2 X_3 \quad (8)$$

From the new polynomial models for both responses it was clearly observed that almost all coefficients involving the enzyme concentration variable (X_3) were much lower than the other coefficients and of the order of their standard deviations and are therefore evaluated as non-significant. This observation indicates that this variable and its interactions hardly influence the Naringinase stability (logk_2 value) or the specific activity of its intermediate state (β_1 value) within the tested region (0.1 – 1 g l^{-1} Naringinase powder concentration). As can be observed from Table 2, experimental and predicted values from equations 4, 5 and 6 (values in parentheses) for the 6 complementary experiments are in acceptable agreement within experimental error confirming the former assumeption.

Enrichment of α-L-rhamnosidase and its stability

Since the commercial preparation used seems to be a raw powder of only 7.8 % w/w protein content (according to Bradford) containing foreign proteins of lower molecular weights (data not shown), it can be worthwhile to perform incubation experiments with a more purified α-rhamnosidase to support the above observations. Activity was eluted in two peaks from an anion adsorbent, one portion eluting before the elution buffer was applied and a later peak together with unwanted proteins. A shift of the second activity peak into the first one was achieved by lowering the pH of the buffer system. The activity recovery in the first peak was then increased from 66 % at pH 7.5 to 70 % at pH 7.0 and 93 % for pH 6.5. Figure 3 shows a typical chromatogram under optimal conditions. At large scale, a partial purification of Naringinase was achieved. The enzyme concentrate of the pooled fractions resulted in a 2.8-fold increase in specific activity with 82 % activity recovery. The specific protein activity of the initial sample was 52.5 U mg^{-1} and of the enriched enzyme 148 U mg^{-1}.

Stability studies of the enriched α-L-rhamnosidase under different temperature and pH values were carried out. For all conditions tested it was again not possible to fit the experimental points to the common exponential deactivation. However, the data could be

appropriately fitted to the proposed double exponential mechanism. Table 3 gives the values of the parameters k_1, k_2 and β_1 for the conditions tested. These values agree with the values predicted by the models (equations 4 and 5) for deactivation of the unpurified α-L-rhamnosidase (Naringinase) and it can therefore be concluded: 1) that the enriched enzyme is as stable as the mixed unpurified powder, and 2) any influence of low molecular weight substances (e.g. additives, contaminants or stabilizers) on the enzyme stability was negligible.

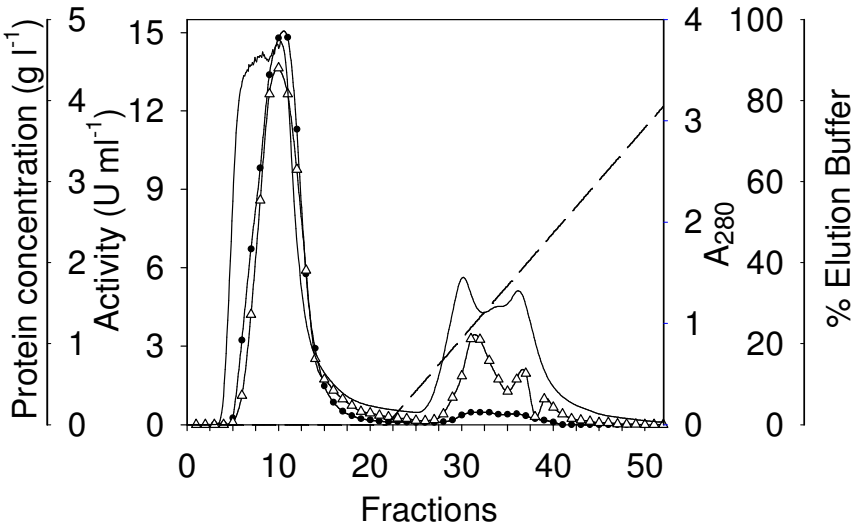

Figure 3: Anion exchange chromatography of Naringinase on Hitrap-Q- FF. Black circles, Rhamnosidase activity; white triangles, protein concentration; full line, absorption at 280 nm and; dashed line, percentage of elution buffer in the running buffer

Table 3: Responses of the stability assays of the enriched α-L-rhamnosidase. In parentheses, calculated values with non-purified enzyme (Naringinase) from equation 4 and 5. All experiments were carried out at a protein concentration of 40 mg l^{-1}

Temperature (°C)	pH-Value (-)	$k_1 \times 10^2$ (h^{-1})	$k_2 \times 10^2$ (h^{-1})	$ß_1$ (-)	$t_{1/2}$ (h)
60	4.50	438	0.6 (0.6)	0.95 (0.91)	116 (103)
61	5.13	50.3	0.8 (0.6)	0.89 (0.91)	72 (105)
65	5.13	32.6	1.2 (1.2)	0.82 (0.89)	46 (48)
78	5.13	503	36.8 (28.4)	0.74 (0.68)	1.3 (1.4)

Discussion

Many examples of soluble, immobilized and chemically modified enzymes exhibiting series-type deactivation mechanism are available in the literature [9, 25, 37, 38]. Moreover, Soria and Ellenrieder [9] also proposed a series-type mechanism for thermal deactivation of a α-L-rhamnosidase of *Aspergillus terreus*. Although there is no evidence at a molecular level of the formation of an intermediate state during deactivation, some

valuable insights were gained to suggest that the proposed model may apply: First, the incubation conditions are similar for obtaining lower deactivation constants (k_2) and greater activity of the intermediate state (β_1), which both promote greater enzyme stabilities. This indicates congruent tendencies. Moreover, the enriched enzyme also exhibited series-type deactivation kinetics supporting the assumption that the deactivation mechanism may be an intrinsic characteristic of the enzyme.

Gabor and Pittner [17] reported that Naringinase tends to self-digestion, cleaving 160 - 170 mole of glucose per mole of enzyme and being in this digested state less active and less stable. In account of this, the first faster deactivation step observed may correspond to the unfolding and self-digestion of the carbohydrate portion, lowering its activity relative to the initial state (β_1) afterwards the common phenomena involving enzyme inactivation may apply for the second slower step. The digestion- and unfolding-grade of this intermediate state may also be controlled by the pH and temperature of incubation.

On the other hand, elution from the Q-column in two activity peaks may indicate existence of α-L-rhamnosidases with different grade of glycosidation having different affinity to the matrix, or even coexistence of different enzymes molecules with different active centres. However, SDS-page revealed protein bands at about 90 kDa for both fractions (data not shown). Mutter et al. [6] and Manzanares et al. [7] detected two different α-L-rhamnosidase activities from *Aspergillus aculeatus.* Young et al. [4] reported purification of *Penicillium decumbens* α-rhamnosidase in a Mono Q column. They also observed activity elution in two peaks however the adsorption onto the column was stronger since at pH 6.0 the major peak was still the later one coming together with the ß-glucosidase portion. The observed double exponential deactivation kinetics may be explained in this case by a stability profile resulted by the contributions of the different deactivation mechanism of the two species.

Concerning stability data it can be concluded that 1) the glyco-enzyme is a rather thermo-stable enzyme preserving its initial activity for long times when incubated at its optimal pH up to temperatures of 65°C; 2) the stability of the enzyme is insensitive to the enzyme concentration; 3) a pH-optimum for enzyme stability could be observed at pH 4.5 – 5.0 by analysis of the response surfaces at constant temperature, being, however, quite sensitive to lower pHs (< 3.5). Ellenrieder and Daz [5] and Tsen et al. [19] reported deactivation data of *Penicillium* Naringinase at pH 3.5 – 3.7; however our measurements exhibited higher stability at the same conditions. Ellenrieder and Daz [5] also observed an increasing stability at higher Naringinase concentrations; however the range tested by these authors was wider (0.5 – 5 g l^{-1}). They also achieved thermostabilization by cross-linking modification and by immobilization on protein-rich supports. Many studies of pH-stability on *Aspergillus* rhamnosidases are reported [1, 6-9,

13, 14]. *Aspergillus aculeatus* α-L-rhamnosidase [6] was shown to be insensitive to pH in the range 3 - 8, whereas *Aspergillus terreus* [8] and *Aspergillus nidulans* [14] α-L-rhamnosidases rapidly lost activity when incubated at pH values lower than 4.0. Comparing our measurements with available stability data of purified fungal α-L-rhamnosidases published in the literature [1, 6-9, 13, 14], it can be further pointed out that α-L-rhamnosidase from *Penicillium decumbens* exhibited higher thermo-stability than from *Aspergillus* species.

Response surface methodology has been successfully applied for the quantitative study of enzyme stability. Compared to the traditional approach consisting of changing one variable at a time, response surface methodology significantly reduced experimental effort and facilitated data treatment and interpretation of the results. Thus, temperature, pH and enzyme concentration effect on stability were evaluated on a minimum set of optimal selected experiments. Estimations of deactivation parameters at different conditions were chosen as responses for every experiment. With these responses an empirical quadratic model was fitted for predicting enzyme stability within the experimental region serving as a basis for a rational selection of conditions of Naringinase catalysed reactions like *e.g.* rhamnolipid hydrolysis. Further investigations for establishing coexistence of different enzymes molecules in Naringinase by *e.g.* measuring eluted activity with two different substrates from a purification column supported by stability profiles of the different activity peaks are being planned. In case of detection of two different enzymes the proposed series deactivation mechanism should be re-evaluated.

Acknowledgments

The authors would like to thank the financial support of this project, carried out in the framework of a EU-CRAFT project (1999-72243) entitled “Integrated process for biosurfactant synthesis at competitive cost allowing for their application in household cleaning and bio-remediation” (InBioSynAp). We also thank Rebecca Lorenz for her helpful practical input during the research project.

References

1. Dunlap, W.J., Hagen, R.E. and Wender, S.H. (1962) J. Food Sci. 27(6), 597-&.
2. Puri, M. and Banerjee, U.C. (2000) Biotechnology Advances. 18(3), 207-217.
3. Romero, C., et al. (1985) Anal. Biochem. 149(2), 566-571.
4. Young, N.M., Johnston, R.A.Z. and Richards, J.C. (1989) Carbohydr. Res. 191(1), 53-62.
5. Ellenrieder, G. and Daz, M. (1996) Biocatal. Biotransform. 14(2), 113-123.
6. Mutter, M., et al. (1994) Plant Physiol. 106(1), 241-250.
7. Manzanares, P., et al. (2001) Appl. Environ. Microbiol. 67(5), 2230-2234.
8. Gallego, M.V., et al. (2001) J. Food Sci. 66(2), 204-209.
9. Soria, F. and Ellenrieder, G. (2002) Bioscience Biotechnology and Biochemistry. 66(7), 1442-1449.
10. Meiwess, J., Wullbrant, D. and Giani, C. (1994) Alpha-L-rhamnosidase zur Gewinnung von Rhamnose, ein Verfahren zur Herstellung und ihre Verwendung EP0599159
11. Trummler, K., Effenberger, F. and Syldatk, C. (2003) Eur. J. Lipid Sci. Technol. 105(10), 563-571.
12. Mamma, D., et al. (2004) Food Biotechnology. 18(1), 1-18.
13. Manzanares, P., de Graaff, L.H. and Visser, J. (1997) FEMS Microbiol. Lett. 157(2), 279-283.
14. Manzanares, P., et al. (2000) Letters in Applied Microbiology. 31(3), 198-202.
15. Monti, D., et al. (2004) Biotechnol. Bioeng. 87(6), 763-771.
16. Scaroni, E., et al. (2002) Letters in Applied Microbiology. 34(6), 461-465.
17. Gabor, F. and Pittner, F. (1984) Hoppe-Seylers Zeitschrift Fur Physiologische Chemie. 365(9), 914-914.
18. Turecek, P. and Pittner, F. (1986) Applied Biochemistry and Biotechnology. 13(1), 1-13.
19. Tsen, H.Y., Tsai, S.Y. and Yu, G.K. (1989) J. Ferment. Bioeng. 67(3), 186-189.
20. Puri, M., Marwaha, S.S. and Kothari, R.M. (1996) Enzyme Microb. Technol. 18(4), 281-285.

21. Norouzian, D., et al. (1999) World Journal of Microbiology & Biotechnology. 15(4), 501-502.

22. Biselli, M., Krugl, U. and Wandrey, C., (1995), in Enzyme catalysis in organic synthesis - a comprehensive handbook, Vol. 1 (Drauz, K. and Waldman, H.), VCH, Weinheim, pp. 89-155.

23. Klibanov, A.M. (1983) Advances in Applied Microbiology. 29, 1-28.

24. Bisswanger, H. (1999) Enzymkinetik: Theorie und Methoden, 3rd ed. Wiley-VCH, Weinheim

25. Sadana, A. (1991) Biocatalysis: Fundamentals of enzyme deactivation kinetics, Prentice Hall, New Jersey

26. Bradford, M.M. (1976) Anal. Biochem. 72(1-2), 248-254.

27. Aktinson, C. (1992) Optimum experimental designs, Clarendon, Oxford

28. Box, G.E.P., Hunter, W.G. and S., H.J. (1978) Statistic for experimenters: an introduction to design, data analysis and model building, Wiley, New York

29. Khuri, A.I. and Cornell, J.A. (1987) Response surfaces, Design and Analyses, Marcel Dekker, ASQC Quality Press, New York

30. Rasch, D., Verdooren, L.R. and Gowers, J.I. (1999) Grundlagen der Planung und Auswertung von Versuchen und Erhebungen, R. Oldenbourg Verlag, München, Wien

31. BenoitMarquie, F., et al. (1997) Journal of Photochemistry and Photobiology a-Chemistry. 108(1), 65-71.

32. Oliveros, E., et al. (2000) In: Proceedings of the Third Asia Pacific Conference. Singapore, Work Scientific, pp 577-581

33. Oliveros, E., et al. (1997) Chem. Eng. Process. 36(5), 397-405.

34. NEMROD and NEMRODW, v., LPRAI, B.P. no. 7, Marseille - Le Merlan, 13311 Marseille Cedex 14, France (www.nemrodw.com).

35. Scopes, R. (1994) Protein Purification, Principles and practice, 3rd ed. Springer, New York

36. Mozhaev, V.V. (1993) Trends Biotechnol. 11(3), 88-95.

37. Greco, G., et al. (1992) In: Stability and stabilization of Enzymes (Proceedings of an International Symposium). Maastricht, Elsevier science, pp 429-435

38. Prazeres, D.M.F., Garcia, F.A.P. and Cabral, J.M.S. (1992) In: Stability and Stabilization of enzymes (Proceedings of an International Symposium). Maastricht, Elsevier Science, pp 445-450

4.2 Kinetic Analysis of a di-Rhamnolipid Conversion

KINETIC ANALYSIS AND MODELING OF THE LIQUID-LIQUID CONVERSION OF EMULSIFIED DI-RHAMNOLIPIDS BY NARINGINASE FROM *PENICILLIUM DECUMBENS*

Biotechnology and Bioengineering 102 (1) (2009) 9-19

DOI: 10.1002/bit.22057

I. Magario *, O. Vielhauer [a], A. Neumann, R. Hausmann, C. Syldatk

Institute of Engineering in Life Sciences, Chair of Technical Biology, University of Karlsruhe (TH), Germany

[a] Institute of Biochemical Engineering, University of Stuttgart, Germany

* Corresponding author: I. Magario
Tel: +49-721-608-6736/8428
Fax: +49-721-608-4881
E-mail: Ivana.Magario@tebi.uni-karlsruhe.de

Key words: rhamnolipids, liquid-liquid biocatalysis, Naringinase, micellar substrates

Abstract

The enzymatic conversion of an aggregates-building substrate was kinetically analyzed and a model was applied for the prediction of reaction-time courses. A L-rhamnose molecule from a di-rhamnolipid is cleaved by Naringinase from Penicillium decumbens leading to a mono-rhamnolipid. Optimal reaction rates were found when both, substrate and product build large co-aggregates in a slightly acidic aqueous phase. On the other hand, reaction rates were independent of initial di-rhamnolipid concentration and this was interpreted by assuming that the reaction occurs in the aqueous phase according to Michaelis-Menten kinetics in combination with competitive L-rhamnose inhibition. Rhamnolipids were therefore assumed to be highly concentrated in aggregates, a second liquid phase, whereas diffusive rhamnolipid transport from and to the aqueous phase occurs due to the enzymatic reaction. Furthermore, ideal surfactant mixing between di- and mono-rhamnolipid was assumed for interpretation of the negative effect of the last on the reaction rate. A model was created that describes the system accordingly. The comparison of the experimental data, were in excellent agreement with the predicted values. The findings of this study may beneficially be adapted for any bioconversions involving aggregate-forming substrate and/or product being catalyzed by hydrophilic enzymes.

Introduction

Rhamnolipids (RL) are amphiphilic compounds produced by *e.g. Pseudomonas* sp. from hydrophobic carbon sources as e.g. vegetable oils. Because of their biodegradability, high tensioactive properties and production from renewal and inexpensive raw materials they are of special interest as an alternative to chemically synthesized surfactants. Besides their use as detergents, RL also have potential industrial applications in food, cosmetic, pharmaceuticals, as well as in bioremediation of pollutants (Banat et al. 2000; Mulligan 2005; Nitschke et al. 2005). RL are produced as an extracellular mixture of different species, which composition strongly varies according to process conditions (Lang and Trowitzsch-Kienast 2002; Nitschke et al. 2005). The main species commonly encountered are often termed di-rhamnolipid (di-RL) and mono-rhamnolipid (mono-RL) (see Figure 1). RL are very potent biosurfactants showing decreased surface tension of water at very low concentrations (26 mg l^{-1}) (Lang and Trowitzsch-Kienast 2002; Ozdemir et al. 2004). Although having similar critical micelle concentration values (cmc), mono-RL shows higher surface and interfacial activity than di-RL at concentrations below the cmc. This property is attributed to the more favorable hydrophilic/hydrophobic balance of mono-RL molecules (Ozdemir et al. 2004).

The interest of RL was often targeted to the production of L-rhamnose and therefore RL were chemically or enzymatically hydrolyzed for obtaining this desoxy sugar (Giani et al. 1993; Linhardt et al. 1989; Meiwes et al. 1997; Mixich et al. 1996; Trummler et al. 2003). L-rhamnose is mainly used as a starting material for the production of the flavor agent Furaneol® (Lang and Trowitzsch-Kienast 2002; Trummler et al. 2003). Enzymatic hydrolysis of di-RL, as displayed in Figure 1, could be a conclusive method for the simultaneous production of pure mono-RL as well as L-rhamnose.

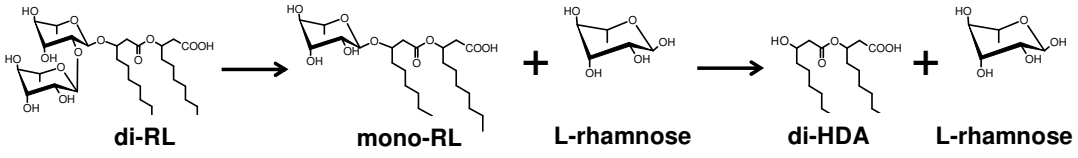

Figure 1: Hydrolysis of di-rhamnolipid and mono-rhamnolipid

Therefore, the objective of this study was the characterization and modeling of the hydrolysis kinetics of di-RL for the production of mono-RL and L-rhamnose by Naringinase. Besides, the subsequent reaction with formation of L-rhamnose and 3-(3-hydroxydecyloxy)decanoic acid (di-HDA) from mono-RL was also investigated. To understand the kinetics of an enzymatic conversion of aggregates-building substrates such as RL, a kinetic analysis for describing reaction-time courses was set-up.

Reaction kinetics modeling

At concentrations above the *cmc* RL build micelles. One of the approaches of thermodynamic treatments of micelle formation considers the micelles to form a separate phase at the *cmc* (Attwood and Florence 1983; Holland and Rubingh 1992). In account of this RL micelles were assumed to be a highly- RL-concentrated liquid phase termed as the micelle-phase. On the other hand, an enzyme attack was assumed to be only possible for dissolved molecules or monomers. Therefore, a diffusive mass transport of di-RL from the micelle-phase to the aqueous phase has to occur due to the decomposition of this species by the enzyme. Equally, a diffusive mass transport of the emerging reaction product mono-RL occurs in the opposite direction whereas the product L-rhamnose accumulates in the aqueous phase. The influence of liquid-liquid mass transfer on the overall reaction rate was checked according to Levenspiel (1999) and Straathof (2003).

The overall RL content was measured as the sum of aqueous and micelle-phase concentration, represented as $C^{T}_{di\text{-}RL}$ and $C^{T}_{mono\text{-}RL}$. Thereby, mole fractions $X^{T}_{di\text{-}RL}$ and $X^{T}_{mono\text{-}RL}$ were calculated. Assuming that RL is concentrated in the micelle-phase and under steady-state condition of the aqueous phase (Straathof 2003) the mass balance for mono-RL corresponds to:

$$C^{T}_{RL} \cdot \frac{dX^{T}_{mono-RL}}{dt} = -r \frac{V_{aq}}{V_T} \tag{1}$$

In equation 1, r represents the reaction rate. It was assumed that 1) the RL diffusion into and from the aqueous phase is not accelerated by the enzymatic reaction, 2) no reaction takes place in the interface film and, 3) constant volumes of aqueous and micelle phases during reaction time. The reaction rate was described by the Michaelis-Menten kinetic with competitive product inhibition by L-rhamnose. The Michaelis-Menten constant K_m was assumed to be much higher than the aqueous di-RL concentration since the last was determined to be rather low (see results section) and thus unlikely as being as high as the K_m value considering typical K_m values for other substrates (Romero et al. 1985). Therewith, r equals:

$$r = \frac{-A_s \cdot \rho_E \cdot C^{aq}_{di-RL}}{K_m \cdot \left(1 + \frac{C_{Rha}}{K_I}\right)} \tag{2}$$

Combining equation 2 with the di-RL mass transfer rate $\phi_{di\text{-}RL}$ an expression for $C^{aq}_{di\text{-}RL}$ was derived:

$$C_{di-RL}^{aq} = \frac{k_{L,di-RL} \cdot a \cdot C_{di-RL}^{aq,eq} \cdot \left(1 + \frac{C_{Rha}}{K_I}\right)}{\frac{A_s}{K_M} \cdot \rho_E + k_{L,di-RL} \cdot a \cdot \left(1 + \frac{C_{Rha}}{K_I}\right)} \tag{3}$$

Considering the separate phase approach for characterizing mixed surfactants systems and assuming ideal mixing, the monomer concentration of di-RL in equilibrium and its total mole fraction were related according to Holland and Rubingh (1992) and Milioto (2006):

$$C_{di-RL}^{aq,eq} = X_{di-RL}^{T} \cdot cmc_{di-RL} \quad \text{for} \quad C_{RL}^{T} >> cmc_{di-RL} \tag{4}$$

Furthermore, C_{Rha} was calculated as the difference of the initial total di-RL concentration and the total di-RL concentration at every time. For integration of equation 1, the following boundary condition was used:

$$t = 0; \qquad X_{mono-RL}^{T} = X_{mono-RL,0}^{T}$$

For low RL total concentrations (< 0.01 M) the ratio of aqueous to total volume of equation 1 was assumed to be unity. For numerical integration of equation 1 by the Runge-Kutta method and fitting to experimental data the program ModelMaker Version 3.0.3 (Cherwell Scientific Publishing Ltd., Oxford, UK) was used.

Materials and Methods

Materials

Naringinase (N-1385; Lot N° 110K16471; 511 U g^{-1} L-rhamnosidase activity, 55 U g^{-1} ß-glucosidase activity) from *Penicillium decumbens* was purchased from Sigma Aldrich (Steinheim, Germany). Pure crystalline di-RL was by courtesy of Hoechst AG (Frankfurt, Germany) (97 %). The model substrate p-nitro-phenyl-rhamnoside (pnpR) for assaying α-rhamnosidase activity was obtained from Extrasynthese (Genay, France). Highly pure standards of mono-RL and di-HDA were prepared by enzymatic hydrolysis of 1 g and 2 g di-RL, respectively according to Trummler et al. (2003). After production and solvent extraction, mono-RL and di-HDA were further purified by adsorption chromatography: Silica gel (60 DM 0.04 – 0.063 mm) was used as stationary phase and a system methanol-chloroform as mobile phase (ratio 15:85 for mono-RL and 5:95 for di-HDA). After evaporation of the mobile phase, silica gel impurities were removed by extraction with water from the re-dissolved products in ethyl acetate for mono-RL and in hexane for di-HDA. After drying, the organic phase was evaporated under high vacuum. 300 mg mono-RL and 454 mg di-HDA were obtained as honey-like substances.

HPLC measurements of the products gave single peaks and elemental analysis was in accordance with theoretical values. Mono-RL used as substrate for biotransformation assays was also produced by enzymatic hydrolysis of di-RL without further purification (condition: pH 4.5, temperature 57°C, with free Naringinase). All other reagents, chemicals and co-solvents were of analytical grade.

Activity assays with rhamnolipids

Di-RL biotransformations were initiated by addition of a Naringinase solution to a temperate di-RL emulsion in a ratio 1 to 20 (see Table I for concentration settings). Under thermo-stated conditions and shaking in a thermo-bloc unit (*Thermomixer* comfort, Eppendorf AG) 500 µl samples were withdrawn at different times and the reaction was stopped by acidification with 50 µl 1 M phosphoric acid followed by RL extraction in 500 µl ethyl acetate. After centrifugation, the ethyl acetate phase was sampled and evaporated at 60°C over 1 h and the RL was re-dissolved in acetonitrile for analysis. Di-RL emulsions were prepared by adding a buffer solution to a weighted amount of RL followed by equilibration at the desired temperature. Following 0.1 M buffer solutions were used: sodium formate for pH 2.5 – 3.5, sodium acetate for pH 4.0 – 5.5 and sodium phosphate for pH 6.0 – 6.5. Table 1 shows experimental conditions of different arrays of biotransformations carried out for optimization and kinetic studies.

Table 1: Experimental conditions of RL biotransformations

Array of biotransformations	pH (/)	T (°C)	$C_{di\text{-}RL,0}^{T}$ * (mM)	$C_{mono\text{-}RL,0}^{T}$ * (mM)	ρ_E ** (mg l^{-1})	$R_{E/S}$ *** (%)
Temperature-curve (Fig. 2)	5.5	40 – 80	1	0	6	0.92
pH-curve (Fig. 2)	2.5 – 6.5	60	1	0	6	0.92
Co-solvents assays (Table 2)	4.5	50	5	0	26	0.80
Ethanol assays (Fig. 3)	4.5	60	10	0	26	0.40
Enzyme assays (Fig. 4A and 6A)	4.5	60	10	0	260 – 6.5	4.0 – 0.10
Substrate assays (Fig. 4B and 6B)	4.5	60	0.1 – 10	0	4.9	7.5 – 0.075
Rhamnose assays (Fig. 4C)	4.5	60	3	0	4.9	0.25
Mole fraction assays (Fig. 6C)	4.5	60	3	0 - 9	4.9	0.25
High-substrate assays (Fig. 6D)	4.5	60	91	0	325	0.50
	4.5	60	47	0	4.9	0.015
	4.5	60	24	0	4.9	0.030
Mono-RL-conversions (Fig. 7)	4.5	60	0	10	0.5	7.7
	4.5	60	10	0	0.5	9.9

* $C_{di\text{-}RL,0}^{T}$ and $C_{mono\text{-}RL,0}^{T}$: initial total di-RL and mono-RL concentrations, respectively
** ρ_E : enzyme concentration
*** $R_{E/S}$: mass ratio enzyme to substrate

For bioconversion with organic solvents, samples were diluted with buffer before ethyl acetate extraction to avoid impairment of RL extraction due to co-solvent addition. Shaking speed was 1400 min^{-1} for pH and temperature-curve setups and 700 min^{-1} for all other experiments. Initial volumetric activities were calculated as the derivative at time zero of mono-RL mole fraction-time curves multiplied by the total nominal RL

concentration. Since a linear time course could not be reached due to the experimental constraint of under-saturation conditions ($C^{aq}_{di\text{-}RL} << K_m$), experimental mole fraction-time values were fitted to the following equation:

$$X^{T}_{mono-RL} = b \cdot (1 - e^{-c \cdot t}) \tag{5}$$

The program SigmaPlot Version 9.01 (Systat software, Inc. 2004) was used for the fitting procedure. One unit was defined as the enzyme amount that converts 1 µmole mono-RL from di-RL in 1 minute at specified conditions of temperature and pH.

Activity assays with pnpR

Activities of Naringinase solutions were always checked with pnpR before di-RL biotransformation: An enzyme solution was added to an 8 mM pnpR solution in 0.1 M sodium acetate buffer pH 5.5, into a plastic cuvette, at 60 °C. The increase of p-nitrophenolate (pnp) concentration was followed by monitoring the absorption at 400 nm (extinction coefficient for pnp at pH 5.5 and 60 °C: 1.2 l $mmol^{-1}cm^{-1}$) during 5 min reaction in a photometer (Amersham Biosciences, Uppsala, Sweden) equipped with a heated cell changer and coupled to the software Swift II reaction kinetics (Biochrom Ltd., Cambridge, UK). For pnpR activity test with ethanol as co-solvent (Figure 3), a 2 mM pnpR solution in sodium acetate buffer pH 4.5 and ethanol (0 – 50 %) with and without addition of a RL solution (end concentration 10 mM) was heated at 60 °C. Enzyme solution was added and activity was assayed according to Romero et al. (1985): At different times, samples were withdrawn and 100 µl were added into a cuvette with 1.5 ml 0.1 M sodium hydroxide and the absorption was immediately measured at 400 nm (Extinction coefficient for pnp at pH 12 and room temperature: 18.9 l $mmol^{-1}cm^{-1}$).

Determination of the solubility, *cmc* and pK_a-value of rhamnolipids

Di-RL emulsions (0.5 – 10 mM) prepared in 0.1 M sodium acetate buffer pH 4.5 and equilibrated for 3 h at 60 °C under shaking were let to stand at 60 °C for 2 days for complete sedimentation of the micelle-phase. Then, samples of the aqueous phase were taken and treated as described above for HPLC analysis. Emulsion mixtures with different ratios di-RL to mono-RL were prepared by carrying out biotransformations of di-RL (10 mM di-RL, 65 mg l^{-1} enzyme concentration, 60 °C and pH 4.5), which were stopped at different times before reaction completion. After analysis of the di-RL to mono-RL proportion, the ethyl acetate phase was evaporated and the RL emulsified in 0.1 M sodium acetate buffer pH 4.5 (10 mM final RL-concentration). After equilibration at 60 °C under shaking, emulsions were centrifuged (Avanti™ J-30I, Beckman Coulter™, California, USA) at 75600 g and 25°C for 1h. Samples of the aqueous phase were taken and treated as described above for HPLC analysis. The superficial tension of a set of di-RL solutions at defined pH and increasing concentrations was measured with

a tensiomenter (Digital-tensiometer K10, Krüss, Hamburg, Germany) using the plate method and the *cmc* was defined as the concentration up to non further decrease of superficial tension was observed. Determination of di-RL acidic constant (K_a) was determined potentiometrically by back-titration of a basic 5 mM di-RL solution with 0.1 M hydrochloric acid.

Rhamnolipids analytics

RL were analyzed by an HPLC device coupled to a UV detector (1100 Series, Agilent, Santa Clara, USA) according to Schenk et al. (1995): RL were pre-derivatized into esters of bromophenacylbromide (Fluka, Steinheim, Germany) in acetonitrile over 1.5 h at 60°C and applied to a RP-18 column (Supelcosil LC-18)(150 mm x 4.6 mm, 5 µm silica gel) thermo-stated at 25°C. Then, RL-bromophenacyl-esters were eluted at a flow rate of 0.8 ml min^{-1} with a linear gradient acetonitrile(Acn)-water (0 min: 70% Acn, 4 min: 70% Acn, 14 min: 100% Acn, 28 min: 100% Acn, 33 min: 70% Acn; 38 min: 70% Acn) and detected at 265 nm. Calibration curves of di-RL, mono-RL and di-HDA were carried out in the range 0.1 - 1 mM with the same preparation protocol as for the biotransformation samples (acidification and extraction from a buffer solution). RL were also qualitatively analyzed by thin layer chromatography with a methanol-chloroform solution in a ratio 15:85 as mobile phase. RL spots in the plates were detected by immersion into an ammonium molibdate/cerium sulphate acidic solution (0.42% w/v ammonium molibdate, 0.2% w/v cerium(IV) sulphate and 6.2% v/v sulfuric acid) and after heating at 105 °C.

Results

Selection of reaction temperature and pH

Figure 2 shows the influence of temperature and pH on the enzyme activity for di-RL conversion. A linear correlation was observed when plotting specific activities till 70 °C in an Arrhenius array (R^2 = 0.99), and the activation energy of the reaction was therewith estimated to be 54 ± 3 kJ mol^{-1}. A temperature of 60 °C was chosen for further experiments, where enzyme half-life values larger than 100 h were obtained (Magario et. al, 2008a). A wide pH optimum between 4.0 and 5.0 is observed, which is in agreement with the optimum pH for stability (Magario et. al, 2008a).

Measurements of *cmc* of di-RL at 61 °C resulted in 0.08 mM at pH 7.0 and 0.03 at pH 4.5 whereas *cmc* of di-RL at pH 4.5 and 34°C resulted in 0.03 mM. These values indicate that the *cmc* increases with increasing pH however being not influenced by the temperature. This *cmc* tendency with pH was already obtained by Ozdemir et al. (2004) and by Syldatk et al. (1985). However, as observed in Figure 2 enzyme activities may

be more influenced by the optimal catalytic activity of Naringinase at acidic pH rather than by the higher availability of di-RL monomers at higher pHs.

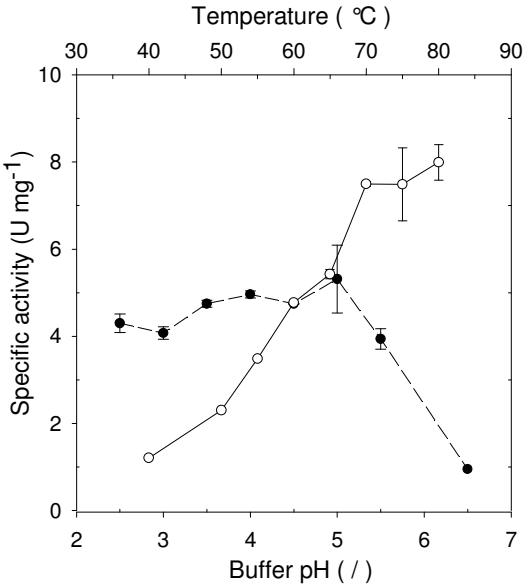

Figure 2: Influence of temperature (○) and pH (●) on the enzyme activity for di-RL conversion.

At acidic pH values di-RL molecules exist mainly as suspended hydrated crystals. These crystals were solubilized at pH higher than 5. The acidic constant of di-RL was determined to be 7.6 10^{-7} (pK_a 6.12). Thus, a relatively low ionization grade was enough to solubilize the non-protonated form of di-RL. On the other hand, when suspensions of di-RL at pH 4.5 were heated above approximately 50 °C, solid di-RL crystals became a separate liquid phase building a turbid and unstable emulsion. This liquid rhamnolipid phase, the micelle-phase, may correspond to the formation of liquid crystals or large aggregates. This emulsion became a clear solution with increasing pH. This observation is in agreement with the fact that the size of the RL micelle-phase increases with decreasing pH (Champion et al. 1995; Ishigami et al. 1987; Lebron-Paler et al. 2006). Kinetics analysis was further conducted at pH 4.5 taking advantage of maximal reaction rates and the existence of a two-phase system, which simplifies product recovery by decantation or centrifugation of the micelle-phase.

Conversions with co-solvent addition

In order to observe whether the addition of water-soluble solvents increase reaction rates due to an increase in the di-rhamnolipid monomer concentration, different alcohol and non-alcohol type co-solvents were tested. Table 2 lists specific enzyme activities, mono-RL mole fraction reached after 4 h reaction and system appearance after solvent addition. Non-significant influences on reaction rates were observed although the reaction system turned clear after solvent addition in most cases. Slight increase of conver-

sion rates was observed with 2-methoxyethanol and with the branched alcohols iso-propanol and tert-butanol whereas lower rates were detected with linear alcohols like 2-butanol and 1-propanol. Tert-butanol and 2-butanol have a damaging effect on enzyme activity with time as observed when comparing initial rates and conversion after 4 h. A minor increase on reaction rate was also reached with dioxane while all other non-alcohol-type solvents caused a decrease.

Table 2: Enzyme activities for di-RL conversion and emulsion appearance in dependence of co-solvent.

Co-solvent	Addition (%)	Spec activity (U mg^{-1})	Mono-RL mole fraction after 4 h (/)	Emulsion appearance*
-	-	2.37	0.90	turbid
-	-	2.33	0.89	turbid
2-methoxyethanol	5	2.35	0.91	clear
2-methoxyethanol	10	2.47	0.93	clear
1-propanol	5	2.00	0.86	clear
Iso-propanol	5	2.35	0.89	turbid
Iso-propanol	10	2.52	0.94	clear
2-butanol	5	2.36	0.77	turbid
Tert-butanol	5	2.41	0.89	turbid
Tert-butanol	10	2.77	0.89	clear
DMSO	5	1.92	0.86	clear
DMF	5	1.44	0.79	clear
Dioxane	5	2.30	0.90	clear
Dioxane	10	2.38	0.93	clear
Butanone	5	1.97	0.81	turbid
Acetonitrile	5	1.95	0.87	clear

* Solvent added to di-RL emulsion in sodium acetate buffer 0.1 M pH 4.5 and heated at 50 °C

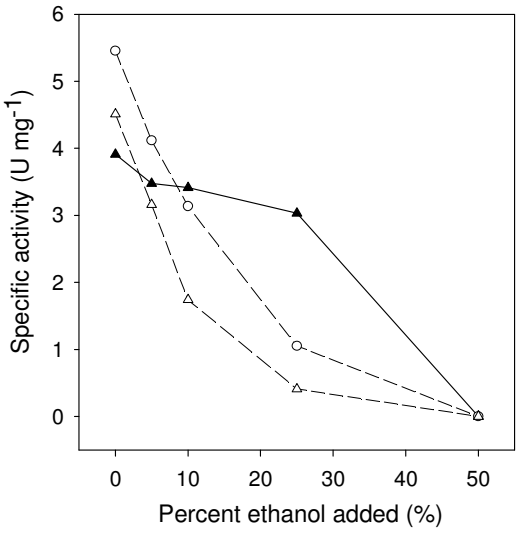

Figure 3: Effect of ethanol addition on enzyme activity. Activity measured with: di-RL (▲), pnpR (○), and pnpR in the presence of RL micelles (Δ)

Figure 3 shows specific activities in dependence of percentage of ethanol added to the reaction system. PnpR-activity decreased abruptly with ethanol addition evidencing its

damaging effect. On the other hand, di-RL-activity decreased much less with solvent addition. To check whether ethanol penetrates in the RL micelle-phase and thus does not affect enzyme activity, ethanol effect on pnpR specific activities was assayed in the presence of di-RL micelle-phase. No protective effect of activity was detected suggesting that ethanol remains in the aqueous phase. Following conversions were conducted without co-solvent addition.

Diffusion effects

Figure 4A shows a linear correlation of initial reaction rate and enzyme concentration up to 0.26 g l^{-1} Naringinase concentration when assaying bioconversion of 10 mM di-RL emulsions. This indicates enzymatically rate-controlled conditions as can be deduced from equation 2 and 3. Since diffusion rate depends on the specific interfacial area *a* which increases with di-RL concentration, this linear correlation suggest that up to a mass ratio of enzyme to di-RL of 4 %, rate limitation due to diffusion is negligible.

Figure 4B shows specific activities in dependence of initial total di-RL concentration. The concentration of aqueous di-RL concentration in equilibrium $C^{aq,eq}_{di\text{-}RL}$ for every total di-RL concentration $C^{T}_{di\text{-}RL}$ is also plotted. Reaction rates and aqueous di-RL concentration remained constant throughout the concentration range 0.1 – 10 mM. This clearly shows that reaction rates are dependent on the aqueous, however, not on the total di-RL concentration. This is also in accordance with equation 2. Since reaction rates were independent of the total RL concentration, and therefore of the specific interfacial area, this is an evidence of enzymatic reaction rate control. Correspondingly; the enzymatic reaction rate is much lower as compared to the diffusion rate of RL. Therefore, the aqueous bulk di-RL concentration $C^{aq}_{di\text{-}RL}$ equals the value in equilibrium; $C^{aq,eq}_{di\text{-}RL}$.

Determination of relevant parameters

To compare theoretical predictions with experimental reaction courses, the parameters $cmc_{di\text{-}RL}$, A_s, K_m and, K_I of equations 2 to 4 need to be known. If possible these parameters should be determined independently. The aqueous di-RL concentrations plotted in figure 4B were determined as the aqueous concentration resulted after complete sedimentation of the micelle-phase. The average value obtained was 0.046 ± 0.001 mM (at pH 4.5, 60°C). Within experimental error, this value was slightly higher, but of the same order of magnitude than the *cmc* of di-RL measured under the same conditions of pH and temperature (0.03 mM). This value was therefore applied as the concentration of free monomers. The rate constant (A_s/K_m) was determined taking the slope of the linear regression of Figure 4A (i.e. equation 2 under enzymatically control at zero reaction time). A value of 0.104 ± 0.004 l min^{-1} mg^{-1} was therewith obtained. The absolute va-

lues A_s and K_m could not be evaluated. However, in equations 2 respectively 3 only the quotient is required, provided that $K_m >> C^{aq}_{di\text{-}RL}$.

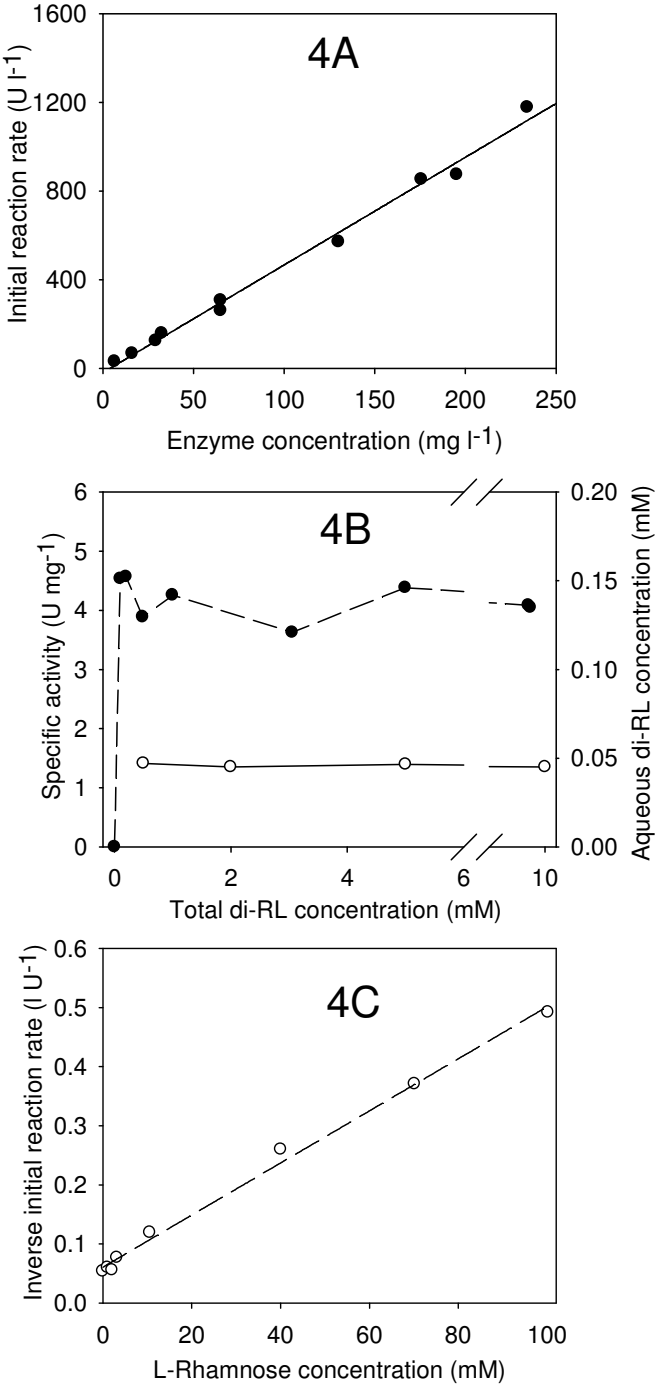

Figure 4: Effect on enzyme, di-RL and rhamnose concentration on initial reaction rates at 60 °C and pH 4.5. 4A: Influence of enzyme concentration. 4B: Aqueous di-RL concentration (○) and influence of initial di-RL concentration (●). 4C: Dixon plot showing L-rhamnose inhibition. Dashed line: linear fitting for determination of inhibition coefficient

Figure 4C shows the influence of L-rhamnose concentration on the inverse initial reaction rate. L-Rhamnose decreased conversion rates probably due to competitive inhibi-

tion since this inhibition type was already observed with other substrates (Romero et al. 1985). A regression quality R^2 of 0.9948 was obtained when experimental points were fitted to the Dixon transformation of equation 2 and an inhibition constant $K_{I,\,di\text{-}RL}$ of 9.7 ± 1.1 mM was therewith calculated. The kind of inhibition was not elucidated due to the difficulty to produce di-RL emulsions with varying di-RL aqueous concentrations. Figure 5 shows mono-RL and di-RL aqueous concentration in dependency of mono-RL total mole fraction of 10 mM emulsions.

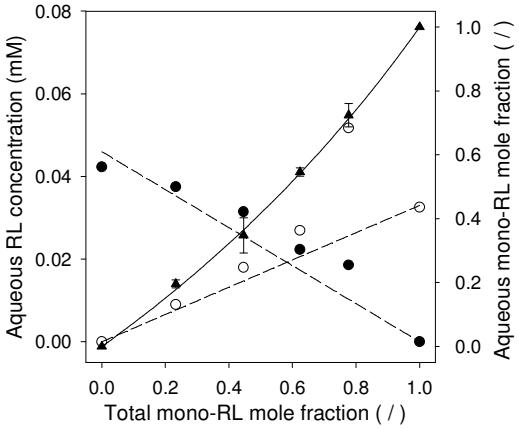

Figure 5: Effect of emulsion composition on the aqueous RL concentration: di-RL aqueous concentration (●), mono-RL aqueous concentration (○), and mono-RL aqueous mole fraction (▲). Dashed and full line: predictions considering ideal surfactant mixing

An agreement between measured concentrations and the linear dependency assuming ideal surfactant mixing (equation 4) was observed. This is an expected correlation since mixtures of two non-ionic surfactants often behave ideally (Holland and Rubingh 1992). By fitting the relation of aqueous to total mole fractions of mono-RL under ideal mixing to the experimental values of Figure 5 and taking $cmc_{di\text{-}RL}$ equals to 0.046 mM, the $cmc_{mono\text{-}RL}$ was estimated to be 0.033 ± 0.002 mM. Mixed emulsions of mono-RL and di-RL were apparently much more stable than pure mono-RL or di-RL emulsions and the micelle-phase could only be fully separated after 1 h centrifugation at 75600 g. The reason for this remains unclear.

Comparison of modeled and experimental reaction courses

Equation 1 simplifies considerably when the rate limiting step is the enzymatic conversion. After rearrangement and replacing C_{Rha} and $C^{aq}{}_{di\text{-}RL}$ as functions of $X^{T}{}_{di\text{-}RL}$ the following expression results:

$$\frac{dX^{T}_{mono-RL}}{dt} = \frac{(A_s / K_m)\cdot \rho_E \cdot cmc_{di-RL}\cdot X^{T}_{di-RL}}{C^{T}_{RL}\cdot\left[1+\dfrac{C^{T}_{RL}\cdot(X^{T}_{di-RL,0}-X^{T}_{di-RL})}{K_{I,di-RL}}\right]}\cdot\frac{V_{aq}}{V_T} \tag{6}$$

Figure 6A to 6D show experimental mono-RL mole fraction-time courses and its predictions by equation 6. Experimental courses are well predicted within the whole bioconversion time. Moreover, results obtained by equation 6 fits very well to experimental data considering variations in enzyme, di-RL and mono-RL concentrations. The goodness of fit between experimental and predicted is as high as 0.99 and parameter optimizations by fitting procedures were not required. Figure 6D shows bioconversion predictions of emulsions of higher RL concentrations. In this case, experimental observations were lower than predicted. Two reasons may account for this disagreement. First, at higher RL concentrations the volume of the micelle-phase can not be neglected and the ratio of aqueous to total volume of equation 6 can no longer be assumed to be unity. Since the micelle-phase consists of di-RL, mono-RL and water and assuming that most RL molecules are located in the micelle-phase the following relation can be derived:

$$\frac{V_{aq}}{V_T} = 1 - C_{RL}^{T} \cdot \frac{W_m}{X_{RL}^{m}} \tag{7}$$

In equation 7, W_m is the molar volume of the micelle-phase and X_{RL}^{m} the mole fraction of RL in the micelle-phase. After settling down the micelle-phase in a 100 mM di-RL emulsion, it was established that 1.6 g water per g di-RL is found in the micelle-phase. Therefore, X_{RL}^{m} equals 0.017. The micelle-phase molar volume was estimated from the molar volume of water and of RL considering its mole fractions as the weighting factor. Molar volumes of di-RL and mono-RL were estimated to be 0.5279 l mol^{-1} and 0.441 l mol^{-1} at 20°C, respectively (SciFinder Scholar database, American Chemical Society, Washington). Taking the mean of the above molar volumes, a value of 0.026 l mol^{-1} was therewith obtained for the micelle-phase. From a settled 100 mM di-RL emulsion at 60 °C the ratio V_{aq} to V_T was found to be 0.82 and W_m can be calculated from equation 7 as 0.029 l mol^{-1}. Thus, estimated and experimentally observed mole volumes were in accordance. Taken into account equation 7 for modeling with W_m equals to 0.029 l mol^{-1}, predictions were re-calculated and are shown in figure 6D as dashed lines. An enhanced prediction to experimental was achieved mainly for 91 mM emulsion.

The second reason for disagreement may have been enzyme deactivation during the longer conversion time. Considering a series-type thermal deactivation model of Naringinase, a correction factor was integrated in equation 6. Thus, the reaction rate r was multiplied by $a(t)$, the residual enzyme activity, which for Naringinase at reaction conditions (60 °C, pH 4.5 and absence of rhamnolipid) equals (Magario et. al 2008a):

$$a(t) = 0.14 \cdot e^{-k_1 \cdot t} + 0.86 \cdot e^{-k_2 \cdot t} \tag{8}$$

The kinetic constant k_1 and k_2 are equal to 8.67 10^{-3} and 5 10^{-5} min^{-1}, respectively (Magario et. al, 2008a). The dotted lines of figure 6D correspond to the prediction of equation 6 multiplied by the factor $a(t)$ and considering volume ratio correction. The residual

enzyme activity is also plotted as the dash-dotted line. A better agreement to experimental values (R^2 0.99) was therewith obtained. Thus, enzyme deactivation as well as volume ratio correction should be taken into account when biotransformations at high rhamnolipid concentrated emulsions are assayed during a larger reaction time.

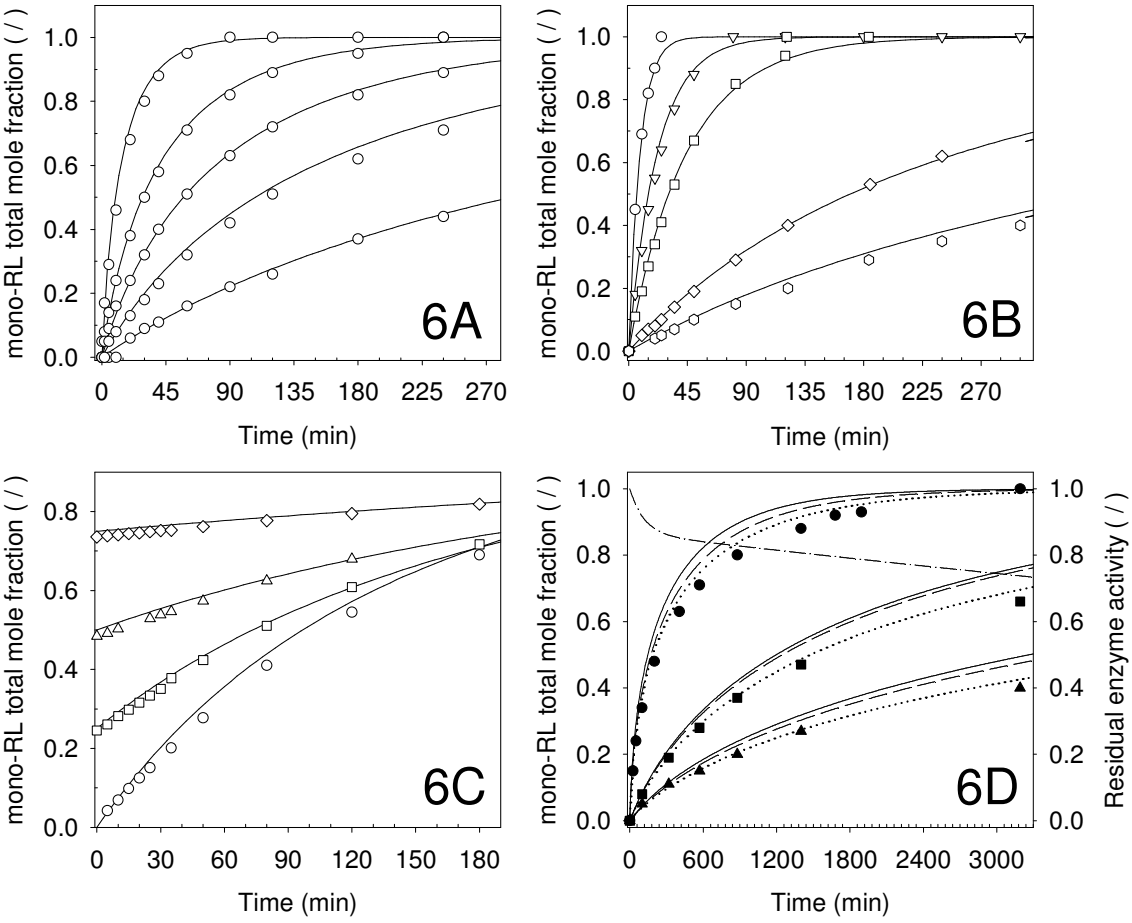

Figure 6: Prediction by equation 6 (full lines) and experimental values (points) of mono-RL mole fraction during different set of biotransformations at pH 4.5 and 60°C. 6A: 195.2; 65.0; 32.5; 16.2 and 6.5 mg l^{-1} enzyme concentration, respectively. 6B: 10; 5; 1; 0.5 and 0.2 mM di-RL, respectively. 6C: 0, 0.25, 0.5 and 0.75 initial mono-RL mole fraction, respectively. 6D: 91 mM di-RL (●), 47 mM di-RL (▲), 24 mM di-RL (■); dashed line: equation 6 multiplied by the volume ratio correction; dotted line: equation 6 multiplied by the volume ratio correction and the factor *a(t)*; dash-dotted line: residual enzyme activity

Consecutive mono-RL conversion

Naringinase is known to convert mono-RL into L-rhamnose and di-HDA however at much lower rates as compared to di-RL conversion (Meiwes et al. 1997; Trummler et al. 2003). Figure 7A shows the reaction course of mono-RL conversion by Naringinase.

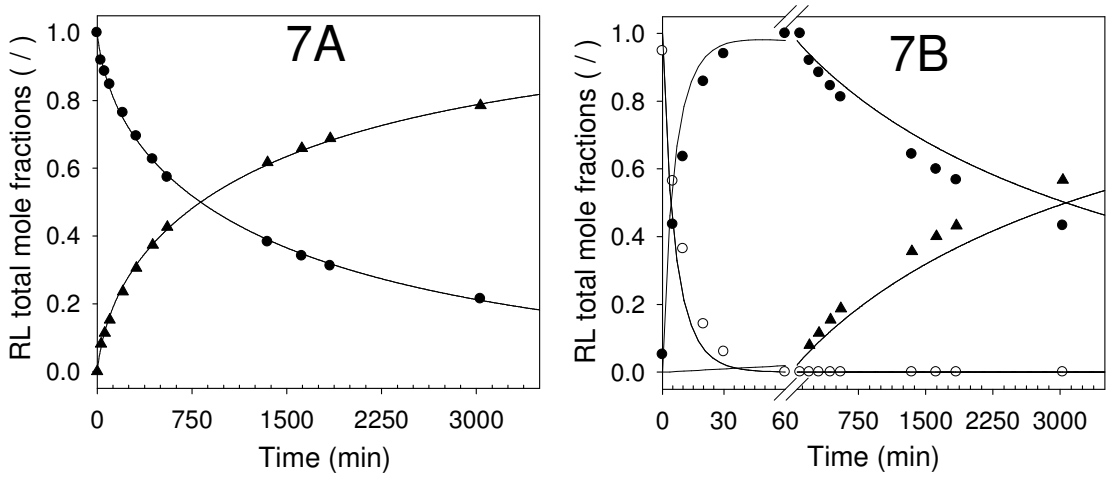

Figure 7: Mono-RL bioconversion. 7A: Bioconversion starting from mono-RL. 7B: Bioconversion starting from di-RL. Experimental mole fractions of di-RL (○), mono-RL (●), and di-HAD (▲). Lines: Prediction by the opposite of equation 6 for di-RL mole fraction, equation 9 for mono-RL mole fraction and the opposite of the second term of the right side of equation 9 for di-HDA mole fractions

Equation 6 can easily be modifed for mono-RL-conversion provided ideal mixing of the surfactants mono-RL and di-HDA. By fitting equation 6 to the experimental points of figure 7A the parameters A_s/K_m and K_I for mono-RL as substrate were deduced. Since substrate and product in this case are mono-RL and di-HDA, respectively, the mole fraction of equation 6 were replaced accordingly for modeling the second reaction. A A_s/K_m value of 0.0019 l min^{-1} mg^{-1} and a K_I value of 1.2 mM were hence obtained with a goodness of fit of 0.99 taking into account enzyme deactivation during reaction according to equation 8. The mono-RL mole fraction can be modeled considering the consecutive reaction by subtracting to the right term of equation 6 the consumption term due to mono-RL- bioconversion:

$$\frac{dX^T_{mono-RL}}{dt} = \frac{(A_s/K_m)_{di-RL}\cdot\rho_E\cdot cmc_{di-RL}\cdot X^T_{di-RL}}{C^T_{RL}\cdot\left[1+\frac{C^T_{RL}\cdot(X^T_{di-RL,0}-X^T_{di-RL})}{K_{I,di-RL}}\right]} - \frac{(A_s/K_m)_{mono-RL}\cdot\rho_E\cdot cmc_{mono-RL}\cdot X^T_{mono-RL}}{C^T_{RL}\cdot\left[1+\frac{C^T_{RL}\cdot(1+X^T_{di-RL,0}-2\cdot X^T_{di-RL}-X^T_{mono-RL})}{K_{I,mono-RL}}\right]} \quad (9)$$

Figure 7B shows the reaction course starting from a di-RL mole fraction equals to 1. Di-RL is nearly totally converted before mono-RL bioconversion becomes detectable and this could properly be predicted by equation 9. Due to product inhibition by the a-

ccumulated L-rhamnose from the former conversion, the higher the initial di-RL concentration, the lower the subsequent mono-RL conversion rate should be. This effect could be utilized as an additional control parameter for avoiding the subsequent mono-RL conversion. Table 3 gives an overview of all parameter values used for prediction equations.

Table 3: Value of the model parameters

	cmc (mM)	A_s/K_m (l min^{-1} mg^{-1})	K_I (mM)	W_m (l mol^{-1})
di-RL	0.046 ± 0.001 *	0.104 ± 0.004 *	9.7 ± 1.1 *	0.029 *
Mono-RL	0.033 ± 0.002 *	0.0019 ± 0.00026 **	1.2 ± 0.3 **	

* Experimental determination

** Determined by fitting equation 6 to the experimental points of figure 7A. Initial parameters values were set at 0.001 l min^{-1} mg^{-1} for $(A_s/K_m)_{mono\text{-}RL}$ and at 9.7 mM for $K_{I,mono\text{-}RL}$.

Discussion

A number of publications deal with modeling of enzymatic reactions with mixed micellar substrates assuming enzyme adsorption in the interface. Although kinetic courses could be predicted by assuming reaction in the aqueous phase, enzyme adsorption to the micelles with consequent interfacial hydrolysis can also occur. Straathof (2003) postulated that the location of the reaction is difficult to determine from measurement of changes in substrate concentration alone. In the case of interfacial reaction the first step is the fixation of a water-soluble enzyme to a lipid/water interface followed by a 2D Michaelis-Menten catalytic step (Panaiotov et al. 1997). However, the enzymes involved there were lipases and phospholipases, some of them showing interfacial activation, and whose natural substrates are insoluble and located into aggregates (Panaiotov et al. 1997; Rubingh 1996). On the other hand, Naringinase used in this study is not expected to adsorb to an interface for substrate attack and no observations were made that may indicate interfacial activation. To our knowledge there are no glycosidases other than cellulases showing interfacial activity. The terms “interfacial activation” or “interfacial catalysis” seems only to be applicable for lipases and phospholipases (Straathof 2003). Chopineau et al. (1998) observed from kinetic studies that ß-D-glucosidase did not accept micelles as substrates but only the monomeric form of octyl-ß-D-glucopyranoside. Furthermore, there are some observations supporting the idea of aqueous phase reaction: 1) in the case of bioconversion of micellar substrates with lipases a Michaelis-Menten behavior between reaction rate and total bulk concentration was often observed (Deems et al. 1975; Redondo et al. 1995; Rubingh and Bauer 1992). In the present case the reaction rate was independent of the total bulk RL concentration indicating that aqueous reaction may apply; 2) in co-incubation experiments, Naringinase was able to cleave pnpR in the presence of RL micelle-phase in a similar rate that without RL. This may indicate that most enzyme molecules remained in the aque-

ous phase; 3) recent results regarding kinetic data of di-RL conversion with immobilized Naringinase on porous supports (Magario et al. 2008b), could be interpreted considering high intern diffusion-limited reaction rate due to the very low aqueous di-RL concentration.

Low-molecular alcohols are known to increase the *cmc* of non-ionic surfactants due to a weakening of its hydrophobic bonding. Higher alcohols cause however a *cmc* decrease as a consequence of its penetration into the micelles (Attwood and Florence 1983). Assuming aqueous reaction applies, variation in *cmc* of di-RL should strongly affect reaction rates. However, when trying to increase *cmc* values by addition of co-solvents or varying bulk pH increasing reaction rates were not observed and an overall little effect was detected. Changes in the reaction rates are presumably the result of two coupled phenomena, namely increased reaction rates due to increased monomer availability (*cmc*) and decreased enzyme activity due to condition variations. This explanation may be supported by the observation that decreasing reaction rate due to alcohol addition or bulk pH are more pronounced for other substrates like pnpR (Romero et al. 1985).

Romero et al. (1985) determined kinetic data with pnpR and Naringin at optimal conditions (pH 3.5 and 57°C): A_s values of 10.7 and 150 U mg^{-1}; K_m values of 1.52 and 7.0 mM. This results in A_s/K_m values of 0.007 and 0.021 l min^{-1} mg^{-1} for pnpR and Naringin, respectively. The rate constants A_s/K_m for di-RL and mono-RL are 0.104 and 0.0019 l min^{-1} mg^{-1}, respectively. This indicates that the substrate specificity of Naringinase is in the sequence: di-RL > Naringin > pnpR > mono-RL (see Table 3) and following conclusions may be extracted: 1) The 1->2 Rha-Rha linkage of di-RL can be hydrolyzed more efficiently than the 1->2 Rha-glucose linkage of Naringin; 2) Rhamnose is cleaved from mono-RL much slower than from pnpR probably due to steric hindrance of the larger aglycone portion of mono-RL. Moreover, the larger specificity towards substrates as di-RL or Naringin compared with pnpR and mono-RL is in agreement with the findings of Michon et al. (1989), who established that Naringinase can hydrolyze more rapidly rhamnose from glycosidic linkage rather than from an aglycone linkage.

Conclusion

From this study it can be concluded that Naringinase from *Penicillium decumbens* is an appropriate catalyst for the bioconversion of di-RL into mono-RL and L-rhamnose. Kinetic data of the hydrolysis of an aggregating substrate, di-RL by Naringinase was properly modeled. The apparent non-Michaelis-Menten behavior was interpreted by assuming an enzymatically rate-controlled reaction in the aqueous phase. Moreover, the well predicted effects to changes in the initial mono-RL mole fraction suggest that the strong influence of mono-RL on reaction rates is exclusively due to ideal surfactant

mixing, and further effects like product inhibition are negligible. This approach may also be applied when RL other than di-RL and mono-RL are present in the reaction system. Moreover, the findings of this study may beneficially be adapted for any bioconversions involving aggregate-forming substrate and/or product being catalyzed by hydrophilic enzymes.

Acknowledgments

We would like to thank for the financial support of this project carried out in the framework of an EU-CRAFT project (1999-72243) entitled "Integrated process for biosurfactant synthesis at competitive cost allowing for their application in household cleaning and bio-remediation" (InBioSynAp).

Nomenclature

a	Interfacial area relative to the aqueous phase (m^{-1})
A_s	Maximal specific enzyme activity (mmol min^{-1} mg^{-1})
$a(t)$	Residual enzyme activity (/)
C	Substrate or product concentration (mM)
cmc	Critical micelle concentration
di-HDA	3-(3-hydroxydecyloxy)decanoic acid
k_1 and k_2	Enzyme deactivation constants (min^{-1})
K_I	Rhamnose inhibition constant (mM)
$k_{L,di\text{-}RL}$	di-RL lumped mass transfer coefficient (m min^{-1})
K_m	Michaelis-Menten constant (mM)
pnpR	p-nitrophenyl-L-α-rhamnoside
r	Enzymatic reaction rate (mmol l^{-1} min^{-1})
mono-RL	Mono-rhamnolipid or rhamnolipid 1
di-RL	Di-rhamnolipid or rhamnolipid 3
Rha	L-Rhamnose
RL	Rhamnolipids
V	Volume (l)
W_m	Molar volume of the micelle-phase (l mol^{-1})
X	Mole fraction
$\phi_{di\text{-}RL}$	di-RL mass transfer rate; $\phi_{di-RL} = k_{L,di-RL} \cdot a \cdot \left(C_{di-RL}^{aq,eq} - C_{di-RL}^{aq}\right)$ (mmol min^{-1} l^{-1})
ρ_E	Enzyme mass concentration (mg l^{-1})

Sub- and super-indices

aq	Aqueous phase
eq	In equilibrium

m	Micelle-phase
T	Sum of aqueous and micelle phases

References

Attwood D, Florence AT. 1983. Surfactant systems: their chemistry, pharmacy and biology. London: Chapman and Hall.

Banat IM, Makkar RS, Cameotra SS. 2000. Potential commercial applications of microbial surfactants. Appl. Microbiol. Biotechnol. 53(5):495-508.

Champion JT, Gilkey JC, Lamparski H, Retterer J, Miller RM. 1995. Electron-Microscopy of Rhamnolipid (Biosurfactant) Morphology - Effects of Ph, Cadmium, and Octadecane. J. Colloid Interface Sci. 170(2):569-574.

Chopineau J, Lesieur S, Carion-Taravella B, Ollivon M. 1998. Self-evolving microstructured systems upon enzymatic catalysis. Biochimie 80(5-6):421-435.

Deems RA, Eaton BR, Dennis EA. 1975. Kinetic analysis of phospholipase-A2 activity toward mixed micelles and its implications for study of lipolytic enzymes. J. Biol. Chem. 250(23):9013-9020.

Giani C, Wullbrandt D, Reinhardt R, Meiwes J; Hoechst AG, assignee. 1993. *Pseudomonas aeruginosa* and its use in a process for the biotechnological preparation of L-rhamnose. Germany patent US5501966.

Holland PM, Rubingh DN. 1992. Mixed surfactant systems - an overview. ACS Symp. Ser. 501:2-30.

Ishigami Y, Gama Y, Nagahora H, Yamaguchi M, Nakahara H, Kamata T. 1987. The pH-sensitive conversion of molecular aggregates of Rhamolipid bisurfactant. Chem. Lett.(5):763-766.

Lang S, Trowitzsch-Kienast W. 2002. Biotenside. Stuttgart Leipzig Wiesbaden: Teubner.

Lebron-Paler A, Pemberton JE, Becker BA, Otto WH, Larive CK, Maier RM. 2006. Determination of the acid dissociation constant of the biosurfactant monorhamnolipid in aqueous solution by potentiometric and spectroscopic methods. Anal. Chem. 78(22):7649-7658.

Levenspiel O. 1999. Chemical Reaction Engineering: John Wiley & Sons.

Linhardt RJ, Bakhit R, Daniels L, Mayerl F, Pickenhagen W. 1989. Microbially produced Rhamnolipid as a source of rhamnose. Biotechnol. Bioeng. 33(3):365-368.

Magario I, Neumann A, Oliveros E, Syldatk C. 2008a Deactivation kinetics and response surface analysis of the stability of alpha-L-rhamnosidase from *Penicil-*

lium decumbens. Appl. Biochem. Biotechnol. In press. DOI: 10.1007/s12010-008-8204-5

Magario I, Xiaotian M, Neumann A, Syldatk C, Hausmann R. 2008b Non-porous magnetic micro-particles: Comparison to porous enzyme carriers for a diffusion rate-controlled enzymatic conversion. J. Biotechnol. 134:72-78. DOI: 10.1016/j.jbiotec.2007.12.001.

Meiwes J, Wullbrandt D, Giani C; Hoechst AG, assignee. 1997. alpha -l-rhamnosidase for obtaining rhamnose, a process for its preparation and its use. Germany patent US5641659.

Michon F, Pozsgay V, Brisson JR, Jennings HJ. 1989. Substrate specificity of Naringinase, an alpha-L-rhamnosidase from *Penicillium decumbens*. Carbohydr. Res. 194:321-324.

Milioto S. 2006. Mixed micellar systems. In: Somasundaran P, editor. Encyclopedia of surface and colloid science. 2 ed. New York: Taylor & Francis. p 3233-4198.

Mixich J, Rapp K, Vogel M; Suedzucker AG. 1996. Method for the preparation of rhamnose monohydrate from rhamnolipids. Germany patent US5550227.

Mulligan CN. 2005. Environmental applications for biosurfactants. Environ. Pollut. 133(2):183-198.

Nitschke M, Costa S, Contiero J. 2005. Rhamnolipid surfactants: An update on the general aspects of these remarkable biomolecules. Biotechnol. Prog. 21(6):1593-1600.

Ozdemir G, Peker S, Helvaci SS. 2004. Effect of pH on the surface and interfacial behavior of rhamnolipids R1 and R2. Colloids Surf., A 234(1-3):135-143.

Panaiotov I, Ivanova M, Verger R. 1997. Interfacial and temporal organization of enzymatic lipolysis. Curr. Opin. Colloid Interface Sci. 2(5):517-525.

Redondo O, Herrero A, Bello JF, Roig MG, Calvo MV, Plou FJ, Burguillo FJ. 1995. Comparative kinetic study of lipase-A and lipase-B from *Candida rugosa* in the hydrolysis of lipid p-nitrophenyl esters in mixed micelles with Triton-X-100. Biochim. Biophys. Acta 1243(1):15-24.

Romero C, Manjon A, Bastida J, Iborra JL. 1985. A method for assaying the Rhamnosidase activity of Naringinase. Anal. Biochem. 149(2):566-571.

Rubingh DN. 1996. The influence of surfactants on enzyme activity. Curr. Opin. Colloid Interface Sci. 1(5):598-603.

Rubingh DN, Bauer M. 1992. Lipase catalysis of reactions in mixed micelles. ACS Symp. Ser. 501:210-226.

Schenk T, Schuphan I, Schmidt B. 1995. High performance liquid chromatographic determination of the Rhamnolipids produced by *Pseudomonas aeruginosa*. J. Chromatogr. A 693(1):7-13.

Straathof AJJ. 2003. Enzymatic catalysis via liquid-liquid interfaces. Biotechnol. Bioeng. 83(4):371-375.

Syldatk C, Lang S, Wagner F, Wray V, Witte L. 1985. Chemical and physical characterization of four interfacial-active rhamnolipids from *Pseudomonas* spec. DSM 2874 grown on n-alkanes. Z Naturforsch [C] 40(1-2):51-60.

Trummler K, Effenberger F, Syldatk C. 2003. An integrated microbial/enzymatic process for production of rhamnolipids and L-(+)-rhamnose from rapeseed oil with Pseudomonas sp DSM 2874. Eur. J. Lipid Sci. Technol. 105(10):563-571.

4.3 Enzyme Carrier Evaluation for Conversion of Rhamnolipids

EVALUATION OF ENZYME CARRIERS AS BIOCATALYSTS FOR THE CONVERSION OF EMULSIFIED RHAMNOLIPIDS

(Submitted)

I. Magario *, A. Neumann, C. Syldatk, O. Vielhauer [a], R. Hausmann

Institute of Engineering in Life Sciences, Chair of Technical Biology, University of Karlsruhe (TH), Germany

[a] Institute of Biochemical Engineering, University of Stuttgart, Germany

* Corresponding author: I. Magario
Tel: +49-721-608-6736/8428
Fax: +49-721-608-4881
E-mail: Ivana.Magario@tebi.uni-karlsruhe.de (I. Magario)
Rudolf.Hausmann@tebi.uni-karlsruhe.de (R. Hausmann)

Key words: immobilization, micro-carriers, Naringinase, rhamnolipids, α-L-rhamnosidase

Abstract

Different carriers were evaluated for Naringinase immobilization with respect to activity yield, activity loading and operational stability for the conversion of emulsified di-rhamnolipid to mono-rhamnolipid and L-rhamnose. Highest specific carrier activities of 88 U g^{-1} with activity yields of 36 % were obtained with micro non-porous carriers. Specific activities of porous-type carriers were much lower due to strong diffutional substrate limitations. Furthermore, the effect of protein and activating-reagent concentration on immobilized enzyme activities on micro non-porous carriers was investigated by response surface methodology. Immobilized enzyme activities gradually decreased with protein loading whereas the activating-reagent concentration hardly affected them.

Introduction

Rhamnolipids are microbial biosurfactants produced as a mixture of species containing one (mono-rhamnolipid) or two (di-rhamnolipid) rhamnose molecules attached to ß-hydroxy fatty acid moieties (Lang and Trowitzsch-Kienast 2002; Syldatk et al. 1985). For industrial applications pure species are generally more desirable than mixtures. The most straightforward approach for achieving pure rhamnolipids is by enzymatic modification. The α-L-rhamnose cleavage of di-rhamnolipid (di-RL) by α-L-rhamnosidase from *Penicillium decumbens* (termed Naringinase) is illustrated in Figure 1 (Trummler et al. 2003).

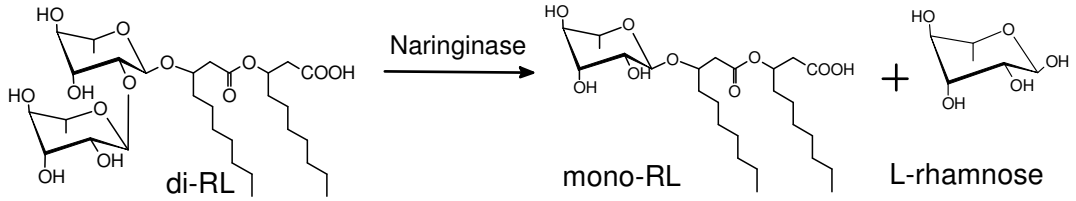

Figure 1: Hydrolysis of di-rhamnolipid (di-RL) into mono-rhamnolipid (mono-RL) and L-rhamnose

In this system nearly total rhamnolipids are bound to micelles, whereas only truly dissolved molecules are available for enzymatic hydrolysis. Thus, the substrate concentration is very low at reaction conditions, 0.05 mM. Reaction kinetics by free α-L-rhamnosidase was successfully described considering the aggregation state of substrate and product. Details will be published elsewhere.

In order to allow enzyme re-use and facilitate product recovery enzyme immobilization is required. A number of previous works reported on α-L-rhamnosidase immobilization (Ellenrieder and Daz 1996; Manjon et al. 1985; Norouzian et al. 1999; Puri et al. 2001; Puri et al. 1996; Sekeroglu et al. 2006; Soares and Hotchkiss 1998; Tsen et al. 1989; Turecek and Pittner 1986). However, the emphasis was to use immobilized Naringinase in column reactors for juice debittering or for preparation of aglycones and none of these works used rhamnolipids as substrate for testing immobilized activity.

The aim of this work was to select a suitable carrier material for α-L-rhamnosidase immobilization for the conversion of di-rhamnolipid to mono-rhamnolipid. Due to the low substrate solubility, immobilized enzyme on micro non-porous carriers is expected to display a higher activity as compared to immobilized enzyme on conventional porous carriers. Immobilized enzyme activities were also co-evaluated with the well-soluble substrate p-nitrophenyl-rhamnoside. Additionally, due to the use of a rather impure enzyme preparation, foreign proteins may be co-immobilized and thus account for a lowering of immobilized enzyme activity. To establish if a more specific immobilization

increases activity, two different strategies were pursued: biospecific immobilization by adsorption of the target glyco-enzyme on a Concanavalin A pre-coupled carrier material (Saleemuddin and Husain 1991) and immobilization of an enriched α-L-rhamnosidase.

Materials and methods

Materials

Naringinase was purchased from Sigma Aldrich (Lot N° 110K16471). Crystalline di-rhamnolipid (di-RL) (97 % purity) was a kind gift from Hoechst AG (Frankfurt, Germany) whereas p-nitro-phenyl-rhamnoside (pnpR) was obtained from Extrasynthese (Genay, France). Amine-functionalized poly-(vinyl-alcohol)-coated micro beads (M-PVA) were obtained from Chemagen AG (Baesweiler, Germany). Eupergit 250L were kindly donated by Degussa, Röhm GmbH & Co. KG (Darmstadt, Germany) whereas CNBr-Sepharose 4B, ConA-Sepharose, NHS-Sepharose and DEAE-Sepharose were purchased from Amersham Biosciences Ltd. (Uppsala, Sweden). Table 1 lists all relevant carrier properties. All other chemicals, solvents and immobilization reagents were of analytical grade.

Table 1: Relevant carrier properties (supplier information)

	Matrix	Particle size	Functionality	Pore size
Micro-carriers	Poly-(vinyl) alcohol	1-3 µm	Amine	-
Eupergit 250L	Copolymer of methacrylamide	190 µm	Oxirane	200 nm
Eupergit C	Copolymer of methacrylamide	170 µm	Oxirane	20 nm
CNBr-Sepharose	4% agarose	90 µm	Cyanate esters	NK [b]
ConA-Sepharose	4% agarose	90 µm	Concanavalin A	NK [b]
NHS-Sepharose	6% agarose	34 µm	Activated carboxylate [a]	NK [b]
DEAE-Sepharose	4% agarose	90 µm	Diethylaminoethyl	NK [b]

[a] 10-atom spacer arms of 6-aminohexanoic acid attached by epichlorohydrin and activated by N-hydroxysuccinimide . [b] NK: not known

Immobilization of Naringinase

Immobilization on M-PVA was conducted by the carbodiimide method according to Ragnitz et al. (2001). 25 mg beads per ml enzyme solution at different concentrations were applied. Immobilization on Eupergit C and Eupergit 250L was carried out according to supplier recommendations. The bead concentration was set at 166 mg ml^{-1} and different protein concentrations were applied. After immobilization the beads were incubated with Tris-HCl, pH 8.0 for abreacting remaining oxirane groups. Immobilization on CNBr-Sepharose, ConA-Sepahrose, and NHS-Sepharose was performed according to supplier recommendations. The bead concentration was always set at 400 mg ml^{-1} and different protein concentrations were applied. After immobilization, CNBr- and

NHS-Sepharose beads were incubated with Tris-HCl, pH 8, for abreacting remaining active groups while ConA-Sepharose beads were let to stand with 0.2 % glutaraldehyde solution in phosphate buffer pH 6.1 for 2 h at 30°C to facilitate cross-linking (Iqbal and Saleemuddin 1985). For washing-steps after immobilization, suspensions were dumped into a disposable filtration device (Vivaspin 4 - 0.2 µm PES membrane, Vivascience-Sartorius group, Hannover, Germany). For ionic adsorption on DEAE-Sepharose, 2 ml Naringinase solution at 2 g l^{-1} in Tris-HCl 20 mM pH 8.0 were incubated with 250 mg wet particles for 3 h at 30°C. Particles were centrifuged and washed several times with coupling buffer and stored at 4°C as wet beads (Ono et al. 1977). Calcium alginate derivates were prepared according to Puri et al. (1996) by mixing 3 ml of a 0.6 g l^{-1} Naringinase solution with 7 ml 3 % sodium alginate.

Determination of protein coupling yields

Protein coupling yields Y_P (%) as well as protein loadings q_P (mg g^{-1}) were calculated based on protein mass balances. Therefore, protein content of Naringinase start-solution, supernatant and first three wash solutions after immobilization were determined by the Bradford assay.

α-L-Rhamnosidase enrichment

Enrichment of α-L-rhamnosidase from the commercial powder was carried out with an ÄKTAexplorer equipment coupled to a control system (UNICORN) (both: Amersham Biosciences, Uppsala, Sweden). 5 g Naringinase powder (7.8 % protein content) were charged on a 20 ml Hiload Q-sepharose HP column (Amersham Biosciences, Uppsala, Sweden) and eluted in 50 mM potassium phosphate buffer pH 6.5 at 4 ml min^{-1} after 12 column-volume (CV) equilibration time with a 40 CV linear gradient from 0 to 0.5 M potassium chloride. Fractions containing α-L-rhamnosidase were pooled, desalted and concentrated in a stirred ultrafiltration cell (Amicon Inc., Beverly, USA) with a 30 kDa exclusion size membrane (Millipore, Bedford, USA). 103 mg enriched enzyme with about a 2-fold increase in specific activity (132 U mg^{-1}) compared to start preparation were obtained.

Activity determination

Di-RL-activity assays were carried out by adding an enzyme solution to a 5 mM di-RL emulsion at 60°C in 0.1 M sodium acetate pH 4.5, in a ratio 1 to 20. A sample volume of 500 µl was admixed with 50 µl 1 M phosphoric acid and rhamnolipids were extracted with 500 µl ethyl acetate for stopping of the enzymatic reaction. Then, rhamnolipids were gained by evaporation of the ethyl acetate phase and re-dissolving in acetonitrile for analysis. Activity assays with immobilized Naringinase were modified as follows:

wet beads of derivates (Eupergit C, Eupergit 250L, CNBr-Sepharose, ConA-Sepharose and alginate beads) were weighted and mixed with a temperate substrate solution or; derivate suspensions (NHS-Sepharose and M-PVA beads) were added to the substrate solution. Samples were centrifuged or magnetically separated from the beads after solvent extraction. The activity was calculated as the average of initial increase of monorhamnolipid (mono-RL) and initial decrease of di-RL concentration. One unit di-RL was defined as the amount that converts 1 µmol di-RL to mono-RL in 1 minute at 60°C and pH 4.5. PnpR-activities were carried out by adding 50 µl enzyme solution to 950 µl of a 4 mM pnpR solution in 0.1 M sodium acetate pH 5.5 at 60°C. The increase of p-nitrophenolate concentration was followed by monitoring the absorption at 400 nm. For conversion with immobilized Naringinase the derivates were added to the substrate solution as described above and the activity was assayed according to Romero et al. (1985). One unit pnpR was defined as the amount that converts 1 µmol pnpR to pnp in 1 minute at 60°C and pH 5.5. Activity determination of alginate beads was carried out at 45°C and a calcium chloride solution was added to the reaction medium to a final concentration of 0.1 M. Single activity determinations were always carried out. Immobilized activity u^{IM} (U mg^{-1}) was calculated as the quotient between activity loading q_A (U g^{-1}) and protein loading q_P (mg g^{-1}). The overall activity yield, Y_A (%) was calculated as the ratio between units recovered after immobilization (q_A multiplied by the applied amount of carrier) and the total units offered for immobilization (specific activity of the free enzyme (U mg^{-1}) multiplied by the amount of applied enzyme).

Determination of the operational stability

The stability of derivates was measured by repeated batch conversion of a 5 mM di-RL emulsion in sodium acetate buffer pH 4.5 at 60°C in 2 h intervals. Between each batch step, the derivates were washed with buffer. Conversions in a termo-block unit were applied for M-PVA derivates whereas conversions by ConA-Sepharose derivates were conducted in a stirred ultrafiltration cell with a 0.2 µm cellulose filter (Millipore, Bedford, USA).

Rhamnolipid analytics

Rhamnolipids were analyzed by chromatography on a HPLC device coupled to a UV detector (Agilent 1100 Series) according to Schenk et al. (1995). High pure standard of mono-RL was prepared according to Trummler et al. (2003). Mono-RL was further purified by adsorption chromatography with fine silica gel as stationary phase and a chloroform/methanol 3:1 v/v solution as mobile phase. After elution, the mobile phase was evaporated and mono-RL was re-dissolved in ethyl acetate. After drying, the organic phase was fully evaporated under high vacuum.

Optimization of coupling conditions

Coupling conditions for immobilization on M-PVA were optimized by experimental design methodology (Aktinson 1992; Box et al. 1978; Khuri and Cornell 1987; Rasch et al. 1999). Experimental responses were fitted to an empirical quadratic polynomial model of the form:

$$Y = b_0 + \sum b_i \cdot X_i + \sum b_{ii} \cdot X_i^2 + \sum \sum b_{ij} \cdot X_i \cdot X_j \qquad (1)$$

In equation 1, b_0 is the average of all experimental responses, b_i the main effect coefficient of the variable X_i, b_{ii} the second order effect coefficient of the variable X_i and b_{ij} the interaction effect coefficient between variables X_i and X_j $(i \neq j)$. The least-square estimates of the coefficients of the model were calculated from the values of the response Y for each experiment in the chosen experimental matrix. As a result three-dimensional representations of the responses were obtained (BenoitMarquie et al. 1997; Oliveros et al. 1997; Oliveros et al. 2000). Among all immobilization parameters two of them were selected for optimization: the mass ratio protein to bead, $q_{P,0}$ (in mg g^{-1}) and the mass ratio between the activating-reagent EDC (N-(3-dimethylaminopropyl)-N´-ethylcarbodiimide hydrochloride) and the protein, $R_{EDC/P}$ (in µmol mg^{-1}). The resulted immobilized activity u^{IM} was taken as the response Y_i for every assay. A Doehlert array (BenoitMarquie et al. 1997; Oliveros et al. 1997; Oliveros et al. 2000) was selected as experimental design. This array consisted of 7 experiments optimally distributed within the experimental region. Additionally, two replicates at the centre of the experimental matrix were conducted for determination of the standard deviation of the response. The independent variables were modified within the ranges 0.5 – 18.7 mg g^{-1} for $q_{P,0}$ and 7 – 180 µmol mg^{-1} for $R_{EDC/P}$. The value at the centre of the range (U_0) was set to 9.6 for $q_{P,0}$ and 94 for $R_{EDC/P}$ and the step (ΔU) was equal to 9.1 for $q_{P,0}$ and 100 for $R_{EDC/P}$.

Table 2 lists the experimental matrix in normalized and effective variables. For building the experimental matrix, calculating the coefficients of the model, evaluating the significance of regression and performing the validity tests, the program NEMRODW (LPRAI, Marseille, France) was used.

Table 2: Applied experimental matrix at 5 levels for $q_{P,0}$ and 3 levels for $R_{EDC/P}$

Assay N°	$q_{P,0}$ (mg g^{-1})[a]		$R_{EDC/P}$ (µmol mg^{-1})[b]		C_P (mg l^{-1})[c]	C_{EDC} (mM)[d]
	coded	Effective	coded	Effective	Effective	Effective
1	1.000	18.7	0	94	468	44
2	-1.000	0.5	0	94	12.5	1.2
3	0.500	14.1	0.866	180	354	64
4	-0.500	5.0	-0.866	7	126	0.9
5	0.500	14.1	-0.866	7	354	2.5
6	-0.500	5.0	0.866	180	126	23
7	0	9.6	0	94	240	23
8	0	9.6	0	94	240	23
9	0	9.6	0	94	240	23

[a] $q_{P,0}$: Initial protein to carrier mass ratio. [b] $R_{EDC/P}$: Activating reagent to protein mass ratio. [c] C_P: Protein concentration. [d] C_{EDC}: activating-reagent concentration.

Results

Effect of carrier type

Results of protein and activity coupling are summarized in Table 3. Protein coupling yields were rather high compared to the theoretical maximum for all carriers tested suggesting a potentially greater loading capacity. Protein activities of free enzyme u^F were equal to 55 and 65 U mg^{-1} for di-RL and pnpR, respectively. Thus, for all methods immobilized enzyme activities u^{IM} values were lower than the corresponding values for free enzyme.

Table 3: Protein- and activity-coupling results for immobilization on different carriers. 4 mg protein mass per ml carrier volume was incubated for immobilization in each case.

	Protein coupling		Substrate: di-RL			Substrate: pnpR		
	q_P[a] (mg g^{-1})	Y_P[b] (%)	q_A[c] (U g^{-1})	Y_A[d] (%)	u^{IM}[e] (U mg^{-1})	q_A[c] (U g^{-1})	Y_A[d] (%)	u^{IM}[e] (U mg^{-1})
Eupergit C	2.4	72	4	2	1.5	11	5	4.5
Eupergit 250L	3.7	93	11	5	3.0	33	13	8.8
CNBr-Sepharose	4.1	98	14	6	3.3	64	24	15.7
NHS-Sepharose	3.2	69	30	12	9.2	114	37	35.4
Micro-carrier	1.5	74	48	43	32.0	21	16	14.1

[a] q_P: Protein loading. [b] Y_P: Protein coupling yield (100 % equals to coupling of total protein-mass offered for immobilization). [c] q_A: Activity loading. [d] Y_A: Overall activity yield (100 % equals to coupling of total di-RL- or pnpR-units offered for immobilization). [e] u^{IM}: Immobilized enzyme activity.

An increase of loaded activity q_A and of activity yield with decreasing particle radius is observed. For conversion of di-RL the highest carrier activity and simultaneously the highest overall activity yield were found with M-PVA derivates of 1 µm size. Concerning pnpR activities, higher yields compared to di-RL conversions were observed for all

derivates. One exception occurred with M-PVA derivates, where low activity values resulted.

Higher protein loadings were achieved with Eupergit 250L than for Eupergit C although the type C has a higher density of epoxy groups (Boller et al. 2002). The smaller pores of the type C may obstruct enzyme diffusion resulting in a lower protein loading than for the type 250L. Similar results were also obtained by Manjon et al. (1985) when testing Naringinase immobilization on controlled pores glass particles of different pore sizes. As expected, substrate diffusion is also retarded in comparison with the type 250L resulting in lower immobilized activity values for both substrates.

Anionic adsorption and entrapment on alginate beads were tested as comparison, since it was expected that these methods would be relatively gentle. High protein coupling was obtained on DEAE-Sepharose. However, enzyme leaching was detected at reaction conditions and therefore this method was discarded. On the other hand, poor activity yields were observed when Naringinase was assayed for entrapment on 2 % alginate beads. The beads lost 90 % of the initial activity when assayed in a second conversion batch presumably due to enzyme leaching.

Specific immobilization

Direct biospecific adsorption of Naringinase on ConA-Sepharose resulted in enzyme leaching under reaction conditions. Therefore, Naringinase had to be covalently bond to Concanavalin A by glutaraldehyde cross linking after adsorption (Saleemuddin and Husain 1991). No leaching could be observed when the immobilized enzyme was treated with the strong eluent α-D-methylglucoside, thus confirming its covalent attachment (Iqbal and Saleemuddin 1985). Figure 2 shows the ratio of immobilized to free enzyme activity (u^{IM}/u^{F}) for immobilizations carried out from the raw enzyme powder and from the enriched preparation. This ratio is also shown for immobilization of the raw enzyme powder on the non-specific CNBr-Sepharose and on ConA-Sepharose. Activities were determined with pnpR for reducing diffusion effects that could mask any improvement due to specific immobilization. Since ConA-Sepharose consists of Concanavalin A pre-coupled on CNBr-Sepharose particles, both resin types are best compared to establish specific immobilization in the former.

The ratio u^{IM}/u^{F} was enhanced for immobilization from the enriched compared to the raw-powder preparation for both carrier types, Eupergit 250L and M-PVA. However, the overall activity yield was enhanced in a lower extend since the protein coupling was lower for the enriched preparations. With ConA-derivates a 2-fold enhancement of the u^{IM}/u^{F} value was observed in comparison with CNBr-derivates. A purification effect during immobilization was detected as the specific activity of the remained protein in the supernatant was dramatically lowered for ConA-supernatant (5 U mg^{-1}) in compari-

son to the CNBr-supernatant (37 U mg^{-1}). However, increasing the protein loading on ConA-derivates did not improve immobilized activities compared to CNBr-derivates and were even lower than for the latter (see Table 4).

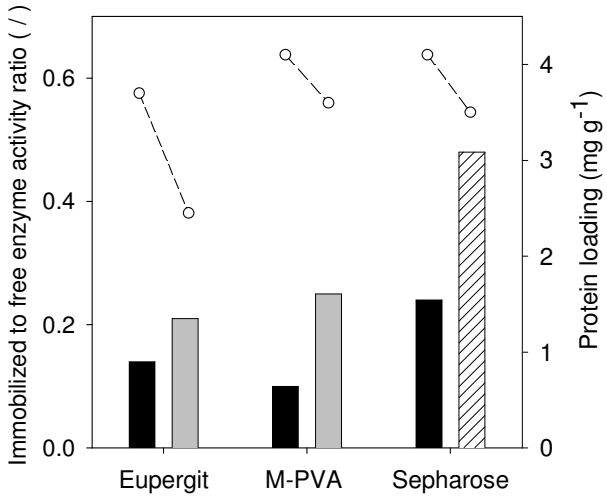

Figure 2: Ratio of immobilized to free enzyme activity of different derivates. Black columns: immobilization of the raw powder preparation on Eupergit 250L, micro-carrier M-PVA and CNBr-sepharose, respectively (Ratio 1 equals to 65 U mg^{-1} immobilized enzyme activity). Grey columns: immobilization of the enriched enzyme preparation (Ratio 1 equals to 132 U mg^{-1} immobilized enzyme activity). Striped column: immobilization of the raw powder preparation on ConA-sepharose (Ratio 1 equals to 65 U mg^{-1} immobilized enzyme activity). Activity determined with p-nitrophenyl-rhamnoside. White points: Protein loading values.

Table 4: Activities of ConA- and CNBr-derivates

	Protein coupling		Substrate: di-RL			Substrate: pnpR		
	q_P [a] (mg g^{-1})	Y_P [b] (%)	q_A [c] (U g^{-1})	Y_A [d] (%)	u^{IM} [e] (U mg^{-1})	q_A [c] (U g^{-1})	Y_A [d] (%)	u^{IM} [e] (U mg^{-1})
CNBr-Sepharose	11.4	79	38	5	3.4	233	25	20.5
ConA-Sepharose	12.6	81	29	3	2.3	92	9	7.3

[a] q_P: Protein loading. [b] Y_P: Protein coupling yield (100 % equals to coupling of total protein-mass offered for immobilization). [c] q_A: Activity loading. [d] Y_A: Overall activity yield (100 % equals to coupling of total di-RL- or pnpR-units offered for immobilization). [e] u^{IM}: Immobilized enzyme activity

Operational stability

Figure 3 shows consecutive conversions reached after 2 h relative to the first cycle of M-PVA and ConA-Sepharose derivates. Both derivates preserved activity upon batch-cycles confirming the covalent enzyme attachment. The 25 % activity lost by M-PVA derivates after the first cycle is commonly observed and may be associated with some enzyme leaching or enzyme deactivation. However, ConA-Sepharose derivates were mechanically disrupted upon magnetic stirring as observed in micrographs. The increa-

sing activity with cycle number observed with these derivates may be attributed to an increasing activity due to reducing particle radius. In account of this, stability determinations for CNBr-derivates, NHS-derivates and Eupergit derivates in the stirred Amicon cell were not further conducted.

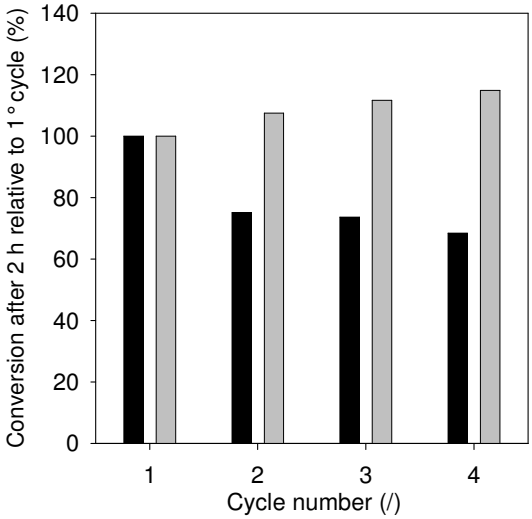

Figure 3: Operational stability of micro-carrier derivates (M-PVA) (black columns, 100 % equals to 61 % conversion) and of ConA-derivates (grey columns, 100 % equals to 72 % conversion) in repeated 2 h biotransformation cycles. Activity determined with di-rhamnolipid.

Optimization of coupling conditions on M-PVA

The highest carrier activities for di-RL were obtained with M-PVA. Therefore, coupling parameters $q_{P,0}$ and $R_{EDC/P}$ of this method were optimized. The resulting activities of the subsequent optimization are summarized in Table 5. The multiple regression coefficients R^2 of the multiple regression analysis are equal to 0.989 for $u^{IM}_{di\text{-}RL}$ and 0.982 for u^{IM}_{pnpR}. The results of F-tests shows that the polynomial regressions are statistically significant at a confidence level higher than 95 % (F = 74.0 for $u^{IM}_{di\text{-}RL}$ and F = 48.1 for u^{IM}_{pnpR}). The good agreements between experimental and calculated values confirmed the validity of the polynomial models. However, some model coefficients are statistically insignificant and were taken out since their absolute values are much lower and of the order of their deviations. After this simplification, the model equations result as:

$$u^{IM}_{di-RL} = 11.4_{(\pm 1.0)} - 15.2_{(\pm 1.0)} X_1 + 9.2_{(\pm 1.5)} X_1^{\,2} + 4.3_{(\pm 1.5)} X_2^{\,2} \quad (2)$$

$$u^{IM}_{pnpR} = 4.3_{(\pm 0.3)} - 3.8_{(\pm 0.3)} X_1 + 1.8_{(\pm 0.5)} X_2^{\,2} \quad (3)$$

Table 5: Responses of the experimental matrix assays. See Table 2 for experimental conditions of assays 1 – 9.

Assay N°	Protein coupling		Substrate: di-RL				Substrate: pnpR			
	q_P [a] (mg g^{-1})	Y_P [b] (%)	u^{IM} [e] (U mg^{-1})		Y_A [d] (%)	q_A [c] (U g^{-1})	u^{IM} [e] (U mg^{-1})		Y_A [d] (%)	q_A [c] (U g^{-1})
			Exp [f]	Calc [g]	Exp [f]	Exp [f]	Exp [f]	Calc [g]	Exp [f]	Exp [f]
1	12.2	61	5.1	5.4	6	62	1.3	1.1	1	16
2	0.4	59	36.1	35.8	39	13	8.4	8.6	8	3
3	9.2	64	10.0	9.7	12	92	3.0	3.2	3	28
4	3.7	82	23.8	24.1	36	88	8.0	7.8	10	29
5	7.8	54	9.4	9.1	9	74	4.4	4.6	4	34
6	3.6	80	24.4	24.7	35	88	7.7	7.5	10	28
7	7.1	73	10.4	11.4	14	74	3.8	4.3	4	27
8	6.6	70	10.1	11.4	13	66	4.1	4.3	5	27
9	6.2	67	13.7	11.4	17	85	4.9	4.3	5	30

[a] q_P: Protein loading. [b] Y_P: Protein coupling yield (100 % equals to $q_{P,0}$, the protein to mass ratio setting). [c] q_A: Activity loading. [d] Y_A: Overall activity yield (100 % equals to coupling of total di-RL- or pnpR-units offered for immobilization). [e] u^{IM}: Immobilized enzyme activity . [f] Exp: experimental determination. [g] Calc: Values calculated with equation 2 and 3 for di-RL and pnpR, respectively.

From equation 2 and 3 it can clearly be deduced that the protein to mass ratio (X_1) significantly affects immobilized enzyme activities whereas the activating-reagent to protein mass ratio (X_2) hardly affects them. Moreover, no interactions between both variables were found and thus influences of $q_{P,0}$ on the immobilized activities were independent of the $R_{EDC/P}$ setting within the experimental region tested. These observations are clearly represented by the plots of the model equations in Figure 4.

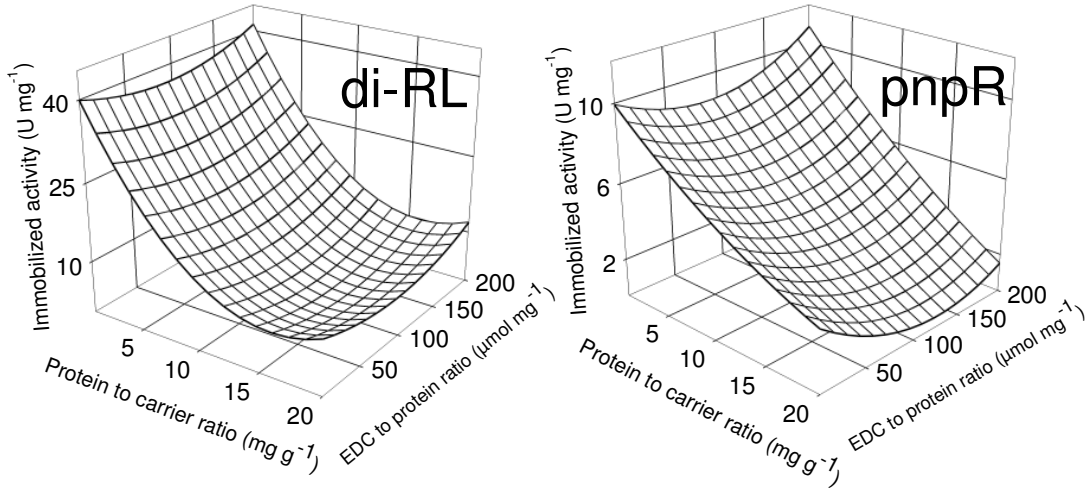

Figure 4: Quadratic model for describing the influence on the immobilized enzyme activity of the immobilization parameters protein to carrier ratio and activating reagent (EDC) to protein ratio. Carrier used: micro-carriers. Activity determined with di-rhamnolipid (di-RL) and with p-nitrophenyl-rhamnoside (pnpR).

Unfortunately, it was not possible to find a statistically valid model for the responses activity yield Y_A and loaded activity q_A. For both substrates, immobilized enzyme activities gradually decreased with protein loading and no maximum resulted. Immobilized enzyme was about 3 times more active with di-RL than with pnpR, in spite of having similar activity values in the free form. On the other hand, the activating-reagent to protein mass ratio did not influence immobilized enzyme activities at all, till values of about 200 µmol EDC per mg of protein. Generally, a saturation profile should be reached until the EDC-reagent starts to become damaging (Ragnitz et al. 2001). This saturation level was presumably not reached in the region tested.

Discussion

Non-porous micro carriers seem to be an appropriate biocatalyst for conversion of emulsified rhamnolipids reaching high carrier activities and simultaneously high activity yields as compared to porous carriers. Enzyme molecules immobilized on the outer surface of micro-non porous particles enable high substrate accessibility and a kinetically controlled reaction may be established. Excluding negative matrix effects that could modify intrinsic activities, the results of Table 3 indicate the existence of an increasing diffusion limitation with particle radius. This effect is also observed by the stability determinations with ConA-derivates, where the mechanically disrupted particles showed higher conversion rates upon cycle number. Additionally, higher activity yields resulted for the well soluble substrate pnpR as compared to di-RL. This is also an indication of diffusion limitation for the last. In accordance to this, Bozhinova et al. (2004) observed higher efficiency, stereoselectivity and selectivity of penicillin amidase immobilized on micro-carriers as compared to larger and porous carriers.

Immobilization by ConA-derivates or by using an enriched preparation produced a 2-fold increase of the activity yield. Surprisingly, this factor is in accordance with the increase of specific activity achieved upon enrichment. This indicates that immobilization of foreign proteins was diminished hereby. However, this improvement was no longer observed when higher protein loading were immobilized on ConA-derivates. This correlation may be interpreted as a strong decrease of the intrinsic activity in ConA-derivates with increasing protein loading. Iqbal and Saleemuddin (1983) also reported a similar lowering with glucose oxidase and invertase immobilized on ConA-sepharose. In conclusion, non-specific immobilization contributes to the lowering of immobilized activity observed (Table 3). However, effects like enzyme damaging upon immobilization or diffusion limitations may also be of importance.

Response surface methodology was successfully applied for studying the effect of coupling conditions on M-PVA immobilization. However, the reason why immobilized activities decreased with increasing protein loading for both substrates remains unclear.

Possibly, substrate diffusion limitations may be a factor. With increasing protein loading the reaction rate gradually increases relative to the substrate diffusion, the later becoming the rate-limiting step at higher loadings. However, substrate diffusion through the stagnant film around a non-porous bead is not expected to be rate-limiting especially for the well-soluble substrate pnpR.

Concluding, an M-PVA derivate at 3.7 mg g^{-1} protein loading with 88 U g^{-1} and 36 % activity yield are the optimized point where highest specific activities with simultaneously high activity yields were achieved. Due to the type of di-RL conversion kinetics the derivates may be best utilized in repeated batch conversion cycles.

Acknowledgments

We would like to thank the University of Karlsruhe for the financial support of this project in the frame of the *Landesgraduiertenförderungsgesetz*. We also thank to Pr. Esther Oliveros of the Université Paul Sabatier, France for her input when interpreting the responses surfaces and also to Xiaotian Ma for his practical input.

References

Aktinson C (1992) Optimum experimental designs. Clarendon, Oxford

BenoitMarquie F, PuechCostes E, Braun A M et al (1997) Photocatalytic degradation of 2,4-dihydroxybenzoic acid in water: Efficiency optimization and mechanistic investigations. J Photochem Photobiol, A 108(1): 65-71

Boller T, Meier C and Menzler S (2002) Eupergit oxirane acrylic beads: How to make enzymes fit for biocatalysis. Org Process Res Dev 6(4): 509-519

Box G E P, Hunter W G and S. H J (1978) Statistic for experimenters: an introduction to design, data analysis and model building. Wiley, New York

Bozhinova D, Galunsky B, Yueping G et al (2004) Evaluation of magnetic polymer micro-beads as carriers of immobilised biocatalysts for selective and stereoselective transformations. Biotechnol Lett 26(4): 343-350

Ellenrieder G and Daz M (1996) Thermostabilization of Naringinase from *Penicillium decumbens* by proteins in solution and immobilization on insoluble proteins. Biocatal Biotransform 14(2): 113-123

Iqbal J and Saleemuddin M (1983) Activity and stability of glucose-oxidase and invertase immobilized on Concanavalin-A-Sepharose - Influence of lectin concentrations. Biotechnol Bioeng 25(12): 3191-3195

Iqbal J and Saleemuddin M (1985) Sucrose hydrolysis using invertase immobilized on Concanavalin-A-Sepharose. Enzyme Microb Technol 7(4): 175-178

Khuri A I and Cornell J A (1987) Response surfaces, design and analyses. Marcel Dekker, ASQC Quality Press, New York

Lang S and Trowitzsch-Kienast W (2002) Biotenside. B G Teubner, Stuttgart

Manjon A, Bastida J, Romero C et al (1985) Immobilization of Naringinase on glycophase-coated porous-glass. Biotechnol Lett 7(7): 477-482

Norouzian D, Hosseinzadeh A, Inanlou D N et al (1999) Various techniques used to immobilize Naringinase produced by Penicillium decombens PTCC 5248. World J Microbiol Biotechnol 15(4): 501-502

Oliveros E, Göb S, Bossmann S H et al (2000) Waste water treatment by the photochemical enhanced fenton reaction: modeling and optimization using experimental design and artificial neural networks. Proceedings of the Third Asia Pacific Conference, Singapore, Work Scientific

Oliveros E, Legrini O, Hohl M et al (1997) Industrial waste water treatment: large scale development of a light-enhanced Fenton reaction. Chem Eng Process 36(5): 397-405

Ono M, Tosa T and Chibata I (1977) Preparation and properties of Naringinase immobilized by ionic binding to DEAE-Sephadex. J Ferment Technol 55(5): 493-500

Puri M, Marwaha S S and Kothari R M (1996) Studies on the applicability of alginate-entrapped Naringinase for the debittering of kinnow juice. Enzyme Microb Technol 18(4): 281-285

Puri M, Seth M, Marwaha S S et al (2001) Debittering of Kinnow mandarin juice by covalently bound Naringinase on hen egg white. Food Biotechnol 15(1): 13-23

Ragnitz K, Pietzsch M and Syldatk C (2001) Immobilization of the hydantoin cleaving enzymes from *Arthrobacter aurescens* DSM 3747. J Biotechnol 92(2): 179-186

Rasch D, Verdooren L R and Gowers J I (1999) Grundlagen der Planung und Auswertung von Versuchen und Erhebungen. R. Oldenbourg Verlag, München, Wien

Romero C, Manjon A, Bastida J et al (1985) A method for assaying the rhamnosidase activity of Naringinase. Anal Biochem 149(2): 566-571

Saleemuddin M and Husain Q (1991) Concanavalin-A - A useful ligand for glycoenzyme immobilization - A review. Enzyme Microb Technol 13(4): 290-295

Schenk T, Schuphan I and Schmidt B (1995) High-performance liquid-chromatographic determination of the rhamnolipids produced by *Pseudomonas aeruginosa*. J Chromatogr A 693(1): 7-13

Sekeroglu G, Fadiloglu S and Gogus F (2006) Immobilization and characterization of Naringinase for the hydrolysis of naringin. Eur Food Res Technol 224(1): 55-60

Soares N F F and Hotchkiss J H (1998) Naringinase immobilization in packaging films for reducing naringin concentration in grapefruit juice. J Food Sci 63(1): 61-65

Syldatk C, Lang S, Wagner F et al (1985) Chemical and physical characterization of 4 interfacial-active rhamnolipids from *Pseudomonas* Spec DSM 2874 grown on normal-alkanes. Z Naturforsch C 40(1-2): 51-60

Trummler K, Effenberger F and Syldatk C (2003) An integrated microbial/enzymatic process for production of rhamnolipids and L-(+)-rhamnose from rapeseed oil with *Pseudomonas* sp DSM 2874. Eur J Lipid Sci Technol 105(10): 563-571

Tsen H Y, Tsai S Y and Yu G K (1989) Fiber entrapment of Naringinase from *Penicillium* Sp and application to fruit juice debittering. J Ferment Bioeng 67(3): 186-189

Turecek P and Pittner F (1986) Simple enzyme reactors suitable for the by-product-free preparation of the aglycones of naturally-occurring glycosides under mild conditions. Appl Biochem Biotech 13(1): 1-13

4.4 Non-porous micro-Carriers for a Diffusion Rate-Controlled Enzymatic Conversion

NON-POROUS MAGNETIC MICRO PARTICLES: COMPARISON TO POROUS ENZYME CARRIERS FOR A DIFFUSION RATE-CONTROLLED ENZYMATIC CONVERSION

Journal of Biotechnology 134 (2008) 72-78

DOI:10.1016/j.jbiotec.2007.12.001

I. Magario *, X. Ma, A. Neumann, C. Syldatk, R. Hausmann

Institute of Engineering in Life Sciences, Chair of Technical Biology, University of Karlsruhe (TH), Germany

* Corresponding author: I. Magario
Tel: +49-721-608-6736/8428
Fax: +49-721-608-4881
E-mail: Ivana.Magario@tebi.uni-karlsruhe.de (I. Magario)
Rudolf.Hausmann@tebi.uni-karlsruhe.de (R. Hausmann)

Key words: rhamnolipids, magnetic micro-beads, Naringinase, enzyme immobilization, effectiveness factor

Abstract

In this study the kinetics of conversion of a low-soluble substrate by an immobilized enzyme was investigated with respect to the diffusion limitation within porous and non-porous carriers. Non-porous micro-magnetic beads in comparison to conventional porous supports like Eupergit and Sepharose were tested. Due to their small diameters and their magnetic properties, micro-magnetic beads are especially applicable in diffusion rate-controlled processes in biological suspensions. The enzymatic reaction studied was the conversion of emulsified dirhamnolipid by immobilized Naringinase from *Penicillium decumbens* to monorhamnolipid and L-rhamnose. Taking into account mass transfer phenomena, the variation of the reaction effectiveness factor with increasing enzyme loading was estimated and compared with experimental efficiencies utilizing different enzyme loaded immobilized preparations. For comparison, carrier activities were also determined with the model substrate p-nitro-phenyl-rhamnoside. Intrinsic enzyme activities were thereby evaluated for porous supports.

Highest specific activities were obtained with the micro-magnetic beads. These non-porous micro-beads demonstrated to be the most suitable carrier for bioconversion of a low-soluble substrate like rhamnolipids, where mass diffusional resistances in the three-phase reaction process are completely overcome. However, the smaller particle surface available limited the specific activity obtained at high protein loadings.

Introduction

Mass transfer within carrier pores is often the rate-limiting process in the conversion of low-soluble substrates by immobilized enzymes. Therefore, low specific enzyme activities as compared to free enzymes are commonly observed. For overcoming diffusion limitation, the use of micro non-porous particles may be advantageous. Micro-magnetic polymer beads with a mean diameter of a few µm hold an ample potential in various fields of biotechnology and bioprocess engineering. Due to their small diameters and their magnetic properties, they are especially applicable in diffusion rate-controlled processes in biological suspensions. Polymer coated micro-non-porous beads have been studied as carrier materials for enzyme immobilization, however in few cases performance comparisons of magnetic micro-beads with non-magnetic carrier are reported [Bilkova et al. 2002; Bozhinova et al. 2004].

As model system for a diffusion rate-controlled reaction, the enzymatic modification of emulsified rhamnolipids was selected. The cleavage of a α-L-rhamnose molecule of a dirhamnolipid (R3) is performed by Naringinase [Meiwes et al. 1997; Trummler et al. 2003]. Monorhamnolipid (R1) and the by-product α-L-rhamnose are therewith gained. In this system nearly total rhamnolipids are bond to micelles, whereas only truly dissolved molecules are available for enzymatic hydrolysis. Thus, the substrate concentration is very low, 0.05 mmol l^{-1}, at reaction conditions. Further details of reaction optimization and the description of the kinetics will be published elsewhere.

The objective of this work was to evaluate the applicability of non-porous magnetic beads as enzyme immobilization carriers for diffusion rate-limited reactions in an emulsion. Due to the small scale of the carrier, higher yields of immobilized activities would be expected as compared to larger but porous carriers.

Theoretical background

Porous diffusion

The approximate expression of efficiencies for Michaelis-Menten kinetics due to pore diffusion given by Aktinson and Davies [1974] was chosen. The relation between the effectiveness factor η^{in} and the Thiele-modulus ϕ for spheres is described as [Aktinson and Davies 1974, Yamane 1981]:

$$\eta^{in}(\phi,\beta_0)=\begin{cases} 1-\dfrac{\tanh\phi}{\phi}\cdot\left[\dfrac{1/\eta_D}{\tanh(1/\eta_D)}-1\right] & \text{for } \dfrac{1}{\eta_D}\le 1 \text{ and } \phi<1 \\ \eta_D-\dfrac{\tanh\phi}{\phi}\cdot\left[\dfrac{1}{\tanh(1/\eta_D)}-1\right] & \text{for } \dfrac{1}{\eta_D}>1 \text{ and } \phi<1 \end{cases} \quad (1)$$

$$\eta_D = \sqrt{2} \cdot \left(\frac{1+\beta_0}{\phi.\beta_0} \right) \cdot \left[\beta_0 - \ln(1+\beta_0) \right]^{1/2} \tag{2}$$

In case of rhamnolipid-3 conversions, the substrate concentration is low, β_0 approaches zero and η converges to the effectiveness factor of the corresponding first-order reaction (Levenspiel 1999):

$$\lim_{\beta \to 0} \eta^{in}(\phi, \beta_0) = \varepsilon(\phi) = \frac{1}{\phi} \cdot \left[\frac{1}{\tanh(3 \cdot \phi)} - \frac{1}{3 \cdot \phi} \right] \tag{3}$$

For applying the above equations a uniform protein distribution within the particle, no external film diffusion limitation and a constant effective diffusion coefficient within the particle have to be assumed. Immobilized activity estimations on porous particles were estimated in dependency of protein loading using equations 1 and 2 for activities with the model substrate p-nitro-α-L-rhamnoside and equation 3 for rhamnolipid-3 activities.

Film diffusion

For the employed non-porous magnetic carriers the enzymatic conversion occurs only at the surface of the particle. For Michaelis-Menten kinetics the effectiveness factor due to film diffusion η^{ex} is related to the Damköhler-number Da_{II} as [Chaplin and Bucke 1990; Kheirolomoon et al. 2002]:

$$\eta^{ex} = \frac{(1+\beta_b) \cdot \left(\varphi - \sqrt{\zeta} \right)}{2 \cdot \beta_b \cdot Da_{II}} \tag{4}$$

$$\varphi = 1 + \beta_b + Da_{II} \tag{5}$$

$$\zeta = \varphi^2 - 4 \cdot \beta_b \cdot Da_{II} \tag{6}$$

In case of rhamnolipid-3 conversion where β_b approaches zero, the effectiveness factor simplifies to [Chaplin and Bucke 1990]:

$$\eta^{ex} = \frac{1}{1 + Da_{II}} \tag{7}$$

Immobilized activity estimations of the non-porous magnetic particles were estimated in dependency of the protein loading using equations 4 - 6 for activities with p-nitro-α-L-rhamnoside and equation 7 for rhamnolipid-3 activities. In Appendices 2, a more detailed description of the equation used is presented.

For the calculation of the Thiele-modulus and Damköhler-number for pnpR activities the value of the intrinsic Michaelis-Menten constant was assumed to be equal to the value for free enzyme. The program ModelMaker-Version 3 (Cherwell Scientific Publishing Ltd) was used for fitting theoretical immobilized activities curves to experimental values. The fitting procedure was according to the Mardquard method [Walker and Crout 1997] and a 10 % relative standard error of experimental results was assumed.

Materials and Methods

Materials

Naringinase was purchased from Sigma Aldrich (Lot N° 110K16471). Crystalline rhamnolipid 3 (R3) (97% purity) was a kind gift from Hoechst AG (Frankfurt, Germany) whereas p-nitro-phenyl-rhamnoside (pnpR) was obtained from Extrasynthese (Genay, France). Amine-functionalized poly-(vinyl-alcohol)-coated micro beads (M-PVA) were obtained from Chemagen AG (Baesweiler, Germany). Eupergit 250L were kindly donated by Degussa, Röhm GmbH & Co.KG (Darmstadt, Germany) whereas CNBr-Sepharose 4B and NHS-Sepharose were purchased from Amersham Biosciences Ltd. (Uppsala, Sweden). Table 1 lists relevant carrier properties. All other chemicals, solvents and immobilization reagents were of analytical grade.

Table 1: Carrier properties

	Matrix	Size	Functionality	Density	Surface	Spacer arm
M-PVA	Poly-(vinyl) alcohol	2 µm	Amine	1.8 g ml^{-1}	1.7 m^2 g^{-1} [a]	-
Eupergit 250L	Copolymer of methacrylamide	190 µm	Oxirane	1.1 g ml^{-1} [b]	13 m^2 g_{wet}^{-1}	-
CNBr-sepharose	4% agarose	90 µm	Cyanate esters	1.0 g ml^{-1} [b]	not determined	-
NHS-sepharose	highly cross-linked 6% agarose	34 µm	Activated carboxylate	1.0 g ml^{-1} [b]	not determined	10-atom spacer arms [c]

[a] Calculated considering smooth surface
[b] Wet particle densities were measured by the pyknometer method
[c] (6-aminohexanoic acid) attached by epichlorohydrin and activated by N-hydroxysuccinimide

Immobilization of Naringinase

Immobilization on M-PVA through the carbodiimide method (EDC-method) was according to Ragnitz et al. [2001]. The mass ratio N-(3-dimethylaminopropyl)-N′-ethylcarbodiimide hydrochloride (EDC) to protein was set at 94 µmol mg^{-1}. Immobilization on M-PVA through the glutaraldehyde-method (GA-method) was according to Bozhinova et al. [2004]. The beads were activated by pre-incubation with 12.5 % GA

solution for 2 h at 30°C. For both methods 25 mg beads per ml enzyme solution at different concentrations (0.01 – 0.47 g l^{-1}) were applied. Immobilization on Eupergit 250L was carried out according to supplier recommendations. The bead concentration was set at 166 mg ml^{-1} and different protein concentrations (0.1 – 4 g l^{-1}) were applied. After immobilization the beads were incubated with Tris-HCl, pH 8.0 for abreacting remaining oxirane groups. Immobilization on Sepharose beads was performed according to supplier recommendations. The bead concentration was always set at 400 mg ml^{-1} whereas the protein concentration was varied between 0.1 and 8 g l^{-1}. For washing-steps after immobilization, suspensions were dumped into a disposable filtration device (Vivaspin 4 - 0.2 µm PES membrane, Vivascience-Sartorius group, Hannover, Germany).

Protein assay

Protein content of Naringinase start-solution, supernatant and first three wash solutions after immobilization were determined by the Bradford method (Bio-rad Laboratories, Munich, Germany) using bovine serum albumin (BSA) as standard. Supernatants of the GA-method were concentrated with disposable ultrafiltration devices (Vivaspin 500-10,000 MWCO PES, Vivascience-Sartorius group) before measurement. Protein coupling yield and protein loading q (mg g^{-1}) were derived by mass balance calculation.

Activity assays of immobilized and free Naringinase

For activity assays with R3, an enzyme solution was added to 5 mmol l^{-1} R3 emulsion at 60°C in 0.1 mol l^{-1} sodium acetate buffer, pH 4.5, in a ratio 1 to 20. 500 µl samples were withdrawn and the reaction was stopped by acidification with 50 µl 1 mol l^{-1} phosphoric acid and rhamnolipids extraction in 500 µl ethyl acetate. Then, a certain volume of ethyl acetate was evaporated and the rhamnolipids were re-dissolved in acetonitrile for analysis. Activity assays with immobilized Naringinase were modified as follows: wet beads of derivates (Eupergit 250L, CNBr-Sepharose) were weighted and mixed with a temperate substrate solution or; derivate suspensions (NHS-Sepharose and M-PVA beads) were added to the substrate solution. Samples were centrifuged or magnetically separated from the beads after solvent extraction. The activity was calculated as the average of initial increase of R1 and initial decrease of R3 concentration. One unit R3 was defined as the amount that converts 1 µmol R1 from R3 in 1 minute at 60°C and pH 4.5. For activity assays with pnpR, 50 µl of enzyme solution was added to 950 µl of a 4 mmol l^{-1} pnpR solution in 0.1 mol l^{-1} sodium acetate buffer, pH 5.5 at 60°C. The increase of p-nitrophenolate concentration was followed by monitoring the absorption at 400 nm. For conversion with immobilized Naringinase the derivates were added to the substrate solution as described above and the activity was assayed according to Romero et al. [1985]. One unit pnpR was defined as the amount that converts 1 µmol pnp from

pnpR in 1 minute at 60°C and pH 5.5. Observed protein activity u_P^{obs} was calculated as the quotient between activity of the derivates (U g^{-1}) and protein loading.

HPLC Analytics

Rhamnolipids were analyzed by an HPLC device coupled to a UV detector (Agilent 1100 Series) according to Schenk et al. [1995]. High pure standards of R1 were prepared by enzymatic hydrolysis of R3, according to Trummler et al. [2003]. R1 was further purified by adsorption chromatography with fine silica gel as stationary phase and a chloroform-methanol 3:1 solution as mobile phase. After elution, the mobile phase was evaporated and R1 was re-dissolved in ethyl acetate. After drying, the organic phase was fully evaporated under high vacuum. 300 mg R1 (49% overall yield) were obtained. Elemental analysis of the product was in accordance with theoretical values.

Results and discussion

To evaluate the performance of every support type and identify the extent of diffusion limitation on the overall reaction rate, a set of derivates with different protein loadings was prepared and their activities with both substrates were assayed. The observed specific protein activity u_P^{obs} as well as the volumetric carrier activity v were then compared with the theoretical predictions according to the diffusion-reaction effectiveness models.

Substrate Diffusivities and mass transfer estimations

Substrate diffusivities were estimated by the method of Hayduk and Laudie at 60°C [Liley et al. 1997]:

$$D_W = \frac{8.621 \cdot 10^{-14}}{\mu^{1.14} \cdot VB^{0.589}} \tag{8}$$

The values of the substrate molar volume, *VB*, at the boiling point temperature required for the calculation were approximated to the corresponding values at 20°C. The last were obtained from the SciFinder Scholar database (American Chemical Society, Washington, USA). The diffusion coefficient values thus obtained were 13.9 10^{-10} and 7.6 10^{-10} m^2 s^{-1} for pnpR and R3, respectively. Substrate diffusion within porous particles is expressed as [Walas 1997]:

$$D_{eff} = D_W \cdot \frac{\vartheta}{\tau} \tag{9}$$

Walas [1997] recommends a porosity ϑ value of 0.5 and a tortuosity τ value of 4. Therefore, D_{eff} values for every support and every substrate were estimated as being 12.5 % of

the diffusivities in the bulk solution. This approximation enables to fit effectiveness factor prediction curves to experimental activity data. Thus, a first estimation of the intrinsic enzyme activity u^I_P can be carried out. For effectiveness calculation with M-PVA an estimation of the mass transfer coefficient k_L is also required. For a stirred particle suspension with Reynolds numbers $Re_p < 1$ the following correlation can be applied [Friedlander 1961; Herndl and Mersmann 1981]:

$$Sh = 2 + 0.991 \cdot \mathrm{Re}_p^{1/3} \cdot Sc^{1/3} \qquad (10)$$

For the very small non-porous magnetic carriers, the value of Re_p tends to zero and the Sh number approaches its minimal value of 2. The resulting k_L values were then 7.6 and 13.9 10^{-4} m s^{-1} for R3 and pnpR, respectively.

Activities with porous supports

Figure 1 and 2 show activity values of porous supports for R3 and pnpR, respectively. The discontinuity observed in the diffusion-reaction prediction of Figures 2A and 2C is due to the constraint change at $\eta_D^{-1} > 1$ of the approximated expression (equations 1 and 2). Intrinsic protein activity values u^I_P were estimated by fitting diffusion-reaction curves to experimental values.

An overall agreement between experimental and predicted tendency is observed for all supports, which confirms the applicability of the diffusion reaction theory for describing immobilized enzyme activities. A pronounced decrease of observed protein activity with increasing protein loading was observed for the diffusion-controlled R3 bioconversion, which implies a corresponding decrease of the activity efficiency of the immobilization process. For the reaction model it is assumed that R3 molecules have first to diffuse from the emulsified aggregates to the aqueous phase and finally penetrate inside the porous particle for its enzymatic conversion. Then, the low aqueous solubility of R3 molecules causes a low driving force for the diffusion into the particles.

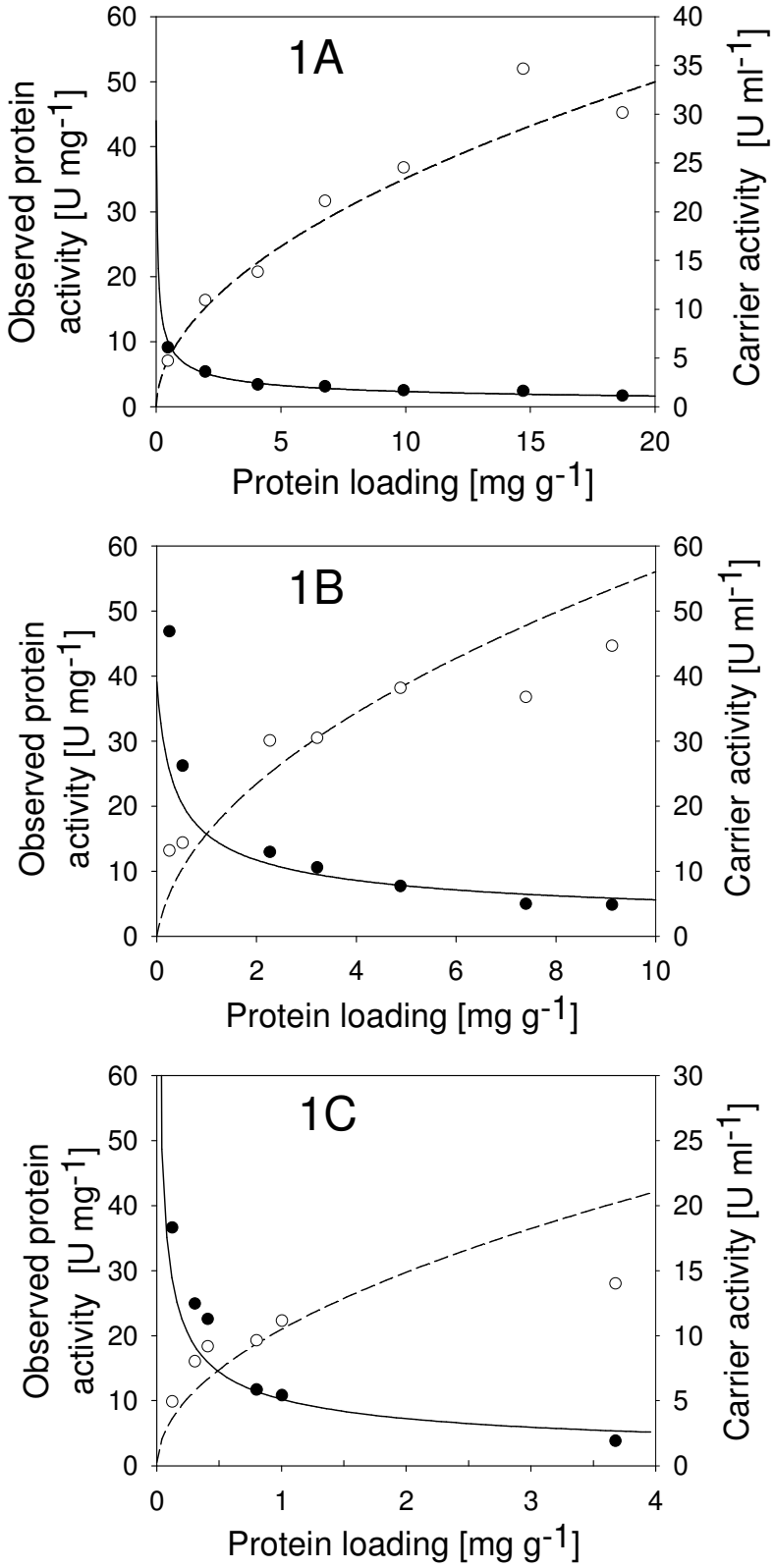

Figure 1: R3-activity of porous derivates in dependency of protein loading. 1A: Enzyme coupling on CNBr-sepharose. 1B: Enzyme coupling on NHS-sepharose. 1C: Enzyme coupling on Eupergit 250L. Black dots and full lines: experimental and theoretical prediction of observed protein activities. White dots and dashed lines: experimental and theoretical prediction of carrier activities. Predictions by equation 3

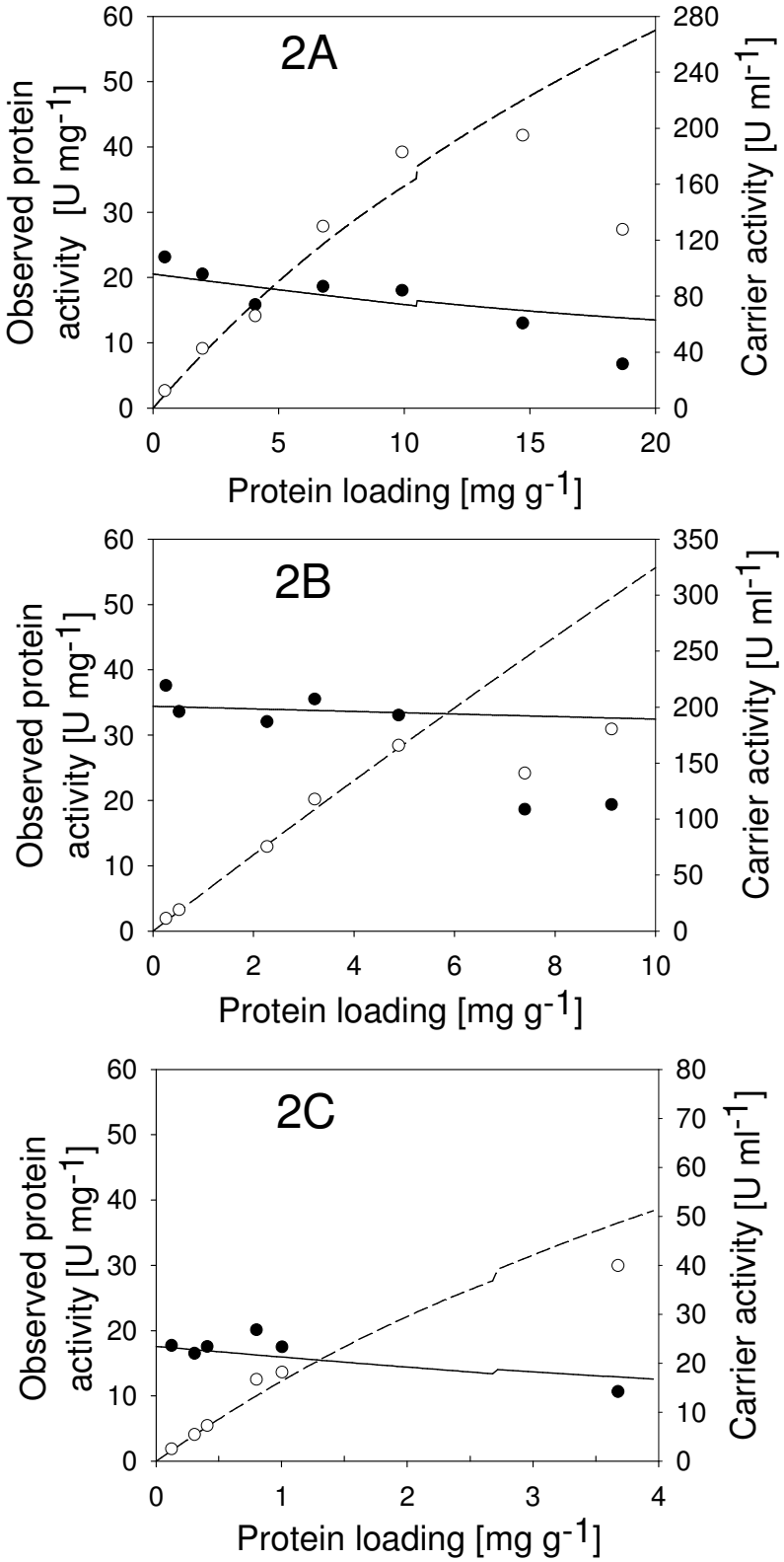

Figure 2: pnpR-activity of porous derivates in dependency of protein loading. 2A: Enzyme coupling on CNBr-sepharose. 2B: Enzyme coupling on NHS-sepharose. 2C: Enzyme coupling on Eupergit 250L. Black dots and full lines: experimental and theoretical prediction of observed protein activities. White dots and dashed lines: Experimental and theoretical prediction of carrier activities. Predictions by equations 1 - 2

The variation of the observed activity with protein loading in case of pnpR is much less pronounced due to the less diffusion-limited reaction. This behavior could also be predicted from the diffusion-reaction calculations since greater substrate solubility and diffusivity resulted in low Thiele-modulus values. However, at higher protein loadings, the observed activity decreased beyond the expected values for pnpR and these biases were taken out for the fitting procedure (last point of CNBr-sepharose in Figure 2A and two last points of NHS-sepharose in Figure 2B). Presumably, intrinsic protein activity u^I_P decreased with increasing loaded protein accounting for such observations. Clark and Bailey [2002] also observed decreasing of intrinsic activities with protein loading by immobilization of chymotrypsin on CNBr-sepharose.

Table 2 summarizes results of the u^I_P estimations as well as the quality of fit in every case. As expected, intrinsic activities were lower than the corresponding values for the soluble enzyme, except for activities of Eupergit with R3. Apart from the difference in size between CNBr- and NHS-sepharose, the last possesses 10-atom spacer arms that may protect the enzyme of matrix damaging effects. Thus, that may account for the higher uIP value obtained for pnpR with NHS- as compared with CNBr-derivate. However, intrinsic activities of CNBr- and NHS-derivates for R3 are of the same order of magnitude and somewhat higher than for pnpR. In case of Eupergit with R3, the intrinsic activity obtained was 7 times higher than for the soluble enzyme. Here, experimental activities were greater than predicted. Many reasons may account for this observation such as 1) non-uniformly distributed immobilized enzyme; 2) larger pore sizes; or 3) the high hydrophobicity of Eupergit matrix. This last may cause substrate partition accumulating R3 molecules at the particle surface thus promoting higher apparent intrinsic activity due to increase of the enzymatically available R3 molecules [Yamane et al. 1981].

Table 2: Intrinsic protein activities of Naringinase immobilized on different supports

	Intrinsic protein activity with R3 at s_b = 0.05 mmol l^{-1} (U mg^{-1})		Intrinsic protein activity with pnpR at s_b = 4 mmol l^{-1} (U mg^{-1})	
Soluble enzyme	55 ± 3		65 ± 4	
CNBr-Sepharose	45 ± 2	R^2 = 0.733	20.5 ± 0.7	R^2 = 0.957
NHS-Sepharose	39 ± 2	R^2 = 0.729	34 ± 1	R^2 = 0.839
Eupergit 250L	384 ± 23	R^2 = 0.841	17.6 ± 0.6	R^2 = 0.841

Activities with non-porous supports

Figure 3 and 4 shows protein and carrier activity in dependency of enzyme loading on micro non-porous magnetic particles. Independently of the immobilization method and substrate used, a constant decrease of activity with loading was detected, which did not agree with the diffusion-reaction calculations. None or little diffusion influence on the reaction process is expected for this carrier. At about 2 mg g^{-1} loading, the carrier activity no longer increased.

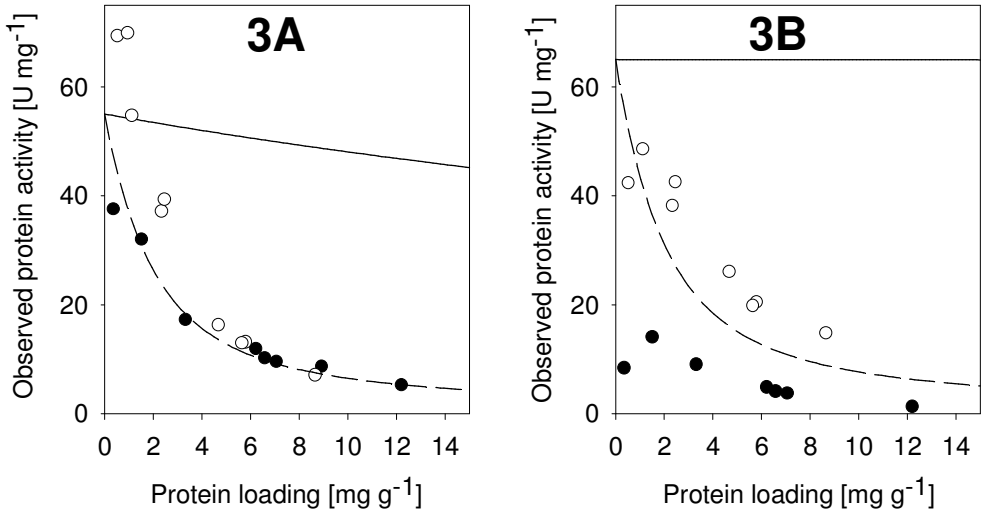

Figure 3: Activity of enzyme coupled on M-PVA in dependency of protein loading. 3A: Activities with R3. 3B: Activities with pnpR. Black dots: Observed enzyme activity; enzyme coupling by the EDC-method. White dots: Observed enzyme activity; enzyme coupling by the GA-method. Full lines: Predictions by equations 4 – 6 for pnpR and 7 for R3. Dashed lines: Predictions by equations 12 - 14

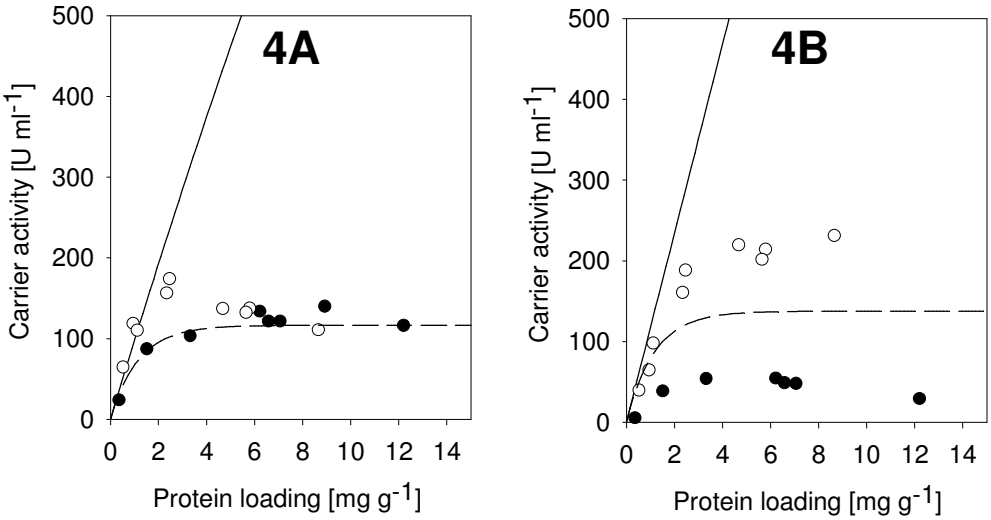

Figure 4: Carrier activity of M-PVA derivates in dependency of protein loading. 4A: Activities with R3. 4B: Activities with pnpR. Black dots: Carrier activity; enzyme coupling by the EDC-method. White dots: Carrier activity; enzyme coupling by the GA-method. Full lines: Predictions by equations 4 – 6 for pnpR and 7 for R3. Dashed lines: Predictions by equations 11 - 13

Taking into account the restricted particle surface available for immobilization, it is possible that immobilization occurs in multi layers. However, only the outer enzyme layer is accessible for substrate conversion. Wu et al. [1998] observed a similar pattern when immobilizing ß-lactamase on non-porous micro-spheres of polystyrene. Enzyme molecules may compete for free places on the particle surface and may be adsorbed or

covalently bond to an already bound enzyme molecule. In case of the EDC-method, immobilization in multi-layers by covalent binding can easily occur, as the bi-functional reagent EDC activates carboxyl groups of the enzyme that react with amino groups of the carrier or with amino groups of proteins. In case of the GA-method, covalent binding of proteins is not possible, because GA is used for activating the amino groups of the carrier and then is washed before the enzyme solution is added for immobilization. Protein-protein adsorption can nevertheless occur by intermolecular interactions.

Assuming that only proteins at the surface are effectively accessible for substrate molecules, the volumetric carrier activity υ should be proportional to the amount of protein on the outer layer rather than to the total amount of immobilized protein. Thus, the definition of υ can be modified for multi-layer immobilization as:

$$\upsilon_{OL} = u_{P_{OL}} \cdot q_{OL} \cdot \rho \tag{11}$$

$$q_{OL} = \left(n_C \frac{w_{EM}}{w_C} \right) \cdot f(q) \tag{12}$$

q_{OL} is assumed to be a function of the total protein loading q as shown in equation 12. n_C is the number of places on a single particle available for immobilization, w_{EM} is the weight of an enzyme molecule in mg and w_C the weight of a single particle in g. Thus, the factor ($n_C\ w_{EM}\ w_C^{-1}$) is then equal to 1.2 mg g^{-1}, corresponding to the maximal capacity of active immobilized enzymes placed on the outer layer of the particle. For the calculation of n_C and w_C it is assumed that there is a smooth surface average particle of 2 µm diameter and an approximated Naringinase diameter of 16.5 nm, corresponding to its molecular weight (90 kDa). Assuming as equally probable an enzyme immobilization to the particle surface or to an already immobilized enzyme and equaling the probability n^{-1}, a simple function is postulated for *f(q)*:

$$f(q) = 1 - \left(1 - \frac{1}{n} \right)^{q \cdot \frac{w_C}{w_{EM}}} \tag{13}$$

Therefore, q_{OL} approaches in an asymptotic manner to a value of 1.2 mg g^{-1} with increasing loading. Combining the definition of υ and of υ_{OL} (equation 11), the observed protein activity can be calculated as:

$$u_P^{obs} = u_{P_{OL}} \cdot \frac{q_{OL}}{q} \tag{14}$$

Equations 11 - 14 were used to predict the variation of activity with M-PVA derivates and it is shown in figures 3 and 4 as dashed lines. The value of u_{POL} was set equal to the specific activity of soluble enzyme, and diffusion resistances were not taken into ac-

count for the calculations due to their little influence on the overall reaction rate (see full lines). The tendency of experimental activities can effectively be explained by considering this multi-layer immobilization model. This suggests that, the decrease of activity with protein loading for M-PVA derivates is attributed to multi-layer immobilization due to the restricted surface available instead of due to diffusion limitations. Deviations of experimental values from this simple multi-layer model could be caused by: 1) variation of the enzyme activity upon immobilization compared with the specific value for free enzyme; 2) unequal probability of immobilization on the particle surface, compared to enzyme-enzyme immobilization; 3) existence of uneven particle surfaces offering an actually greater surface for immobilization and 4) systematic error for determination of protein loadings, since an external protein was used as standard for calibration. However, three interesting observations can be extracted: 1) higher activities were obtained with the GA-method for both substrates; 2) activities by the EDC-method were 3 times more active for R3 than for pnpR for every loading tested. This effect was no longer observed for the enzyme derivates attached by the GA-method; 3) as with Eupergit particles, a similar tendency to higher intrinsic activities as compared to the soluble enzyme is observed for R3 with the GA method. Possible substrate partition at the PVA carrier surface may be responsible for the apparent higher activity.

In conclusion, relatively high carrier activities were reached with the non-porous micro carriers for the conversion of R3 in comparison to porous carriers. Non-porous micro beads demonstrated to be the most appropriate carrier type for an enzymatic conversion of a low-soluble substrate, where strong diffusion limitations of the reaction rate are avoided.

Acknowledgements

We would like to thank the University of Karlsruhe for the financial support of this project in the frame of the *Landesgraduiertenförderungsgesetz*. We also thank to PD. Dr. Matthias Franzreb of the Institute for Technical Chemistry of *Forschungszentrum Karlsruhe* for his fruitful discussions and also to Dipl.-Ing. Martin Silvestre for particles surface area determinations carried out in the same institution.

Nomenclature

a	Surface to volume ratio (m^{-1})
Da_{II}	Damköhler-number defined as $Da_{II} = \frac{V^{I}_{\max}}{k_L \cdot a \cdot K^{I}_{M}}$ (-)
D_{eff}	Effective substrate diffusivity within a porous particle ($m^2\ s^{-1}$)
D_w	Substrate diffusivity ($m^2\ s^{-1}$)
EDC	N-(3-dimethylaminopropyl)-N′-ethylcarbodiimide hydrochloride

$f(q)$	Probability function for prediction of multi-layer immobilization (-)
GA	Glutaraldehyde
k_L	Mass transfer coefficient (m s^{-1})
K^I_M	Michaelis-Menten constant (mmol l^{-1}) ($K^I_{M,pnpR}$ = 6.1 mmol l^{-1})
M-PVA	non porous micro-magnetic-(polyvinyl alcohol)-particles
n_C	Number of places on a single particle available for immobilization (-)
pnpR	p-nitro-α-L-rhamnoside
q	Protein or enzyme loading (mg g^{-1})
R	Particle radius (m)
R1	Rhamnolipid-1 or monorhamnolipid
R3	Rhamnolipid-3 or dirhamnolipid
Re_p	Particle Reynolds-number (-)
s	Fluid substrate concentration (mmol l^{-1})
Sc	Schmid-number (-)
Sh	Scherwood-number, (k_L 2R D_w^{-1}) (-)
u_P	Specific protein activity (U mg^{-1})
VB	Molar volume at boiling point temperature (m^3 $kmol^{-1}$)
V^I_{max}	Maximum reaction rate (U ml^{-1})
w_C	Weight of a single particle (g)
w_{EM}	Weight of an enzyme molecule (mg)

Greek symbols

μ	Viscosity of water at 60°C (Pa s)
η	Effectiveness factor defined as $\eta = \frac{\upsilon^{obs}(s_b)}{\upsilon^{I}(s_b)} = \frac{u_P^{obs}(s_b)}{u_P^{I}(s_b)}$ (-)
ε	Effectiveness factor of a first order reaction (-)
ϑ	Particle porosity (-)
ϕ	Thiele-modulus defined as $\phi = \frac{R}{3} \cdot \sqrt{\frac{V^I_{\max}}{K^I_M \cdot D_{eff}}}$ (-)
τ	Tortuosity (-)
υ	Volumetric carrier activity defined as $\upsilon = u_P \cdot q \cdot \rho$ (U ml^{-1})
ρ	Wet particle density (g ml^{-1})
β	Dimensionless substrate concentration defined as: s $(K^I_M)^{-1}$

Sub- and super-indices

I	intrinsic
obs	observed
0	At particle surface

b	At bulk fluid conditions
ex	extern
in	intern
OL	outer layer

References

Atkinson, B., Davies, I.J. (1974) Overall rate of substrate uptake (Reaction) by microbial films.1. biological rate equation. T. I. Chem. Eng.-Lond. 52, 248-259

Bilkova, Z., Slovakova, M., Horak, D., Lenfeld, J., Churacek, J. (2002) Enzymes immobilized on magnetic carriers: efficient and selective system for protein modification. J. Chromatogr. B. 770, 177-181

Bozhinova, D., Galunsky, B., Yueping, G., Franzreb, M., Koster, R., Kasche, V. (2004) Evaluation of magnetic polymer micro-beads as carriers of immobilised biocatalysts for selective and stereoselective transformations. Biotechnol. Lett. 26, 343-350

Chaplin, M., Bucke, C. (1990) Enzyme Technology. Cambridge University Press

Clark, D.S., Bailey, J.E. (2002) Structure-function relationships in immobilized chymotrypsin catalysis. Biotechnol. Bioeng. 79, 539-549

Friedlander, S.K. (1961) A note on transport to spheres in stokes flow. Aiche J. 7, 347-348

Herndl, G., Mersmann, A.B. (1981) Fluid-dynamics and mass-transfer in stirred suspensions. Chemical Engineering Communications. 13, 23-37

Kheirolomoom, A., Khorasheh, F., Fazelinia, H. (2002) Influence of external mass transfer limitation on apparent kinetic parameters of penicillin G acylase immobilized on nonporous ultrafine silica particles. J. Biosci. Bioeng. 93, 125-129

Levenspiel, O. (1999) Chemical Reaction Engineering, Third edn. John Wiley & Sons

Liley, P., Thomson, G., Fried, D., Daubert, T., Buck, E. (1997) Physical and chemical data. In: Perry R.H., Green D.W. (eds) Perry`s Chemical Engineer´s Handbook, seventh edn. McGraw-Hill, New York, pp 2/371-372

Meiwes, J., Wullbrant, D., Giani, C. (1997) alpha-L-rhamnosidase for obtaining rhamnose, a process for its preparation and its use. US19950465414 19950605, Germany

Ragnitz, K., Pietzsch, M., Syldatk, C. (2001) Immobilization of the hydantoin cleaving enzymes from *Arthrobacter aurescens* DSM 3747. J. Biotechnol. 92, 179-186

Romero, C., Manjon, A., Bastida, J., Iborra, J.L. (1985) A method for assaying the rhamnosidase activity of naringinase. Anal. Biochem. 149, 566-571

Schenk, T., Schuphan, I., Schmidt, B. (1995) High-performance liquid-chromatographic determination of the rhamnolipids produced by *Pseudomonas aeruginos*a. J. Chromatogr. A. 693, 7-13

Trummler, K., Effenberger, F., Syldatk, C. (2003) An integrated microbial/enzymatic process for production of rhamnolipids and L-(+)-rhamnose from rapeseed oil with *Pseudomonas* sp DSM 2874. Eur. J. Lipid Sci. Tech. 105, 563-571

Walas, S. (1997) Chemical reactors. In: Perry R.H., Green D.W. (eds) Perry`s Chemical Engineer´s Handbook, seventh edn. McGraw-Hill, New York, p 23/29

Walker, A., Crout, N. (1997) Model Maker user manual. Cherwell-Scientific-Publishing, Oxford

Wu, C.W., Lee, J.G., Lee, W.C. (1998) Protein and enzyme immobilization on non-porous microspheres of polystyrene. Biotechnol. Appl. Bioc. 27, 225-230

Yamane, T. (1981) (a) On approximate expressions of effectiveness factors for immobilized biocatalysts. J. Ferment. Technol. 59, 375-381

Yamane, T., Araki, S., Sada, E. (1981) (b) Overall effectiveness factor incorporating partition-coefficient for gel-immobilized enzyme pellet. J. Ferment. Technol. 59, 367-374

5 Conclusion and Outlook

In this work it was established that the production of mono-rhamnolipid by conversion of di-rhamnolipid by Naringinase from *Penicillium decumbens* is feasible and straightforward. Thus, this study provides a solid background for the set-up of a biotechnological process of industrial interest. Regarding process optimization, following steps were achieved:

- Reaction conditions were selected based on biocatalyst activity and stability data. Moreover, the use of organic solvents for increasing reaction rates was evaluated. Optimal conditions seem to be determined by enzyme characteristics but not on a higher availability of substrate molecules.
- Under selected reaction conditions a mathematical description of the reaction kinetics was carried out. The selection of a suitable reactor-type is therewith possible. Since reaction rates increases with substrate concentration and decreases by the presence of both product mono-rhamnolipid and L-rhamnose, the most promising arrangements are a batch-conversion in a well mixed tank reactor or a continuous conversion in a reactor column (plug flow model).
- Naringinase immobilization was evaluated for enhancing the efficiency of the process. Different carrier types and coupling methods were tested for obtaining high activities yields and simultaneously high loaded activities. Best results were obtained with non-porous micro-magnetic particles compared to large but porous carriers. Due to its small size this particles are only applicable to repeated batch-conversions in a well mixed tank reactor with magnetic separation of the particles after each reaction cycle.

Furthermore, at academic level following observations were gained:

- Regarding Naringinase characterization, new data about its stability and also its activity-optima with the substrate di-rhamnolipid were found. The mixed Naringinase preparation was enriched by application on an anionic exchange column and elution in two activity peaks was observed. Enzyme deactivation based on a series-type mechanism was proposed assuming that only one α-L-rhamnosidase species is present in the preparation. However, the presence of two different iso-enzymes with different regio-selectivities *i.e.* cleavage of a rhamnose-rhamnose bond in di-rhamnolipid or cleavage of a rhamnose-aglycone bond in p-nitro-phenyl-rhamnoside or mono-rhamnolipid can not be discarded.

- A kinetic model was set-up for kinetics analysis considering the enzymatic reaction taking place in the aqueous phase whereas rhamnolipids must diffuse from or to the micelle-phase. Excellent agreement between expected and experimental values was achieved. This model may be extended to other systems involving aggregate-building substrates. This new representation may serve as an alternative to already existing kinetic models considering reaction taking place on the surface of the substrate aggregates. An independent experiment to establish the real location of the reaction should be rather conducted since that can not be observed from kinetic data.
- Immobilized enzyme activities of different protein loaded preparations were compared to predictions based on the diffusion-reaction theory for heterogeneous catalysts. This is a completely innovative approach for analyzing initial reaction rates of immobilized enzymes considering the influence of diffusion limitation. Moreover, estimation of intrinsic enzyme activities were therewith possible which are otherwise very difficult to determine by diffusion-rate controlled reactions. Intrinsic enzyme activity values higher than free enzyme activity were estimated by the hydrophobic support Eupergit 250L. Partition and or adsorption of the surface active di-rhamnolipid molecules on the matrix surface may have been the reason for such high intrinsic enzyme activity. Regarding the non-porous micro-magnetic particles, unexpected low activities at high protein loading were observed when compared to theoretical values. The reason for this was attributed to a multi-layer immobilization due to the much lower carrier surface available.

Future development could be focused on the testing of di-rhamnolipid conversion on a reactor with immobilized Naringinase. Two different reactor configurations could be compared and evaluated: 1) a tank reactor coupled to a magnetic separation device with Naringinase immobilized on non-porous micro magnetic particles and 2) a column reactor with Naringinase immobilized on porous Eupergit particles. Based on the kinetic model for the conversion with free Naringinase the reactor kinetics could then be modeled taking into account diffusion limitations. In order to compare expected and experimental conversion values some relevant parameters should be determined as the effective diffusion coefficient within the porous Eupergit and the partition coefficient of di-rhamnolipid molecules around the outer surface of the carriers.

6 References

Amersham-Biosciences (2002) Affinity chromatography. Principles and methods. Editon AD, Uppsala

Atkinson B and Davies I J (1974) Overall rate of substrate uptake (Reaction) by microbial films.1. biological rate equation. T I Chem Eng-Lond 52(3): 248-259

Attwood D and Florence A T (1983) Surfactant systems. J.W. Arrowsmith Ltd., Bristol

Bahar T and Celebi S S (1999) Immobilization of glucoamylase on magnetic poly(styrene) particles. J Appl Polym Sci 72(1): 69-73

Banat I M, Makkar R S and Cameotra S S (2000) Potential commercial applications of microbial surfactants. Appl Microbiol Biotechnol 53(5): 495-508

Bilkova Z, Slovakova M, Horak D et al (2002) Enzymes immobilized on magnetic carriers: efficient and selective system for protein modification. J Chromatogr, B: Anal Technol Biomed Life Sci 770(1-2): 177-181

Birgisson H, Hreggvidsson G O, Fridjonsson O H et al (2004) Two new thermostable alpha-L-rhamnosidases from a novel thermophilic bacterium. Enzyme Microb Technol 34(6): 561-571

Biselli M, Kragl U and Wandrey C (2002). Reaction engineering for enzyme-catalyzed biotransformations. Enzyme catalysis in organic synthesis - a comprehensive handbook. Drauz K and Waldman H. Weinheim, Wiley-VCH Verlag GmbH. I**:** 185-258.

Bisht K S, Gao W and Gross R A (2000) Glycolipids from Candida bombicola: Polymerization of a 6-O-acryloyl sophorolipid derivative. Macromolecules 33(17): 6208-6210

Bisht K S, Gross R A and Kaplan D L (1999) Enzyme-mediated regioselective acylations of sophorolipids. J Org Chem 64(3): 780-789

Bozhinova D (2004). Synthesis, modification and characterization of magnetic micromatrices for covalent immobilization of biomolecules. Model investigation with penicillin amidase from *E. coli*. Fakultät IV: Chemie und Pharmazie, University of Regensburg. phD Thesis.

Bozhinova D, Galunsky B, Yueping G et al (2004) Evaluation of magnetic polymer micro-beads as carriers of immobilised biocatalysts for selective and stereoselective transformations. Biotechnol Lett 26(4): 343-350

Buchholz K and Kasche V (1997) Biokatalysatoren und Enzymtechnologie. VCH, Weinheim

Buchholz K, Kasche V and Bornscheuer U T (2005) Biocatalysts and enzyme technology. Wiley-VCH Verlag GmbH & Co. KGaA, Weinheim

Cameotra S S and Makkar R S (2004) Recent applications of biosurfactants as biological and immunological molecules. Curr Opin Microbiol 7(3): 262-266

Champion J T, Gilkey J C, Lamparski H et al (1995) Electron-Microscopy of Rhamnolipid (Biosurfactant) Morphology - Effects of Ph, Cadmium, and Octadecane. J Colloid Interface Sci 170(2): 569-574

Chaplin M and Bucke C (1990) Enzyme Technology. Cambridge University Press, Cambridge

Cheetham P and Quail M (1991) Process for preparing L-rhamnose. US5077206 Unilever, Netherlands

Chopineau J, Lesieur S, Carion-Taravella B et al (1998) Self-evolving microstructured systems upon enzymatic catalysis. Biochimie 80(5-6): 421-435

Cooper D G, Macdonald C R, Duff S J B et al (1981) Enhanced production of surfactin from *Bacillus subtilis* by continuous product removal and metal cation additions. Appl Environ Microbiol 42(3): 408-412

Cooper D G and Paddock D A (1984) Production of a biosurfactant from *Torulopsis bombicola*. Appl Environ Microbiol 47(1): 173-176

Dreker T (1998). Immobilisierung und Charakterisierung des Enzyms Naringinase auf magnetischen Silica-Partikeln. Institut für Bioverfahrenstechnik, University of Stuttgart. Studienarbeit.

Dunlap W J, Hagen R E and Wender S H (1962) Preparation and properties of rhamnosidase and glucosidase fractions from a fungal flavonoid glycosidase preparation, Naringinase C-100. J Food Sci 27(6): 597-&

Ellenrieder G and Daz M (1996) Thermostabilization of Naringinase from *Penicillium decumbens* by proteins in solution and immobilization on insoluble proteins. Biocatal Biotransform 14(2): 113-123

Engasser J M and Horvath C (1973) Effect of internal diffusion in heterogeneous enzyme-systems - evaluation of true kinetic parameters and substrate diffusivity. J Theor Biol 42(1): 137-155

Franzreb M, Siemann-Herzberg M, Hobley T J et al (2006) Protein purification using magnetic adsorbent particles. Appl Microbiol Biotechnol 70(5): 505-516

Gabor F and Pittner F (1984) Data on the classification of Naringinase in *Penicillium* species. H-S Z Physiol Chem 365(9): 914-914

Gallego M V, Pinaga F, Ramon D et al (2001) Purification and characterization of an alpha-L-rhamnosidase from *Aspergillus terreus* of interest in winemaking. J Food Sci 66(2): 204-209

Giani C, Wullbrandt D, Reinhardt R et al (1993) *Pseudomonas aeruginosa* and its use in a process for the biotechnological preparation of L-rhamnose. US5501966 Hoechst, Germany

Gottifredi J C and Gonzo E E (2005) On the effectiveness factor calculation for a reaction-diffusion process in an immobilized biocatalyst pellet. Biochem Eng J 24(3): 235-242

Gunata Z, Bitteur S, Brillouet J M et al (1988) Sequential enzymic-hydrolysis of potentially aromatic glycosides from grape. Carbohydr Res 184: 139-149

Guo Z and Sun Y (2004) Characteristics of immobilized lipase on hydrophobic superparamagnetic microspheres to catalyze esterification. Biotechnol Prog 20(2): 500-506

Hashimoto W, Miyake O, Nankai H et al (2003) Molecular identification of an alpha-L-rhamnosidase from *Bacillus* sp strain GL1 as an enzyme involved in complete metabolism of gellan. Arch Biochem Biophys 415(2): 235-244

Hashimoto W and Murata K (1998) Alpha-L-rhamnosidase of *Sphingomonas* sp. R1 producing an unusual exopolysaccharide of sphingan. Biosci Biotech Bioch 62(6): 1068-1074

Hashimoto W, Nankai H, Sato N et al (1999) Characterization of alpha-L-rhamnosidase of *Bacillus* sp GL1 responsible for the complete depolymerization of gellan. Arch Biochem Biophys 368(1): 56-60

Helvaci S S, Peker S and Ozdemir G (2004) Effect of electrolytes on the surface behavior of rhamnolipids R1 and R2. Colloids Surf, B 35(3-4): 225-233

Hooijmans C M, Stoop M L, Boon M et al (1992) Comparison of 2 experimental methods for the determination of michaelis-menten kinetics of an immobilized enzyme. Biotechnol Bioeng 40(1): 16-24

Hut Y M and Ju L K (2003) Lipase-mediated deacetylation and oligomerization of lactonic sophorolipids. Biotechnol Prog 19(2): 303-311

Iqbal J and Saleemuddin M (1985) Sucrose hydrolysis using invertase immobilized on concanavalin-a-sepharose. Enzyme Microb Technol 7(4): 175-178

Ishigami Y, Gama Y, Nagahora H et al (1987) The pH-sensitive conversion of molecular aggregates of rhamolipid bisurfactant. Chem Lett(5): 763-766

Kheirolomoom A, Khorasheh F and Fazelinia H (2002) Influence of external mass transfer limitation on apparent kinetic parameters of penicillin G acylase immobilized on nonporous ultrafine silica particles. J Biosci Bioeng 93(2): 125-129

Kim J S, Powalla M, Lang S et al (1990) Microbial glycolipid production under nitrogen limitation and resting cell conditions. J Biotechnol 13(4): 257-266

Kosaric N (2001) Biosurfactants and their application for soil bioremediation. Food Technol Biotech 39(4): 295-304

Lang S (2002) Biological amphiphiles (microbial biosurfactants). Curr Opin Colloid Interface Sci 7(1-2): 12-20

Lang S and Trowitzsch-Kienast W (2002) Biotenside. B.G.Teubner GmbH, Stuttgart, Leipzig, Wiesbaden

Lang S and Wullbrandt D (1999) Rhamnose lipids - biosynthesis, microbial production and application potential. Appl Microbiol Biotechnol 51(1): 22-32

Lebron-Paler A, Pemberton J E, Becker B A et al (2006) Determination of the acid dissociation constant of the biosurfactant monorhamnolipid in aqueous solution by potentiometric and spectroscopic methods. Anal Chem 78(22): 7649-7658

Levenspiel O (1999) Chemical Reaction Engineering. John Wiley & Sons, New York

Li J, He J L, Shi J G et al (2006) Preparation and adsorption properties of rhamnolipid adsorbent. J Inorg Mater 21(6): 1339-1344

Linhardt R J, Bakhit R, Daniels L et al (1989) Microbially produced rhamnolipid as a source of rhamnose. Biotechnol Bioeng 33(3): 365-368

Liu X Q, Guan Y P, Shen R et al (2005) Immobilization of lipase onto micron-size magnetic beads. J Chromatogr, B: Anal Technol Biomed Life Sci 822(1-2): 91-97

Maier R M and Soberon-Chavez G (2000) *Pseudomonas aeruginosa* rhamnolipids: biosynthesis and potential applications. Appl Microbiol Biotechnol 54(5): 625-633

Mamma D, Kalogeris E, Hatzinikolaou D G et al (2004) Biochemical characterization of the multi-enzyme system produced by *Penicillium decumbens* grown on rutin. Food Biotechnol 18(1): 1-18

Manjon A, Bastida J, Romero C et al (1985) Immobilization of Naringinase on glycophase-coated porous-glass. Biotechnol Lett 7(7): 477-482

Manjon A, Iborra J L, Gomez J L et al (1987) Evaluation of the effectiveness factor along immobilized enzyme fixed-bed reactors - Design of a reactor with Naringinase covalently immobilized into glycophase-coated porous-glass. Biotechnol Bioeng 30(4): 491-497

Manzanares P, de Graaff L H and Visser J (1997) Purification and characterization of an alpha-L-rhamnosidase from *Aspergillus niger*. FEMS Microbiol Lett 157(2): 279-283

Manzanares P, Orejas M, Gil J V et al (2003) Construction of a genetically modified wine yeast strain expressing the *Aspergillus aculeatus* rhaA gene, encoding an alpha-L-rhamnosidase of enological interest. Appl Environ Microbiol 69(12): 7558-7562

Manzanares P, Orejas M, Ibanez E et al (2000) Purification and characterization of an alpha-L-rhamnosidase from *Aspergillus nidulans*. Lett Appl Microbiol 31(3): 198-202

Manzanares P, van den Broeck H C, de Graaff L H et al (2001) Purification and characterization of two different alpha-L-rhamnosidases, RhaA and RhaB, from *Aspergillus aculeatus*. Appl Environ Microbiol 67(5): 2230-2234

Martearena M R, Blanco S and Ellenrieder G (2003) Synthesis of alkyl-alpha-L-rhamnosides by water soluble alcohols enzymatic glycosylation. Bioresour Technol 90(3): 297-303

Mata-Sandoval J, Karns J and Torrents A (1999) High-performance liquid chromatography method for the characterization of rhamnolipid mixtures produced by *Pseudomonas aeruginosa* UG2 on corn oil. J Chromatogr A 864: 211 - 220

Matulovic U (1987). Verfahrenentwicklung zur Herstellung grenzflächenaktiver Rhamnolipide mit immobilisierten Zellen von *Pseudomonas* spec. DSM 2874. Naturwissenschaftliche Fakultät. Braunschweig, Technische Universität Carolo-Wilhelmina. Doktors der Naturwissenschaften (Dr.rer.nat)**:** 157.

Meiwess J, Wullbrant D and Giani C (1994) Alpha-L-Rhamnosidase zur Gewinnung von Rhamnose, ein Verfahren zur Herstellung und Ihre Verwendung. Germany. EP0599159

Miake F, Satho T, Takesue H et al (2000) Purification and characterization of intracellular alpha-L-rhamnosidase from *Pseudomonas paucimobilis* FP2001. Arch Microbiol 173(1): 65-70

Michon F, Pozsgay V, Brisson J R et al (1989) Substrate-specificity of Naringinase, an alpha-L-rhamnosidase from *Penicillium decumbens*. Carbohydr Res 194: 321-324.

Mixich J, Rapp K and Vogel M (1996) Method for the preparation of rhamnose monohydrate from rhamnolipids. Germany. US5550227

Monti D, Pisvejcova A, Kren V et al (2004) Generation of an alpha-L-rhamnosidase library and its application for the selective derhamnosylation of natural products. Biotechnol Bioeng 87(6): 763-771

Mulligan C N (2005) Environmental applications for biosurfactants. Environm Pollut 133(2): 183-198

Mutter M, Beldman G, Schols H A et al (1994) Rhamnogalacturonan alpha-l-rhamnopyranohydrolase - a novel enzyme specific for the terminal nonreducing rhamnosyl unit in rhamnogalacturonan regions of pectin. Plant Physiol 106(1): 241-250

Nitschke M and Costa S (2007) Biosurfactants in food industry. Trends Food Sc Tech 18(5): 252-259

Nitschke M, Costa S and Contiero J (2005) Rhamnolipid surfactants: An update on the general aspects of these remarkable biomolecules. Biotechnol Prog 21(6): 1593-1600

Noordman W H, Brusseau M L and Janssen D B (2000) Adsorption of a multicomponent rhamnolipid surfactant to soil. Environm Sci Technol 34(5): 832-838

Norouzian D, Hosseinzadeh A, Inanlou D N et al (1999) Various techniques used to immobilize naringinase produced by *Penicillium decumbens* PTCC 5248. World J Microb Biot 15(4): 501-502

Ochoa-Loza F J, Noordman W H, Janssen D B et al (2007) Effect of clays, metal oxides, and organic matter on rhamnolipid biosurfactant sorption by soil. Chemosphere 66(9): 1634-1642

Ochsner U A, Reiser J, Fiechter A et al (1995) Production of *Pseudomonas aeruginosa* rhamnolipid biosurfactants in heterologous Hosts. Appl Environ Microbiol 61(9): 3503–3506

Ono M, Tosa T and Chibata I (1977) Preparation and properties of Naringinase immobilized by ionic binding to Deae-Sephadex. J Ferment Technol 55(5): 493-500

Ozdemir G, Peker S and Helvaci S S (2004) Effect of pH on the surface and interfacial behavior of rhamnolipids R1 and R2. Colloids Surfaces A 234(1-3): 135-143

Panaiotov I, Ivanova M and Verger R (1997) Interfacial and temporal organization of enzymatic lipolysis. Curr Opin Colloid Interface Sci 2(5): 517-525

Parra J L, Guinea J, Manresa M A et al (1989) Chemical characterization and physicochemical behavior of biosurfactants. J Am Oil Chem Soc 66(1): 141-145

Peker S, Helvaci S S and Özdemir G (2003) Interface-subphase interactions of rhamnolipids in aqueous rhamnose solutions. Langmuir 19: 5838-5845

Pieters B R and Bardeletti G (1992) Enzyme immobilization on a low-cost magnetic support - kinetic-studies on immobilized and coimmobilized glucose-oxidase and glucoamylase. Enzyme Microb Technol 14(5): 361-370

Piljac G and Piljac V (1993) Pharmaceutical preparation based on rhamnolipid against dermatological diseases, *e.g.* papilloma virus infections. Belgien. WO93/14767

Puri M and Banerjee U C (2000) Production, purification, and characterization of the debittering enzyme Naringinase. Biotechnol Adv 18(3): 207-217

Puri M, Marwaha S S and Kothari R M (1996) Studies on the applicability of alginate-entrapped naringinase for the debittering of kinnow juice. Enzyme Microb Technol 18(4): 281-285

Puri M, Seth M, Marwaha S S et al (2001) Debittering of Kinnow mandarin juice by covalently bound Naringinase on hen egg white. Food Biotechnol 15(1): 13-23

Qiu G M, Zhu B K and Xu Y Y (2005) alpha-Amylase immobilized by Fe_3O_4 poly(styrene-co-maleic anhydride) magnetic composite microspheres: Preparation and characterization. J Appl Polym Sci 95(2): 328-335

Ragnitz K, Pietzsch M and Syldatk C (2001) Immobilization of the hydantoin cleaving enzymes from *Arthrobacter aurescens* DSM 3747. J Biotechnol 92(2): 179-186

Reiling H E, Thaneiwyss U, Guerrasantos L H et al (1986) Pilot-plant production of rhamnolipid biosurfactant by *Pseudomonas aeruginosa*. Appl Environ Microbiol 51(5): 985-989

Rodrigues L, Banat I M, Teixeira J et al (2006) Biosurfactants: potential applications in medicine. J Antimicrob Chemoth 57(4): 609-618

Roitner M, Schalkhammer T and Pittner F (1984) Preparation of prunin with the help of immobilized Naringinase pretreated with alkaline buffer. Appl Biochem Biotech 9(5-6): 483-488

Romero C, Manjon A, Bastida J et al (1985) A method for assaying the rhamnosidase activity of Naringinase. Anal Biochem 149(2): 566-571

Rosenberg E and Ron E Z (1999) High- and low-molecular-mass microbial surfactants. Appl Microbiol Biotechnol 52(2): 154-162

Saleemuddin M and Husain Q (1991) Concanavalin-a - a useful ligand for glycoenzyme immobilization - a review. Enzyme Microb Technol 13(4): 290-295

Sanchez M, Aranda F J, Espuny M J et al (2007) Aggregation behaviour of a dirhamnolipid biosurfactant secreted by *Pseudomonas aeruginosa* in aqueous media. J Colloid Interface Sci 307(1): 246-253

Scaroni E, Cuevas C, Carrillo L et al (2002) Hydrolytic properties of crude alpha-L-rhamnosidases produced by several wild strains of mesophilic fungi. Lett Appl Microbiol 34(6): 461-465

Schalkhammer T and Pittner F (1986) Characterization of rhamno - glucosidase from *Penicillium* species. 17th FEBS Meeting Berlin (West)

Sekeroglu G, Fadiloglu S and Gogus F (2006) Immobilization and characterization of Naringinase for the hydrolysis of naringin. Eur Food Res Technol 224(1): 55-60

Shimomura M, Ohta M, Sugiyama N et al (1999) Properties of alpha-chymotrypsin covalently immobilized on poly(acrylic acid)-grafted magnetite particles. Polym J 31(3): 274-278

Singh A, Van Hamme J D and Ward O P (2007) Surfactants in microbiology and biotechnology: Part 2. Application aspects. Biotechnol Adv 25(1): 99-121

Singh P and Cameotra S S (2004) Potential applications of microbial surfactants in biomedical sciences. Trends Biotechnol 22(3): 142-146

Singh S K, Felse A P, Nunez A et al (2003) Regioselective enzyme-catalyzed synthesis of sophorolipid esters, amides, and multifunctional monomers. J Org Chem 68(14): 5466-5477

Soares N F F and Hotchkiss J H (1998) Naringinase immobilization in packaging films for reducing naringin concentration in grapefruit juice. J Food Sci 63(1): 61-65

Syldatk C (1984). Mikrobielle Bildung und Charakterisierung grenzflächenaktiver Rhamnolipide aus *Pseudomonas* spec. DSM 2874. Naturwissenschaftliche Fakultät. Braunschweig, Technische Universität Carolo-Wilhelmina. Doktors der Naturwissenschaften (Dr.rer.nat)**:** 99.

Syldatk C, Lang S, Matulovic U et al (1985) Production of four interfacial active rhamnolipids from n-alkanes or glycerol by resting cells of *Pseudomonas* species DSM 2874. Z Naturforsch [C] 40(1-2): 61-7

Syldatk C, Lang S, Wagner F et al (1985) Chemical and physical characterization of four interfacial-active rhamnolipids from *Pseudomonas* spec. DSM 2874 grown on n-alkanes. Z Naturforsch [C] 40(1-2): 51-60

Tischer W (1995). Immobilization of enzymes. In: Enzymes catalysis in organic synthesis: A comprehensive handbook. Drauz K and Waldmann H. VCH. I., Weinheim

Trummler K, Effenberger F and Syldatk C (2003) An integrated microbial/enzymatic process for production of rhamnolipids and L-(+)-rhamnose from rapeseed oil with *Pseudomonas* sp. DSM 2874. Eur J Lipid Sci Tech 105(10): 563-571

Tsen H Y, Tsai S Y and Yu G K (1989) Fiber entrapment of Naringinase from *Penicillium* sp. and application to fruit juice debittering. J Ferment Bioeng 67(3): 186-189

Turecek P and Pittner F (1986) Simple enzyme reactors suitable for the by-product-free preparation of the aglycones of naturally-occurring glycosides under mild conditions. Appl Biochem Biotechnol 13(1): 1-13

Van Haesendonck I and Vanzeveren E (2006) Rhamnolipid in bakery products.

Wang W, Deng L, Peng Z H et al (2007) Study of the epoxydized magnetic hydroxyl particles as a carrier for immobilizing penicillin G acylase. Enzyme Microb Technol 40(2): 255-261

Yamane T (1981) On approximate expressions of effectiveness factors for immobilized biocatalysts. J Ferment Technol 59(5): 375-381

Yanai T and Sato M (2000) Purification and characterization of an alpha-L-rhamnosidase from *Pichia angusta* X349. Biosci Biotech Bioch 64(10): 2179-2185

Young N M, Johnston R A Z and Richards J C (1989) Purification of the alpha-L-rhamnosidase of *Penicillium decumbens* and characterization of 2 glycopeptide components. Carbohydr Res 191(1): 53-62

Zhang L, Somasundaran P, Singh S K et al (2004) Synthesis and interfacial properties of sophorolipid derivatives. Colloids Surfaces A 240(1-3): 75-82

Zverlov V V, Hertel C, Bronnenmeier K et al (2000) The thermostable alpha-L-rhamnosidase RamA of *Clostridium stercorarium*: biochemical characterization and primary structure of a bacterial alpha-L-rhamnoside hydrolase, a new type of inverting glycoside hydrolase. Mol Microbiol 35(1): 173-179

7 Appendices

7.1 Selection of Commercial L-Rhamnosidases

Besides the known ability of *Penicillium* Naringinase to hydrolyze rhamnolipids, other technical enzyme preparations containing α-L-rhamnosidase activity were tested. Table 1 shows di-rhamnolipid and p-nitrophenyl-rhamnoside (pnpR) activities found for the different enzyme preparations.

Table 1: Di-rhamnolipid and pnpR activities of commercial L-rhamnosidases

Enzyme preparation	Fungal source	Di-rhamnolipid activity (U mg^{-1})[c]	pnpR activity (U mg^{-1})[c]
Naringinase	*Penicillium decumbens*	3.9	6.1 [a] – 5.6 [b]
Hesperidinase P	*Penicillium* sp.	31.5	46.2 [a]
Viscozyme L	*Aspergillus aculeatus*	not detected	0.0031 [b]
Novozyme 188	*Aspergillus niger*	not detected	0.0034 [b]
Hesperidinase A	*Aspergillus niger*	not detected	not detected

[a] 8 mM initial pnpR concentration. [b] 1.75 mM initial pnpR concentration. [c] Activity per mg of solid or liquid enzyme preparation

Unfortunately, only the *Penicillium decumbens* L-rhamnosidases were able to cleave di-rhamnolipid into mono-rhamnolipid at slightly acidic medium (pH 4.5 – 5.5). On the other hand, the enzyme mixtures Viscozyme L and Novozyme 188 were active against pnpR while Hesperidinase A was not. α-L-Rhamnosidases from *Aspergillus* species are known to be capable of cleaving L-rhamnose from a α-1-2 glycosidic bond (Mutter et al. 1994; Manzanares et al. 1997; Manzanares et al. 2000) and were therefore expected to be able to convert di-rhamnolipid into mono-rhamnolipid. Thus, *Aspergillus* rhamnosidase might be inactivated by rhamnolipids. Trummler et al. (2003) observed inactivation of a recombinant L-rhamnosidase from *Clostridium stercorarium* by co-incubation experiments with di-rhamnolipid and pnpR.

The much more expensive and pure *Penicillium* Hesperidinase-P was able to cleave di-rhamnolipid into mono-rhamnolipid at a rate about 8-fold higher than that of Naringinase. However, after enrichment of Naringinase on a Q-sepharose column, the specific protein activity was as high as that of Hesperidinase-P. The difference in prices did not justify selecting Hesperidinase-P over Naringinase and therefore all conversion experiments throughout the work were carried out with Naringinase.

7.1.1 Material and Methods

Naringinase (N-1385; Lot N° 110K16471; 511 U g^{-1} L-rhamnosidase activity, 55 U g^{-1} ß-glucosidase activity) from *Penicillium decumbens* and Hesperidinase-A (H-8137; 3 U g^{-1}) from *Aspergillus Niger* were purchased from Sigma Aldrich (Steinheim, Germany). The technical grade liquid enzyme mixtures Viscozyme L (VL) (100 U g-1 ß-glucanase activity) from *Aspergillus aculeatus* and Novozyme 188 (N188) (250 U g^{-1} cellobiase activity) from *Aspergillus Niger* containing α-L-rhamnosidase as side activity were kindly donated by Novozymes (Bagsvaerd, Denmark). A second lyophilized preparation Hesperidinase-P (H-8510; 18 U g^{-1} hesperidinase activity, 7 U g^{-1} ß-glucosidase activity) from *Penicillium* sp. was also obtained from Sigma Aldrich. Crystalline di-rhamnolipid was a gift of Hoechst AG (Frankfurt, Germany). p-nitro-phenyl-rhamnoside (pnpR) from Extrasynthese (Genay, France) served as model substrate for α-rhamnosidase activity. All other reagents, chemicals and co-solvents were of analytical grade.

Di-rhamnolipid conversions were carried out at 10 mM initial concentration and started by addition of 10 µl of the enzyme preparation (VL and N188) or by addition of 50 µl of a 1 g l^{-1} enzyme solution (Hesperidinase-A, -P and Naringinase) to 1 ml reaction volume. Conversions with VL and N188 were carried out at 50°C whereas 60°C were applied for all other enzymes. Conversion with VL was carried out in sodium acetate buffer 0.1 M, pH 5.5 whereas conversions with all other enzymes in sodium acetate buffer 0.1 M, pH 4.5. 100 µl samples were withdrawn at different times and the reaction was stopped by acidification with 12 µl 1 M phosphoric acid followed by RL extraction in 100 µl ethyl acetate. Droplets of this solution were qualitatively analyzed by thin layer chromatography with a methanol-chloroform solution in a ratio 15:85 as mobile phase. Di- and mono-rhamnolipid spots were detected in the plates by immersion into a ammonium molibdate/cerium sulphate acidic solution (0.42% w/v ammonium molibdate, 0.2% w/v cerium(IV) sulphate and 6.2% v/v sulfuric acid) and after heating at 105°C. Quantitative determination of rhamnolipid for bioconversion of Naringinase and Hesperidinase P was carried out by HPLC according to the description in the method sub-section of section 4.2 (page 69)

PnpR-conversions were carried out at 1.75 mM (VL and N188) or 8 mM (Hesperidinase-A, -P and Naringinase) initial concentration at 60°C in sodium acetate buffer 0.1 M, pH 5.5. The reaction was started by addition of 10 µl enzyme preparation (VL and N188) or by addition of 50 µl of a 1 g l^{-1} enzyme solution (Hesperidinase-A and -P and Naringinase) to 1 ml reaction volume. Analysis of p-nitro-phenolate for VL and N188 conversions was conducted by withdrawing 100 µl samples at different times till 1 hour and adding into a cuvette with 1.4 ml 0.1 M sodium hydroxide. The absorption was immediately measured at 400 nm (Extinction coefficient for p-nitro-phenolate at pH 12

and room temperature: 18.9 l $mmol^{-1}cm^{-1}$). Analysis for Hesperidinase-A, -P and Naringinase activity was conducted in a cuvette and the reaction was monitored by the increase of p-nitrophenolate concentration at 400 nm (extinction coefficient for pnp at pH 5.5 and 60 °C: 1.2 l $mmol^{-1}cm^{-1}$) during 5 min reaction in a photometer (Amersham Biosciences, Uppsala, Sweden) equipped with a heated cell changer and coupled to the software Swift II reaction kinetics (Biochrom Ltd., Cambridge, UK).

7.2 Calculation of Effectiveness Factor

The estimation of immobilized enzyme activities and loaded carrier activities carried out on chapter 4.4 was based on calculations of effectiveness factor of the enzymatic reaction within and on the surface of the enzyme carrier. In the next paragraphs, a detailed description of the equations used is presented for clarifying the calculation. The list of abbreviations is indicated in page 103 and 104.

7.2.1 Porous diffusion

The differential steady-state mass balance in a porous spherical particle with simultaneous substrate pore diffusion and Michaelis-Menten reaction kinetics can only be solved numerically. Nevertheless, there is a number of approximate expressions in form of simple algebraic equations which can satisfactorily be used for analyzing experimental kinetic data (Atkinson and Davies 1974; Yamane 1981; Hooijmans et al. 1992; Gottifredi and Gonzo 2005). For a first approximation of theoretical carrier activities and considering experimental limitations we chose the equation proposed by Atkinson and Davies (1974) for slab geometries. The generalized definition of the Thiele-Modulus ϕ for Michaelis-Menten kinetics and spherical particles according to Engasser and Horvath (1973) and Atkinson and Davies (1974) equals:

$$\phi = \frac{R}{3} \cdot \sqrt{\frac{V_{\max}^{I}}{K_M^{I} \cdot D_{eff}}} \tag{A-1}$$

The approximate description of efficiencies due to pore diffusion given by Atkinson and Davies (1974) is:

$$\eta^{in}(\phi, \beta_0) = \begin{cases} 1 - \dfrac{\tanh\phi}{\phi} \cdot \left[\dfrac{1/\eta_D}{\tanh(1/\eta_D)} - 1 \right] : \dfrac{1}{\eta_D} \le 1 \\ \eta_D - \dfrac{\tanh\phi}{\phi} \cdot \left[\dfrac{1}{\tanh(1/\eta_D)} - 1 \right] : \dfrac{1}{\eta_D} > 1 \end{cases} \tag{A-2}$$

$$\eta_D = \sqrt{2} \cdot \left(\frac{1+\beta_0}{\phi.\beta_0} \right) \cdot \left[\beta_0 - \ln(1+\beta_0) \right]^{1/2} \tag{A-3}$$

This approximation is valid for estimations with spherical particles, although only at relative small Thiele-Modulus values (< 1) (Yamane 1981). On the other hand, for R3 conversion, where s_0 is low, β_0 approaches zero, and η converges to the effectiveness factor of the corresponding first-order reaction. In this case the expression can be derived analytically as follows (Levenspiel 1999):

$$\lim_{\beta \to 0} \eta^{in}(\phi, \beta_0) = \varepsilon(\phi) = \frac{1}{\phi} \cdot \left[\frac{1}{\tanh(3 \cdot \phi)} - \frac{1}{3 \cdot \phi} \right] \tag{A-4}$$

For applying the above equations, it has to be further assumed that: 1) The protein is uniformly distributed within the porous particle, 2) There is no external film diffusion limitation being $s_0 = s_b$ and 3) The effective diffusion coefficient is constant within the particle. Thus, provided that the intrinsic protein activity and the effective diffusion coefficient for every substrate are known, the reaction effectiveness factor can be estimated in dependency of the protein loading. Equations A-1 to A-3 and A-10 were used for estimating pnpR-immobilized enzyme activities and equations A-1, A-4 and A-10 were used for estimating R3-immobilized enzyme activities.

7.2.2 Film diffusion

For Michaelis-Menten reaction kinetics the external effectiveness factor can be derived from the steady state mass balance equations (Chaplin and Bucke 1990; Kheirolomoom et al. 2002):

$$\eta^{ex} = \frac{(1 + \beta_b) \cdot \left(\varphi - \sqrt{\zeta} \right)}{2 \cdot \beta_b \cdot Da_{II}} \tag{A-5}$$

$$\varphi = 1 + \beta_b + Da_{II} \tag{A-6}$$

$$\zeta = \varphi^2 - 4 \cdot \beta_b \cdot Da_{II} \tag{A-7}$$

The corresponding definition of the substrate modulus for external substrate diffusion, the Damköhler number, Da_{II} equals according to Chaplin and Bucke (1990):

$$Da_{II} = \frac{V^I_{\max}}{k_L \cdot a \cdot K^I_M} \tag{A-8}$$

As pointed out above, β_b approaches zero for R3 conversions and the corresponding effectiveness factor in this condition simplifies according to Chaplin and Bucke (1990):

$$\eta^{ex} = \frac{1}{1 + Da_{II}} \tag{A-9}$$

Thus, provided that the intrinsic protein activity and the mass transfer coefficient for every substrate are known, the reaction effectiveness factor can be estimated in dependency of the protein loading. Equations A-5 to A-8 and A-10 were used for estimation of pnpR immobilized enzyme activities on non-porous supports, whereas equations A-8 to A-10 were used for R3 immobilized enzyme activities estimations.

For the calculation of the Thiele-Modulus (equation A-1) and Damköhler-Number (equation A-8), the quotient $V^I_{max}(K^I_M)^{-1}$ was obtained as:

$$\frac{V^I_{\max}}{K^I_M} = u^I_P(s_0) \cdot q_P \cdot \rho \cdot \frac{(1+\beta_0)}{s_0} \tag{A-10}$$

7.3 Preparation of Immobilized Naringinase

In the following paragraphs a detailed description of the preparation of immobilized Naringinase, which were used in the experiments presented in chapter 4.3 and 4.4 is presented. The list of abbreviations is indicated in page 113 and 114.

7.3.1 Preparation of M-PVA derivates

Aliquots of M-PVA bead suspension were washed 3 times with de-ionized water before use. Each wash step consisted in re-suspension of the beads and separation from the supernatant with a magnet block. 25 mg beads per ml enzyme solution were always employed.

For immobilization through the EDC-method, the beads were mixed with aqueous Naringinase solution at different concentrations and a concentrated aqueous EDC-solution, adjusted at pH 5.0, was added to the suspension drop by drop in a ratio 1 to 8 under intensive stirring. The EDC to protein ratio was set at 94 (µmol mg^{-1}) for every assay. Suspensions were then incubated at 20°C for 20 h under overhead shaking. After 2 h incubation the pH was re-adjusted to 5. The beads were then separated from the supernatant and washed in 3 cycles (3 times each) of different pH buffers (pH 8.5 with Tris-HCl and pH 4.0 with acetate both containing 0.5 mol l^{-1} sodium chloride) (Ragnitz et al. 2001).

For immobilization through the GA-method the beads were activated by pre-incubation with 12.5% GA solution for 2 h at 30°C. After equilibration with coupling buffer, the beads were mixed with Naringinase solution at different concentrations in 1 mol l^{-1} potassium phosphate, pH 7.5, and the suspension was incubated at 20°C for 20 h under overhead shaking. The supernatant was then separated and the beads were washed 3 times with coupling buffer followed by 2 wash-cycles with different pH buffers (acetate buffer pH 4.0 containing 0.5 mol l^{-1} sodium chloride and 0.2 mol l^{-1} potassium phosphate pH 7.5). The wet beads were incubated with sodium borohydride for reduction of the formed Schiff´s base linkages. Finally, the beads were washed again as described above, and stored in 0.1 mol l^{-1} sodium acetate buffer pH 5.5 at 4°C (Bozhinova et al. 2004).

7.3.2 Preparation of Eupergit C and Eupergit 250L derivates

The immobilization procedure, as well as their parameters was chosen according to the standard protocol recommended by the supplier: aqueous Naringinase solution of different concentrations previously diluted with 1 mol l^{-1} potassium phosphate buffer pH 8.0 in a ratio 1 to 2 was added to dried beads at a bead concentration of 0.166 g ml^{-1}. The slurry was let to stand at 23°C under gentle shaking. After 24 h incubation, the

beads were rinsed onto a suction filter with 10 ml incubation buffer, suck off and washed 6 times with 50 ml 0.1 mol l^{-1} potassium phosphate buffer, pH 8.0. The beads were then incubated 1 h with 1 mol l^{-1} Tris-HCl, pH 8.0, at room temperature, for abreacting remaining oxirane groups, and washed again several times with 0.1 mol l^{-1} potassium phosphate buffer, pH 8.0. Wet drained beads were weighted out and stored at 4°C.

7.3.3 Preparation of Sepharose derivates

Preparation of the beads and immobilization parameters were chosen according to the supplier recommendations: Freeze-dried CNBr-Sepharose beads were swollen and washed with 1 mmol l^{-1} HCl. Pre-swollen ConA-Sepharose beads in 20% ethanol were washed with binding buffer. Pre-swollen NHS-Sepharose beads in iso-propanol were washed with ice-cold 1 mmol l^{-1} HCl. Wet drained beads were mixed with Naringinase solution at different concentrations at a bead concentration of 400 g l^{-1}. The respective coupling buffers were as followed: 0.1 mol l^{-1} sodium bicarbonate, pH 8.3, for CNBr-Sepharose, 0.2 mol l^{-1} sodium bicarbonate, pH 8.3, for NHS-Sepharose and 20 mmol l^{-1} Tris-HCl, pH 7.4, with 1 mmol l^{-1} calcium chloride for ConA-Sepharose. All coupling buffers contained 0.5 mol l^{-1} sodium chloride for preventing non-specific ionic interactions. The suspensions were incubated at 25°C in an overhead shaker during 4 h (ConA- and CNBr-derivates) or 2 h (NHS-derivates). The suspension were then dumped into a weighted disposable filtration device (Vivaspin 4-0.2 µm PES membrane, Vivascience-Sartorius group) and centrifuged at 4500 rpm (Multifuge 1S-R, Heraeus). The beads were washed several times by resuspention-centrifugation cycles with coupling buffer. CNBr- and NHS-Sepharose beads were incubated at room temperature with Tris-HCl, pH 8, for abreacting remaining active groups while ConA-Sepharose beads were let to stand with 0.2% GA solution in phosphate buffer pH 6.1 for 2 h at 30°C to facilitate cross-linking (Iqbal and Saleemuddin 1985). After 3 wash-cycles with alternating pH buffers (pH 4 with acetate and pH 8.0 with Tris-HCl, both containing 0.5 mol l^{-1} sodium chloride) filtration devices containing the centrifuged beads were weighted and stored at 4°C, whereas NHS-derivates were stored as a suspension in 1 ml 0.1 mol l^{-1} sodium acetate buffer, pH 5.5.

Considering enzyme catalyzed reactions rhamnolipids are special substrates. In water they form molecular aggregates and therefore the substrate concentration available for the converting enzyme (e.g. α-L-rhamnosidase) is very low and only the critical micelle concentration will be, as monomers, in aqueous solution.

Taken into account this particularity, process optimization was conducted for the enzymatic conversion of di-rhamnolipid to mono-rhamnolipid and resulting in (I) selection of the optimal reaction conditions for enzyme stability and conversion rate, (II) a mathematical description of the reaction time course assuming mixed aggregates as a second phase, and (III) non-porous magnetic micro-beads at low enzyme loading demonstrated to be the most suitable carrier, where mass diffusion resistances in the three-phase reaction system as well as multi-layer immobilization were completely overcome.

ISBN: 978-3-86644-329-7

www.uvka.de